The ER-Golgi-Intermediate Compartment: dynamics and cargo sorting studied by time-lapse video microscopy

Inauguraldissertation

zur

Erlangung der Würde eines Doktors der Philosophie

vorgelegt der

Philosophisch-Naturwissenschaftlichen Fakultät

der Universität Basel

von

Houchaïma Ben-Tekaya

aus Tunis, Tunesien

Basel 2004

Genehmigt von der Philosophisch-Naturwissenschaftlichen Fakultät

auf Antrag von

Prof. Dr. Hans-Peter Hauri und Prof. Dr. Martin Spiess

Basel, den 19 Mai 2004

Prof. Dr. Marcel Tanner

Dekan

Index

Acknowledgements…… 1

Summary…… 3

Introduction…… 4

1. The early secretory pathway…… 4

1.1. Morphology…… 5

1.2. Functions…… 7

1.3. Protein traffic…… 8

1.3.1. Coats…… 9

1.3.2. SNAREs…… 13

1.3.3. Motors…… 17

1.3.4. Transport signals…… 20

1.3.5. Retention and retrieval signals…… 21

1.3.6. Regulatory components, tethers and Rabs…… 22

1.4. Current models of membrane traffic…… 26

2. Live imaging…… 29

2.1. Overview…… 29

2.2. Fluorophores…… 30

2.2.1. Fluorescent proteins…… 30

2.2.2. Organic fluorophores…… 32

2.2.3. Quantum dots…… 33

2.3. Techniques…… 34

2.3.1. Photobleaching…… 35

2.3.2. Photoactivation…… 36

2.3.3. Four-dimensional imaging…… 38

2.4. Quantification…… 40

2.4.1. Image processing…… 41

2.4.2. Kinetic modelling…… 41

2.4.3. Volumes and concentrations…… 44

2.4.4. Single particle tracking…… 44

2.5. Contribution to understanding the early secretory pathway…… 47

2.5.1. Compartmentalization…… 47

2.5.2. Trafficking…… 49
3. Aim of the thesis…….. 51
4. References…….. 52
Results…….. 93
1. Summary……... 94
2. Introduction…….. 94
3. Results…….. 96
3.1. Features of GFP-ERGIC-53 and endogenous ERGIC-53 are indistinguishable. 96
3.2. GFP-ERGIC-53 imaging reveals two populations with different dynamics……. 98
3.3. Trafficking routes of GFP-ERGIC-53…….... 101
3.4. GFP-ERGIC-53 and VSV-G-GFP take different routes from the ERGIC…… 103
3.5. Sorting of anterograde and retrograde cargo in the ERGIC……. ……... 104
4. Discussion…….. 107
5. Experimental procedures…….. 111
5.1. Recombinant DNAs……..... 111
5.2. Cell culture, pulse-chase and immunoprecipitation……..... 112
5.3. Immunofluorescence microscopy…….... 112
5.4. Live cell imaging……..... 113
5.5. Transport blocks…….... 114
5.6. Quantification of directionality……..... 114
6. Acknowledgments…….. 115
7. References…….. 115
8. Supplementary data legends……... 120
Conclusions and perspectives…… 122
1. ERGIC: previous and up-dated view…….. 122
2. ERGIC populations…….. 124
3. Potential machineries controlling ERGIC populations……..……... 129
4. Future directions…….. 132
5. References…….. 133
Curriculum vitae…….. 139

Acknowledgements

I would like to thank Dr. Hans-Peter Hauri for his continuous support, patience and trust regarding my work. I am grateful to him for all what he taught me during my Ph.D. thesis, from addressing the appropriate questions of a problem to presenting and discussing the results in an objective and critical manner. Thank you Hans-Peter.

I would like to thank Käthy Bucher for her technical support especially when I started in the lab. Without those teachings I would not be able to go so far. Thank you Käthy for patiently coaching me in the lab and for correcting my Swiss German; with your help I made an enormous progress.

I would like to thank all the Hauri Group members for their fruitful and critical discussions about my work. Thank you Christian Appenzeller, Lionel Breuza, Sandra Mitrovic, Oliver Nufer, Beat Nyfeler and Cécile Védrenne.

I would like to thank all the Pepperkok Group at the EMBL Heidelberg and the ALMF team for their technical support and the interesting discussions.

I would like to thank all the Neurobiology/Pharmacology present and former members for their help and the nice working atmosphere. Particularly I would like to thank the secretaries Marianne Liechti and Jny Wittker, the department manager Markus Meier (and Markus Hämmerle), the former department manager and our IT support Roger Jenni (and the BioPHit team) and the laboratory helpers Monika Furrer and Angèle Klein.

I would like to thank all the members of the Biozentrum/Pharmazentrum that I crossed and who helped me in any way.

I would like to thank Dr. Martin Spiess for accepting to make part of my thesis committee.

Acknowledgements

I would like to thank Dr. Maria-Suzanna Balda and Dr. Karl Matter for all their instructions, advises, support and friendship.

I would like to thank my aunt, uncles, and cousins in Basel and Lausanne for their help and encouragement.

I would like to thank my parents, my brother and my friend for their endless love and for always being there for me.

Thank you all.

Summary

Membrane trafficking in mammalian cells proceeds through several steps including sorting the correct components to be transported, packaging them into appropriate containers and conveying the carriers to the proper organelles with which they fuse. All these steps are tightly regulated by several machineries like coats, fusion proteins, motors, tethers, Rabs and other regulatory components. The investigation of the molecular mechanisms of these machineries unraveled the trafficking events taking place between different compartments; but these findings did not elucidate how organelles can persist and maintain their integrity in a constantly dynamic environment. Two major controversial models are constantly debated: the stability and the maturation of compartments. The stability model favors the notion that compartments are long-lived stations in which cargo material is sorted from the resident components and transits from one organelle to the other in vesicular carriers. The maturation hypothesis suggests that organelles of the secretory pathway are transient stations that form at the level of the ER; once they leave it, they continuously homo-fuse and recycle back machinery components to the previous station. A particular discordance resides in defining the ER-Golgi-intermediate compartment (ERGIC) features: is it a stable or a maturing organelle?

The ERGIC defined by the cycling lectin ERGIC-53 consists of tubulovesicular clusters. Here, I show by live imaging that GFP-ERGIC-53 mainly localizes to long-lived stationary and some short-lived highly mobile elements. Unlike the anterograde marker VSV-G-GFP, GFP-ERGIC-53 does not vectorially move to the Golgi upon exit from the ERGIC, as assessed by a novel quantitative vector field method. Dual color imaging of GFP-ERGIC-53 and a secretory protein (signal-sequence-tagged DsRed) reveals that the stationary elements are sites of repeated sorting of retrograde and anterograde cargo, and are interconnected by highly mobile elements. Based on these results, I conclude that the ERGIC is a membrane compartment in the true sense and not simply a collection of mobile carriers mediating protein traffic from endoplasmic reticulum to Golgi. The finding that the ERGIC is a true compartment opens new perspectives for the dissection of ERGIC functions and the molecular machineries that are recruited.

Introduction

1. The early secretory pathway

All cells are delimited by an external membrane: the plasma membrane, which is important for regulating the interactions with the environment and in protecting the intracellular content. In eukaryotic cells, in addition to this membrane there are several intracellular membranes delimiting different compartments. It is believed that the organelles of the secretory and endocytic pathways have originated from the cell surface by a mechanism where membrane patches, consisting of clusters of specialized membrane proteins, have invaginated and internalized. Each of the compartments contains a distinct set of enzymes and distinct lipid compositions. A central compartment in the secretory pathway is the Golgi apparatus, which demarcates a boundary: all the organelles up-stream define the early secretory pathway, while the ones down-stream are the late secretory pathway. Here I am mainly interested in the early secretory pathway, which is common for secreted proteins as well as proteins destined for residence at the plasma membrane, endosomes or lysosomes (figure 1).

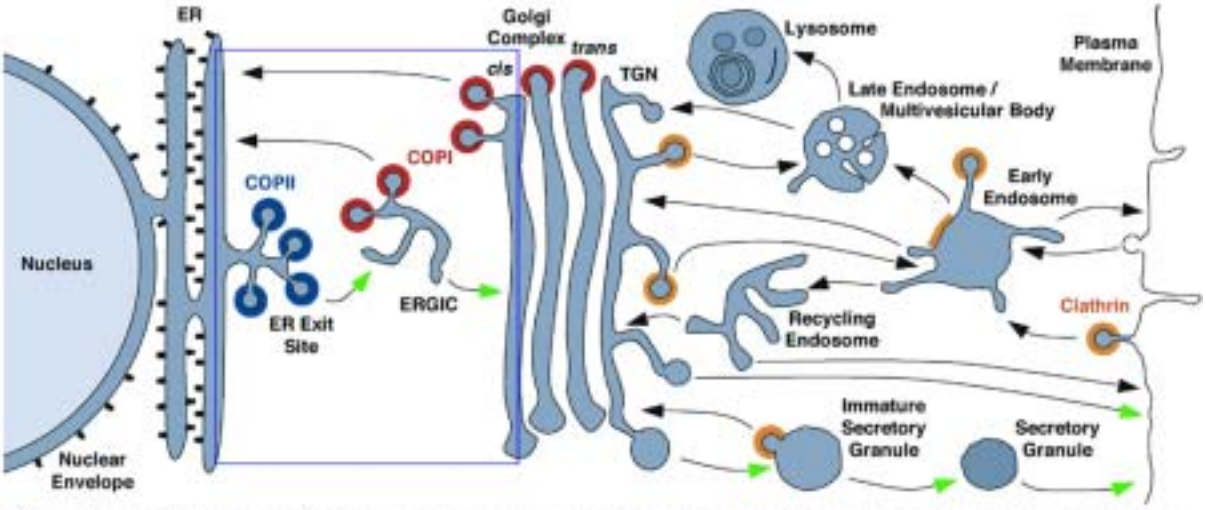

Figure 1: Model representing the secretory, endocytic, lysosomal and vacuolar pathways in mammalian cells.
Green arrowheads represent the secretory pathway. The early secretory pathway is highlighted by the blue box. Traffic through the early secretory pathway is common to all newly synthesised proteins that are targeted to the plasma membrane, or to the endocytic/lysosomal pathway. COP, coat protomer complex; ER: endoplasmic reticulum; ERGIC: ER-Golgi-intermediate compartment; TGN: *trans*-Golgi network. Reproduced and modified from Bonifacino and Glick 2004.

1.1. Morphology

In most cell types, by fluorescence light microscopy using appropriate markers, the ER appears as a reticular network throughout the cytoplasm. The Golgi is generally situated in a juxtanuclear region as a blob or dilated rings. The ER-Golgi intermediate compartment (ERGIC) labeling is characterized by dotty structures spread all over the cell (figure 2).

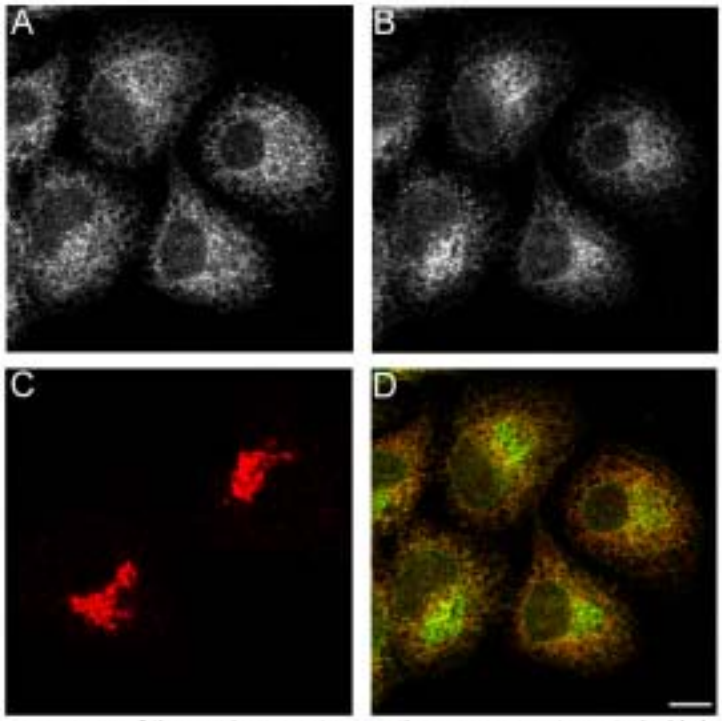

Figure 2: Immunofluorescence of the early secretory pathway compartments in HeLa cells. (A) ER: CLIMP-63 shows a reticular network and is excluded from the nuclear membrane. (B) ERGIC: ERGIC-53 staining shows a low reticular pattern and small dots that concentrate in the juxtanuclear area. Note that the ER and the Golgi stainings of ERGIC-53 are due to its recycling through these compartments. (C) Golgi: giantin stains mainly the Golgi cisternae that are localised in the juxtanuclear region. (D) merge of (A) and (B) where the ERGIC is in green and the ER in red. Bar: 5 µm.

When observed by electron microscopy (figure 3), the ER is a large membrane-bound organelle consisting of membrane bilayers separating an internal lumen from the cytoplasm (Porter et al., 1945). This structure, depending on the cell type, can have a sheet-like morphology in the cell center or consist of a network of interconnected tubules in the periphery of the cell (Porter et al., 1945) (Terasaki and Jaffe, 1991). Large portions referred to as rough ER are covered with ribosomes engaged in synthesis of proteins targeted to the membrane or the lumen of the ER (Caro and Palade, 1964). Other portions, devoid of ribosomes, emit some discrete buds or convoluted networks of

tubules and vesicles (Jamieson and Palade, 1967) (Bednarek et al., 1995) (Orci et al., 1997) (Bannykh and Balch, 1997). These buds are ERES (for ER exit sites, also known as transitional ER sites), which are COPII-coated, closely adjacent and limited to specific regions of the ER (Bannykh et al., 1996). ERES are facing into a region housing several tubulo-vesicular clusters (Bannykh et al., 1996), the ER-Golgi-intermediate compartment (ERGIC) (Hauri and Schweizer, 1992). The ERES/ERGIC complexes were termed export complexes (Bannykh et al., 1996). ERGIC clusters are also named VTCs for vesicular tubular clusters (Bannykh et al., 1996) and pre-Golgi intermediates (Presley et al., 1997). They consist of a complex of tubules apparently not contiguous with ER membranes (figure 3) (Bannykh et al., 1996) (Klumperman et al., 1998). Individual tubules have 50 nm diameter with an average diameter for the cluster of 0.4 micron (Bannykh et al., 1996) (Martinez-Menarguez et al., 1999). ERGIC clusters have a constant average number, are COPI positive and are enriched in cargo proteins. They relocate closer to the Golgi when cells are incubated at 15°C (Klumperman et al., 1998).

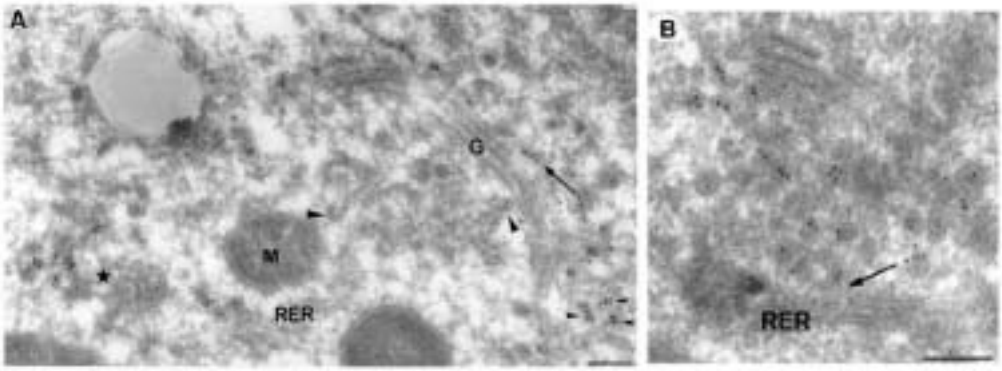

Figure 3: Electron micrograph of the early secretory pathway compartments in HepG2 cells. RER: rough ER, G: Golgi. The ERGIC clusters (* and small arrowheads) are defined by high ERGIC-53 gold particles labelling. ERGIC-53 localises to the *cis*-Golgi cisterna (arrow in A) and to ER exit sites as well (arrow in B). Big arrowheads in A point to clathrin-coated membranes. M: mitochondrion, bar: 200 nm. Reproduced and modified from Klumperman *et al.* 1998.

In most mammalian cells, the Golgi is localized near the microtubule organizing center (MTOC) (Thyberg and Moskalewski, 1985). It is a ribbon composed of stacks of cisternae occasionally connected by tubules (Rambourg and Clermont, 1990) (Tanaka and Fukudome, 1991). The stacks exhibit a *cis*-side and a *trans*-side (figure 3). The *cis* part of the Golgi is facing the ERGIC and corresponds to the entry site of material that

exited the ERGIC. The *trans*-Golgi corresponds to the side from which proteins targeted to the late secretory/endosomal pathway or to the plasma membrane exit.

1.2. Functions

Each compartment of the early secretory pathway has specific functions. These functional units are generated by localized protein–protein assemblies. The ER is a compartment formed by different sub-domains with diverse roles. The rough ER is defined as the membrane compartment that houses the translocation apparatus, oligosaccharyl transferase and associated chaperone proteins (Johnson and van Waes, 1999). It is thus the site where post-translational modifications (as oligomerization) and quality control start taking place. The transitional ER is a collection of domains where transport vesicles are formed. In this area the transport machinery (see below) is concentrated. The smooth ER is the site where enzymes involved in lipid biosynthesis are localized. In some cells as muscle cells, regions of the smooth ER are the site of calcium storage and are called the sarcoplasmic reticulum (Petersen et al., 2001).

The functions of the ERGIC are still under investigation. What is known to date is that in some diseases there is a morphological change of the ERGIC clusters (Roth, 2002). ERGIC is characterized by the type I transmembrane protein ERGIC-53, which is a recycling mannose-binding lectin (Hauri et al., 2000). If we consider ERGIC functions based on the data collected about this bona fide marker, then the ERGIC is a central station where cargo-receptor interactions are released. This release is proposed to be mediated by a low pH in the ERGIC (Appenzeller-Herzog et al., 2004). Indeed, many cargo proteins destined to leave the ER have no cytosolic domain and cannot directly interact with COPII (see below). It has been shown that some proteins as p24 proteins (Muniz et al., 2000), ERGIC-53, and its rat homologue p58 (Fiedler and Simons, 1994) (Itin et al., 1996), function as cargo receptors for these proteins. Such cargo proteins for ERGIC-53 are cathepsin C and cathepsin Z related protein (CatZr) as well as factors V and VIII (Vollenweider et al., 1998) (Appenzeller et al., 1999) (Nichols et al., 1998). In ERGIC-53 knockout humans, factors V and VIII traffic is compromised resulting in hemophilia (Nichols et al., 1998). The molecular mechanism of such a process is currently studied.

In the early secretory pathway, the Golgi is the last step for post-translational modifications. Modifying enzymes are spread in unique gradient-like distributions across the several Golgi cisternae. For example the early (or *cis*) Golgi is enriched in mannosidase I, the medial Golgi in N-acetylglucosamine (GlcNAc) transferase I and the late (or *trans*) Golgi in galactosyltransferase. Hence, through the different Golgi cisternae glycosylation, sulfation and/or proteolytic processing steps occur in an ordered fashion.

1.3. Protein traffic

All these compartments are stations through which secreted proteins or proteins targeted to the plasma membrane, endosomes or lysosomes transit before reaching their final destination. During their translation on ribosomes, newly synthesized proteins enter the ER through interactions of their hydrophobic signal peptide with the ER translocon machinery (Caro and Palade, 1964) (Blobel and Dobberstein, 1975b; Blobel and Dobberstein, 1975a) (Johnson and van Waes, 1999). Proteins inserted into the ER can be integral membrane proteins, proteins attached to membranes (through glycophosphoinositol or other lipid anchors) or proteins that are soluble within the ER lumen. Once the translation is completed, proteins shape up into a specific 3-dimensional structure and oligomerize prior to exiting the ER (Gething, 1986a) (Kreis, 1986). Different quality control machineries guarantee that only completely and correctly folded proteins are competent to exit the ER (Ellgaard and Helenius, 2003). The control process is achieved by sequential binding to chaperones (BiP, calnexin and calreticulin), which recognize and stabilize folding intermediates (Hammond and Helenius, 1994) retaining them in the ER until the proteins are completely folded. The correctly folded and assembled proteins destined for export (termed anterograde cargo) are sorted from ER resident proteins into ERES (Barlowe et al., 1994). ERES were also proposed to be folding stations for some cargo proteins (Mezzacasa and Helenius, 2002). These sites are coated with COPII proteins (see below) (Balch et al., 1994) that generate COPII-coated transport intermediates. These carriers separate from ER membranes and deliver cargo to the ERGIC. Cargo is then transported to the Golgi, where it either moves further anterogradely or retrogradely (figure 1). The proteins that leave the ER for

the ERGIC and/or the Golgi apparatus and move retrogradely are termed recycling proteins (Lippincott-Schwartz et al., 1990) (Palokangas et al., 1998) (Kappeler et al., 1997) (Lewis and Pelham, 1996). These proteins include ERGIC-53, KDEL receptor and some SNAREs (Palokangas et al., 1998) (Appenzeller et al., 1999) (Lewis and Pelham, 1992) (Rothman, 1994) (Cole et al., 1998) (Storrie et al., 1998) (Zaal et al., 1999) (Ward et al., 2001). Other proteins such as toxins that bind receptors or lipids on the plasma membrane travel from the cell surface to the ER (Sandvig and van Deurs, 1996) (White et al., 1999) (figure 1). The retrograde movement of proteins from the Golgi to the ER was primarily uncovered in brefeldin A experiments (Lippincott-Schwartz et al., 1989). From these data, Klausner *et al.* (Klausner et al., 1992) proposed that brefeldin A up regulates a pre-existing retrograde pathway from the Golgi apparatus to the ER. Later, it has been shown that brefeldin A-mediated delivery of Golgi proteins to the ER is not a gradual process but occurs explosively, apparently after the fusion of a single tubule with the ER (Sciaky et al., 1997). It could be a flow process driven by energetically favorable mixing of ER and Golgi lipids (Sciaky et al., 1997). The existence of the cycling between ER and Golgi membranes is now firmly established.

1.3.1. Coats

ER-to-Golgi and Golgi-to-ER traffic is mediated by coated vesicles. There are two types of coats: coatomer protein (COP) I and II. COPII is required for ER exit (Barlowe et al., 1994). The components of the COPII coat are the Ras-like GTPase Sar1p, the Sec23p/Sec24p sub-complex and the Sec13p/Sec31p sub-complex (Barlowe et al., 1994) (figure 4). These components (with the exception of Sar1p (Nakano and Muramatsu, 1989)) were first identified in a genetic screen using *Saccharomyces cerevisiae* (Novick, 1980). COPII complex components undergo several cycles between the cytosol and the ER membranes (Bonifacino and Glick, 2004). The cycle on ER membranes starts with the recruitment of Sar1p-GTP by Sec12p in conjunction with the transmembrane protein Sec16p. Sar1p-GTP associates with the lipid bilayer through a hydrophobic amino-terminal extension and engages its effector the Sec23p/Sec24p sub-complex, thus forming the “pre-budding complex” (Huang et al., 2001) (Bi et al., 2002) (figure 4). This newly formed complex has a positively charged, concave surface that

likely apposes the membrane and induces membrane bending (Bi et al., 2002). While Sec23p makes direct contact with Sar1p-GTP (Bi et al., 2002), Sec24p participates in cargo recognition. Once assembled onto membranes, the pre-budding complex recruits the Sec13p/Sec31p sub-complex, which consists of two Sec13p and two Sec31p subunits (Lederkremer et al., 2001) (figure 4). This mobilization will probably stabilize the curvature generated by the pre-budding sub-complex (Bonifacino and Glick, 2004) and will increase ten fold the ability of Sec23p to stimulate the GTP hydrolysis activity of Sar1p thus triggering coat disassembly (Yoshihisa et al., 1993) (Antonny and Schekman, 2001). Coat polymerization goes on by closing the COPII cage thus driving membrane scission and generating a vesicle that will either fuse with the ERGIC (Pelham, 1989) or fuse homotypically with similar vesicles to form the ERGIC (Lippincott-Schwartz et al., 2000). In the ERGIC, COPII coats shed off and recycle back to the ER.

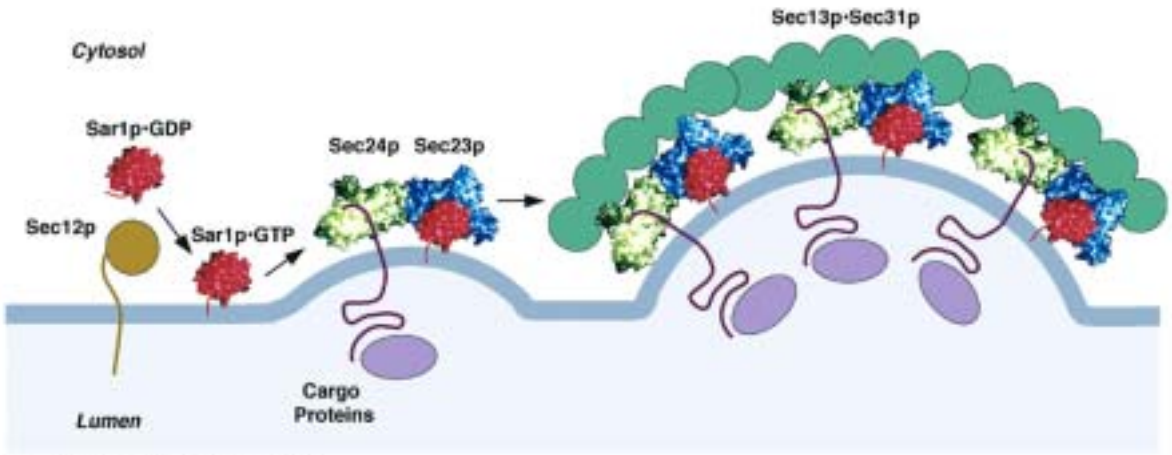

Figure 4: Assembly of COPII
Cytosolic Sar1p•GDP is converted to membrane bound Sar1p•GTP by the transmembrane protein Sec12p. Sar1p•GTP recruits the Sec23p•Sec24p subcomplex by binding to Sec23p, forming the 'pre-budding complex'. Transmembrane cargo proteins gather at the assembling coat by binding to Sec24p. The Sec13p•Sec31p subcomplex polymerizes onto Sec23p•Sec24p and crosslinks the pre-budding complexes. Cargo proteins are further concentrated. Sec16p and Sed4p also participate in the assembly of COPII, but are not represented here. Reproduced from Bonifacino and Glick 2004.

COPI is a complex formed by the small GTPase Arf1 (for adenosine diphosphate-ribosylation factor 1) and a cytosolic protein complex (coatomer, short for coat promoter). Arf1 is myristoylated on an amino terminal glycine residue, and membrane binding and function depend on this post-translational modification (Kahn et al., 1991). It regulates sorting of proteins into COPI vesicles and also the assembly and disassembly

of the coat (Serafini et al., 1991) (Lanoix et al., 1999) (Malsam et al., 1999) (Pepperkok et al., 2000) (Donaldson et al., 1992a) (Palmer et al., 1993) (Tanigawa et al., 1993). Coatomer comprises seven subunits: ζ, η, η', ι, κ, ν, and • (Waters et al., 1991). During COPI coat assembly, Arf-GTP simultaneously recruits the membrane-proximal ηνι• and the membrane distal ζη'κ sub-complexes (Hara-Kuge et al., 1994) (Scales et al., 2000). By means of their WD40 domains, COPI ζ and η' subunits recruit cargo proteins by binding distinct but overlapping sets of dilysine signals (Eugster et al., 2004). The ν COPI subunit binds dilysine signals as well (Harter and Wieland, 1996), while the ι COPI subunit binds a specific sequence containing at least one aromatic residue (Sato et al., 1997). The membrane association of Arf1 coupled to its activation is regulated positively by guanine nucleotide exchange factors (GEFs) and negatively by GTPase-activating proteins (GAPs) (Puertollano et al., 2001). Each GEF processes a 200-amino acid segment referred to as "Sec7 domain" (Chardin et al., 1996) (Chardin and McCormick, 1999). The detailed steps of COPI coats formation are not as well documented as it is the case for COPII. It is presumed that coats in general, although molecularly distinct, form following similar processes where subunits of coat proteins and small guanine triphosphatases play key roles (Barlowe, 2000) (Scales et al., 2000). COPI was initially identified by Rothman and co-workers as the coat protein found on vesicles in an intra-Golgi transport assay (Balch et al., 1984) and by Klausner and co-workers as a protein dispersed from Golgi membranes by brefeldin A (Donaldson et al., 1990). Rothman and co-workers originally proposed that COPI coats mediate intra-Golgi anterograde trafficking (Balch et al., 1984). However, the COPI vesicles could be shown to contain Golgi resident proteins (Lanoix et al., 1999) and proteins that cycle between the Golgi and the ER (Martinez-Menarguez et al., 1999). The supporting evidence that COPI is involved in Golgi-to-ER trafficking comes primarily from yeast genetics and *in vitro* binding experiments. Cosson and Letourneur (Cosson and Letourneur, 1994) (Letourneur et al., 1994) supplied two pieces of data that were taken as evidence that COPI is involved in retrograde trafficking. First, in yeast with mutations in ζ and η' COPI subunits, COPI-binding proteins appeared on the cell surface (Letourneur et al., 1994). Second, direct interactions could be shown between some COPI subunits and specific peptides bound to affinity columns (Cosson and Letourneur, 1994). Klumperman and co-

workers have further investigated these findings in mammalian cells and found, using a detailed quantitative electron microscopy study, that COPI tends to be present on the ends of ERGIC tubules (Martinez-Menarguez et al., 1999); cargo proteins and soluble proteins being excluded from these areas. It is believed that interactions between motifs on the cytoplasmic tails of transmembrane proteins, to be recycled from the ERGIC or the Golgi, and COPI (Cosson and Letourneur, 1994) (Bremser et al., 1999) (Scales et al., 2000) lead to the recruitment of this subset of proteins into COPI-coated buds. These buds then transform into COPI-coated vesicles which uncoat and fuse with ER membranes. Brefeldin A inhibits the GEF required to localize Arf1 to Golgi membranes (Peyroche et al., 1999). Since Arf1 is normally cycling on and off the Golgi membranes (Donaldson et al., 1991) (Vasudevan et al., 1998), inhibiting new recruitment of Arf1 causes its rapid loss from these membranes (Donaldson et al., 1992b) (Donaldson et al., 1992a) (Vasudevan et al., 1998) (Helms and Rothman, 1992). As Arf1 is required to recruit the coat protein COPI to Golgi membranes, the result is that after a short time (60 sec in HeLa cells), both COPI and Arf1 relocate from Golgi membranes to the cytosol (Lippincott-Schwartz et al., 1990) (Donaldson et al., 1991) (Presley et al., 2002). After the mislocalization of these components, there is microtubule-dependent tubulation of Golgi membranes (Lippincott-Schwartz et al., 1990), and eventually the Golgi fuses with the ER (Lippincott-Schwartz et al., 1989) (Lippincott-Schwartz et al., 1990). Based on the brefeldin A studies, Klausner proposed that COPI stabilizes Golgi membranes and negatively regulates the formation of retrograde transport intermediates (Klausner et al., 1992). In support of this, a brefeldin A-like phenotype in which Golgi tubulates and then merges partially with the ER was produced in a mutant CHO cell line (ldlF) (Hobbie et al., 1994) in which the epsilon subunit of COPI was degraded (Guo et al., 1996). Also, brefeldin A-induced tubulation could be prevented with an antibody against COPI (Scheel et al., 1997).

Data from genetic and *in vitro* experiments (Letourneur et al., 1994) (Cosson and Letourneur, 1994) (Rothman and Wieland, 1996), suggested that the anterograde and retrograde vesicles were 60-75 nm in diameter. For instance, COPII-coated vesicles isolated from yeast (Barlowe et al., 1994) or generated *in vitro* using purified components (Matsuoka et al., 1998), were shown to have a diameter of 75 nm. Such small-sized vesicles do not explain the mechanism by which large macromolecular

cargoes are transported. For instance, fibroblasts assemble long (300 nm) rigid trimers of procollagen I that must be exported from the ER, and export is dependent upon the function of both COPII and COPI complexes (Stephens and Pepperkok, 2002). It has been proposed that the subunit composition of the coat complex could allow the accommodation of these large cargoes into coated carriers (Shimoni et al., 2000). Specifically, Lst1p, a homologue of Sec24p in *Saccharomyces cerevisiae*, was found to generate vesicles of larger size than Sec24p itself (Shimoni et al., 2000). Moreover, rapid transport of protein aggregates through the Golgi was uncovered to be mediated by “mega-vesicles”. These vesicles correspond to Golgi cisternal rims that dilated to accommodate the aggregates and that pinched off to form what amounts to a huge transport vesicle (Volchuk et al., 2000). Conversely, data from intact mammalian cells propose that ER-to-Golgi transport intermediates are either large pleiomorphic or tubular (Lippincott-Schwartz et al., 2000) (Stephens and Pepperkok, 2001) structures (Mironov et al., 2003) (Aridor et al., 2001). Golgi-to-ER transport is also found to be mediated by tubules in mammalian cells. Indeed, sorting of ERGIC-53 from ERGIC under 15°C rewarming conditions involves the formation of tubules which exclude cargo proteins and do not appear to have a COPI coat (Klumperman et al., 1998). In these cases, coats would be involved in cargo concentration and sorting, and would probably act in the generation and maintenance of the export domains only.

Recent work suggests that transport of some proteins is independent of COPI (Johannes and Goud, 1998) (Storrie et al., 2000). The discovery was based on the observations that recycling of some Golgi enzymes (such as glycosyltransferases) and toxins (such as Shiga toxin) to the ER was not inhibited in the presence of an Arf1 GTP-bound mutant nor by microinjection of COPI antibodies (Storrie et al., 2000), while such inhibition of COPI function blocked recycling of KDEL receptor and ERGIC-53 from the Golgi to the ER (Girod et al., 1999). Conversely, expression of a GDP-bound mutant of the small GTPase Rab6 blocked recycling of glycosyltransferases and Shiga toxin from the Golgi to the ER (Girod et al., 1999) (White et al., 1999). Under these conditions, recycling of the KDEL receptor and ERGIC-53 is unaffected.

1.3.2. SNAREs

The final steps in the existence of a transport vesicle are the targeting to the appropriate compartment, the coat shedding and the fusion with the acceptor membrane. The targeting and fusion reactions both rely on the same class of proteins, which were identified in a cell-free intra-Golgi transport assay. By treating Golgi membranes with N-ethylmaleimide, this assay allowed the purification of “N-ethylmaleimide-Sensitive Factor” (NSF) (Block et al., 1988), which exists in cytosolic or membrane bound forms (Glick and Rothman, 1987). Electron microscopy demonstrated that when NSF was inactivated, uncoated vesicles accumulated on Golgi membranes, implying that NSF is required for membrane fusion (Malhotra et al., 1988). Cloning of the corresponding gene revealed that NSF was the mammalian ortholog of yeast Sec18p, which had been implicated in ER-to-Golgi transport (Wilson et al., 1989) (Eakle et al., 1988). NSF acts in a wide range of membrane fusion steps in the secretory and endocytic pathways (Beckers et al., 1989) (Diaz et al., 1989). It forms a hexameric ring (Whiteheart et al., 2001) and is a founding member of the AAA protein family (“ATPases associated with diverse cellular activities”), a group of enzymes that catalyze the structural remodeling of protein complexes (Lupas and Martin, 2002). A partner protein called ζ-SNAP (“soluble NSF association protein”) binds NSF to membranes (Clary et al., 1990). ζ-SNAP is the mammalian ortholog of yeast Sec17p (Griff et al., 1992). Using NSF/ζ-SNAP as an affinity reagent to fractionate a brain lysate, Söllner *et al.* identified a set of three membrane-associated “SNAP Receptors,” or SNAREs (Sollner et al., 1993). These same membrane proteins had previously been implicated in linking synaptic vesicles to the plasma membrane (Walch-Solimena et al., 1993). One of the proteins, known as VAMP (for Vesicle-Associated Membrane Protein) or synaptobrevin, was proven to be associated with synaptic vesicles, whereas the other two proteins, syntaxin and SNAP-25 (for SyNaptosome Associated Protein of relative molecular mass 25 kD, no relation to ζ-SNAP), had been localized to the presynaptic plasma membrane. Almost every step in membrane trafficking is carried out by a distinct set of SNARE pairs, and the SNAREs that mediate a given transport step (from ER to Golgi, from Golgi to plasma membrane, and so on) are conserved from yeast to humans (Ferro-Novick and Jahn, 1994). Based on these data the SNARE hypothesis emerged. It proposes that each type of transport vesicle carries a specific “v-SNARE” that binds to a cognate “t-SNARE” on the target membrane (Rothman, 1994). This idea fits with the observations that cells

contain families of proteins related to the synaptic SNAREs and that various SNAREs localize to different intracellular compartments (Bennett and Scheller, 1993) (Weimbs et al., 1998) (Chen and Scheller, 2001). Most SNAREs are C-terminally anchored transmembrane proteins, with their functional N-terminal domains facing the cytosol. Each of these proteins contains a heptad repeat “SNARE motif” of 60–70 amino acids that can participate in coiled-coil formation (Bock et al., 2001). An exception is SNAP-25, which contains two SNARE motifs and binds to the membrane via covalently linked palmitate groups attached to the central part of the protein. Structural and biochemical studies showed that the SNARE complex generated by the pairing of a cognate v- and t-SNARE is a very stable four-helix bundle, with one ζ-helix contributed by the monomeric v-SNARE and the other three ζ-helices contributed by the oligomeric t-SNARE (Fasshauer et al., 1997) (Sutton et al., 1998) . The t-SNARE usually consists of three separate polypeptides. All of the SNARE complexes in the cell appear to fit this general pattern in which the four SNARE motifs are contributed by a protein related to synaptobrevin, a protein related to syntaxin, a protein or protein domain related to the N-terminal part of SNAP-25, and a protein or protein domain related to the C-terminal part of SNAP-25 (Misura et al., 2002). In some cases, the distinction between vesicles and target membranes SNAREs is not meaningful—for example, during the homotypic fusion of organelles—but the general classification scheme of v-SNAREs (one ζ-helix) and t-SNAREs (three ζ-helices) remains useful. An alternative scheme uses the terminology R- or Q-SNAREs, reflecting the presence of an arginine or a glutamine, respectively, at a characteristic position within the SNARE motif (Fasshauer et al., 1998). In each SNARE complex, three glutamines and one arginine form a central ionic layer in the otherwise hydrophobic core of the four-helix bundle (Sutton et al., 1998). Although the two classification schemes are based on different principles, there is a rough correspondence of R-SNAREs with v-SNAREs and of Q-SNAREs with t-SNAREs. A major insight from structural analysis of the SNARE complex was that v- and t-SNAREs pair in a parallel fashion (Hanson et al., 1997) (Lin and Scheller, 1997) (Sutton et al., 1998) (figure 5). Therefore, v- and t-SNAREs in separate membranes can pair to form a *trans*-SNARE complex (“SNAREpin”), or v- and t-SNAREs in the same membrane can pair to form a *cis*-SNARE complex. A *trans*-SNARE complex persists throughout the fusion reaction to become a *cis*-SNARE complex in the fused membrane.

ζ-SNAP then binds along the edge of the SNARE complex (Rice and Brunger, 1999) and recruits NSF (figure 5). ATP hydrolysis by NSF dissociates the *cis*-SNARE complex (Mayer et al., 1996), possibly by exerting rotational force to untwist the four-helix bundle (May et al., 1999) (Yu et al., 1999). Thus, NSF and ζ-SNAP do not participate directly in the fusion reaction, but instead act to recycle the SNAREs for another round of complex formation.

SNAREs seem to perform two major functions (Bonifacino and Glick, 2004). One function is to promote fusion itself. In all transport reactions that have been examined, the formation of *trans*-SNARE complexes is essential for fusion. Assembly of the four-helix bundle is thought to supply the free energy needed to bring apposing membranes close enough to fuse (Hanson et al., 1997) (Weber et al., 1998) (Chen and Scheller, 2001). Support for the idea that SNAREs act as fusogens came from reconstitution experiments showing that purified recombinant SNAREs can promote the fusion of liposomes, provided that v- and t-SNAREs are in different liposomes (Weber et al., 1998). In an elegant extension of this work, Rothman and co-workers recently demonstrated that the fusion of natural biological membranes can be driven by SNAREs in the absence of accessory proteins (Hu et al., 2003). Under some conditions, fusion can apparently proceed even if the *trans*-SNARE complex has already dissociated (Szule and Coorssen, 2003). The meaning of these observations is still being debated, but they suggest that assembly of a *trans*-SNARE complex is not always temporally coupled to membrane fusion. This point may be particularly relevant for the reversible “kiss-and-run” fusion that occurs during regulated exocytosis (Palfrey and Artalejo, 2003). The second major function of SNAREs is to help ensure the specificity of membrane fusion. Different v-/t-SNARE complexes form at different steps of intracellular transport. Surprisingly, purified SNAREs can pair promiscuously *in vitro*. But when purified SNAREs were tested in the liposome fusion assay, the formation of productive *trans*-SNARE complexes was almost exclusively restricted to physiologically relevant v- and t-SNARE combinations (McNew et al., 2000). As a result, the biophysical fusion assay actually has predictive power for identifying SNARE complexes that form *in vivo* (Parlati et al., 2002).

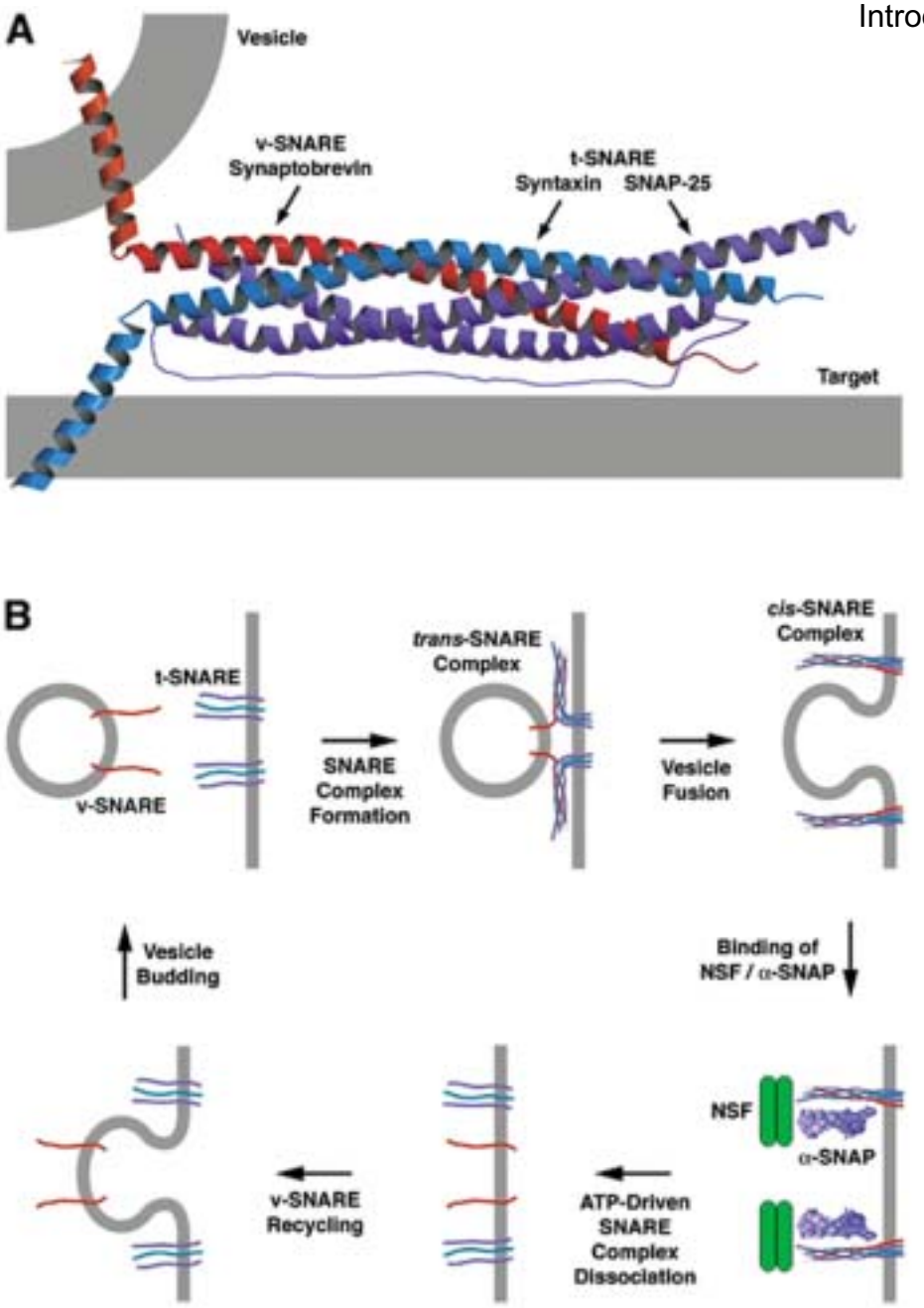

Figure 5: Structure and Function of SNAREs.
(A) Crystal structure of a synaptic trans-SNARE complex. The structures of the two membrane anchors and of the peptide that links the two SNAP-25 helices are hypothetical. (B) The SNARE cycle. A trans-SNARE complex assembles when a monomeric v-SNARE on the vesicle binds to an oligomeric t-SNARE on the target membrane, forming a stable four-helix bundle that promotes fusion. The result is a cis-SNARE complex in the fused membrane. α-SNAP binds to this complex and recruits NSF, which hydrolyzes ATP to dissociate the complex. Unpaired v-SNAREs can then be packaged again into vesicles. Reproduced from Bonifacino and Glick 2004.

1.3.3. Motors

Motors are proteins that bind ATP and are able to move on a suitable substrate with concomitant ATP hydrolysis. Most eukaryotic motor proteins move by binding to a

specific site on either actin filaments (myosin) or on microtubules (dynein, kinesin). They are normally elongated molecules with two active binding sites although some kinesin analogues have a single site. The distal end of the molecule normally binds adaptor proteins that enable them to make stable interactions with membranous vesicles or with filamentous structures, which then constitute the 'cargo' to be moved along the substrate filament.

In the early secretory pathway, substrate filaments implicated in movement are predominantly microtubules. Thus, the motor proteins that are implicated in numerous trafficking events are kinesin and dynein. There are multiple organelle-associated cytoplasmic dyneins (Vaisberg et al., 1996). As described in the “Morphology” sub-section, the ER tubular network extends to the cell periphery. This extension is perturbed in cells with disrupted microtubules (Terasaki et al., 1984) and has been shown to require the (+)-end directed motor kinesin (Feiguin et al., 1994). The ERGIC contains the molecular motors kinesin and dynein. The (+)-end directed motor kinesin was shown to be responsible for the extension of the brefeldin A-induced tubules from the Golgi apparatus towards the cell periphery (Lippincott-Schwartz et al., 1995). It was thus concluded that kinesin serves as a Golgi-to-ER motor (Lippincott-Schwartz et al., 1995). And it was proposed that a COPI coat on Golgi membranes stabilizes the Golgi apparatus and inhibits the kinesin motor required to form the tubular retrograde transport intermediates in non-brefeldin A-treated cells (Klausner et al., 1992) (Lippincott-Schwartz et al., 1995). The (-)-end directed motor dynein complexed with its adaptor protein dynactin (Paschal and Vallee, 1987) (Gill et al., 1991) is required for microtubule-mediated transport of anterograde carriers from the ER to the Golgi apparatus (Presley et al., 1997) (Burkhardt et al., 1997) (Harada et al., 1998). The contribution of the dynein/dynactin complex in anterograde transport was initially uncovered by the finding that over-expression of p50/dynamitin blocks ER-to-Golgi transport of VSV-G-GFP, a typical cargo protein targeted to the cell surface (Presley et al., 1997) (Burkhardt et al., 1997). Various dynein subunits have been identified on ERGIC and Golgi membranes, but the identity of the dynein responsible for ER-to-Golgi trafficking is not resolved at this time (Murshid and Presley, 2004). The dynein/dynactin complex is active in the Golgi apparatus and is partly responsible for the centrosomal localization of this organelle (Burkhardt et al., 1997). Dynein’s ER-to-Golgi activity as an exclusively (-)-end directed

motor is contested by the finding that dynein heavy chain 1a is stably associated with ERGIC and Golgi membranes, not coming off even when the Golgi apparatus is disrupted with the drug brefeldin A (Roghi and Allan, 1999). This suggests that at least some dyneins cycle between the ER and the Golgi apparatus along with their associated membrane (Roghi and Allan, 1999). Thus, they could be on anterograde (-)-end-directed and on retrograde (+)-end directed transport intermediates. As a result, it is suggested that dynein activity must be regulated (Roghi and Allan, 1999). How this would be done is not clear for the moment. But there is evidence that Rab proteins can control binding or activity of microtubule motors as well as membrane recognition.

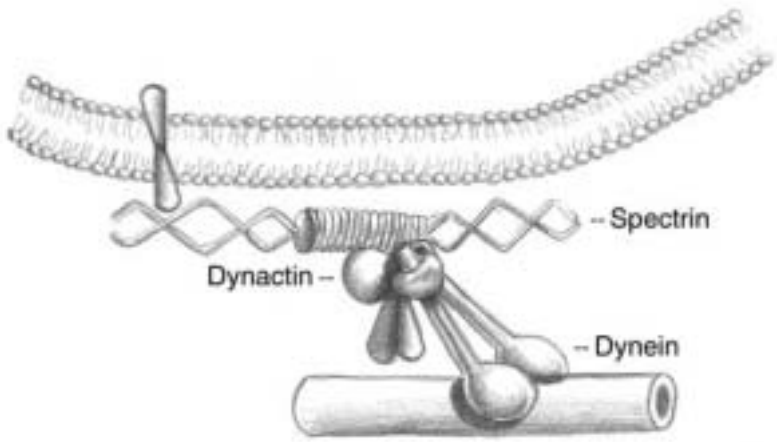

Figure 6: The dynein/dynactin complex. The molecular motor dynein does not attach directly to the plasma membrane of a transport intermediate but is attached indirectly. Dynein binds to the protein complex dynactin. Dynactin may attach to a spectrin lattice anchored to integral membrane proteins in the transport carrier. Reproduced from Mrushid and Presley 2004.

Dynactin is a membrane-associated multi-subunit complex composed of several polypeptides, including at one end a 37-nm-long filament composed of the actin homologue Arp-1, $p150^{Glued}$ and p50/dynamitin (reviewed in (Allan, 1996) (Holleran and Holzbaur, 1998) (Schroer, 1996)). While dynactin has been shown to bind directly to dynein, the mechanism for binding of dynactin to the membrane has not been determined. A spectrin/ankyrin skeleton has been proposed to localize to the ERGIC and to the Golgi apparatus (De Matteis and Morrow, 2000). The Golgi-associated spectrin/ankyrin network elements are lost from Golgi membranes when cells are

treated with BFA suggesting their recycling (Godi et al., 1998). Since binding of the dynactin Arp-1 subunit to ηIII spectrin has been shown (Holleran et al., 2001), a plausible mechanism for binding of dynein to membranes can be postulated (figure 6). In this model ηIII spectrin and Arp1 recruit dynein and dynactin to intracellular membranes and provide a direct link between the microtubule motor complex and its membrane-bound "cargo" (Godi et al., 1998). Recently, dynactin was also proposed to bind kinesin through the $p150^{Glued}$ subunit (Deacon et al., 2003).

1.3.4. Transport signals

Membrane proteins trafficking in the early secretory pathway bind coats via specific signals in their sequence. Molecules with cytosolic sequences either diaromatic as –FF in ERGIC-53 and p24 proteins (Kappeler et al., 1997) (Fiedler and Simons, 1996) (Dominguez et al., 1998) or apolar as –V in TGFζ, MT1-MMP and CD8 (Nufer et al., 2002) (Briley et al., 1997) (Urena et al., 1999) (Iodice et al., 2001) are well characterized for binding Sec24p. A cytosolic diacidic motif as -DXE- in VSV-G has been shown to facilitate export from the ER (Nishimura and Balch, 1997) possibly by interacting with Sar1p (Aridor et al., 2001). SNAREs are packaged into COPII vesicles during ER export and then into COPI vesicles during retrieval from the Golgi (Springer and Schekman, 1998) (Rein et al., 2002). SNAREs involved in ER-to-Golgi transport in mammalian cells are at least Bet1p, ERS24/Sec22b, GOS-28 and syntaxin 5 (Xu et al., 2000). Recent biochemical and structural studies have illuminated the process by which three *S. cerevisiae* SNAREs involved in ER-to-Golgi transport—Sed5p, Bet1p, and Sec22p—interact with the COPII coat (Miller et al., 2003) (Mossessova et al., 2003). These SNAREs bind to distinct sites on the Sec24p subunit: a YNNSNPF signal from Sed5p binds to the A site, a LXX[LM]E signal from Sed5p and Bet1p binds to the B site (as does a diacidic signal from the Golgi protein Sys1p), and an unidentified determinant on Sec22p binds to a site that includes Arg342 (Miller et al., 2003) (Mossessova et al., 2003). Sec24p apparently cannot bind an assembled SNARE complex, but instead selects for the uncomplexed, fusogenic forms of the SNAREs (Mossessova et al., 2003).

Recruitment of cargo into COPI vesicles, is via coatomer subunits that bind directly to cytosolic motifs. The COPI subunits ζ, η', ν and κ bind motifs typically

represented by a KKXX or KXKXX sequence at the carboxy or amino terminus of type I transmembrane proteins (Lowe and Kreis, 1995) (Letourneur et al., 1994) (Fiedler et al., 1996) (Harter and Wieland, 1996) (Cosson and Letourneur, 1994) (Eugster et al., 2004). The COPI ι subunit binds to the sequence W/YXXXW/F/Y also called ιL (for ι COPI ligand) motif (Cosson et al., 1998). The η, ν, and • COPI subunits were reported to bind phenylalanine motifs (Fiedler et al., 1996).

1.3.5. Retention and retrieval signals

Proteins exiting the ER are sorted from proteins that have to be selectively retained in the ER. Sorting (as described above) and retention are mediated by specific signals on proteins. The retained proteins include resident proteins and misfolded, like partially folded, proteins (Gething, 1986b) (Kreis, 1986). Resident proteins as chaperones are retained in the ER through a variety of mechanisms which can be conceptually divided into two categories: direct retention and retrieval/recycling mechanisms. Direct retention could involve aggregation of the protein as was shown for CLIMP63 (Klopfenstein et al., 1998), binding to the ER matrix or other immobile protein complexes, or exclusion from COPII vesicles. Retrieval/recycling mechanisms in which proteins escaped from the ER are captured in ERGIC or Golgi membranes and returned to the ER have been proposed more frequently; but often these mechanisms were not investigated in detail. A cytoplasmic C- or N- terminal K(X)KXX motif in integral membrane proteins and the sequence KDEL (HDEL in yeast) in ER luminal proteins (Pelham, 1996) were indeed found to function primarily as retrieval/recycling signals; although their involvement in retention was also described. The ER retention motif -KKXX is found on many ER-retained transmembrane proteins and in proteins that cycle between the Golgi and the ER (Cosson and Letourneur, 1994) (Letourneur et al., 1994). Data have shown that -KKXX motifs do not result in active retention of -KKXX proteins in ER membranes but rather the proteins that exit the ER and enter the ERGIC or the Golgi apparatus are sorted into COPI-coated vesicles which are targeted back to the ER (Pelham, 1994). However, while the yeast experiments are compelling in showing a role for COPI in retention of -KKXX proteins in the early secretory pathway, there is evidence that -KKXX motifs can also mediate direct retention of proteins. ERGIC-53 containing an engineered

-KKAA motif in its cytoplasmic tail fails to undergo processing of its N-linked oligosaccharides, indicating that it never advances as far as the *cis*-Golgi (Andersson et al., 1999). This ER retention mechanism is not saturable and does not depend on the presence of functional COPI, suggesting that the current models for retention in the early secretory pathway are not completely resolved. In addition to -KKXX motifs, there is evidence that motifs in transmembrane domains of integral membrane proteins, specifically hydrophilic amino acids within these hydrophobic domains, can mediate ER retention of yeast and mammalian proteins through an unknown mechanism (Letourneur and Cosson, 1998) (Sato et al., 1997) (Boehm et al., 1997). KDEL-containing proteins such as the ER chaperone BiP, are not actively excluded from Golgi-destined transport vesicles and are sometimes transported into the Golgi apparatus. Since the Golgi luminal pH is acidic, they bind with high affinity to the KDEL-receptor, a seven-transmembrane spanning protein that cycles between the ER and the Golgi membranes and transports KDEL proteins specifically back to the ER. There, the KDEL protein is released because of the ER neutral luminal pH. Thus, KDEL protein retention in the ER is thought to require its retrieval from later compartments (Pelham, 1996). However, some KDEL-containing proteins, including the chaperone calreticulin, can be held in the ER by KDEL-independent mechanisms that are not clearly known and appear to involve direct retention rather than retrieval (Sonnichsen et al., 1994).

1.3.6. Regulatory components, tethers and Rabs

Rothman and co-workers have shown that purified neuronal v- and t-SNAREs, when reconstituted into distinct liposome vesicles, are themselves capable of driving liposome fusion, albeit at a rate that is significantly slower than the rate of exocytosis of synaptic vesicles (Weber et al., 1998). These results implied that additional components cooperate with SNAREs to “tickle” the membranes and accelerate fusion. This machinery is formed by regulatory factors, AAA-type ATPases, tethering complexes and Rab GTPases (Vale, 2000) (Gerst, 2003) (Pfeffer, 1999) (Pfeffer, 2001). They directly bind to SNAREs and are involved in the regulation of SNARE assembly as well as the ability of SNAREs to participate in trafficking events (Gerst, 2003). They ensure that membranes fuse at the correct time and place.

Key regulatory elements for SNARE complex assembly are present in the SNAREs themselves, many of which contain extensions upstream of the SNARE motif (Misura et al., 2002) (Dietrich et al., 2003). For example, syntaxins have an N-terminal three-helix bundle, which binds internally to the SNARE motif to generate a “closed” conformation that cannot bind to partner SNAREs; and certain members of the synaptobrevin family have an N-terminal “longin” domain that may have a similar auto-inhibitory function (Dietrich et al., 2003). In some cases, SNARE complex formation is regulated by phosphorylation of SNAREs or of interacting components (Gerst, 2003). A wide variety of kinases are known to phosphorylate SNAREs and SNARE regulators, including protein kinase A (PKA), PKC, Ca2 +- and calmodulin-activated kinase II (CaMKII), and casein kinases I and II (Lin and Scheller, 2000) (Gerst, 1999) (Turner et al., 1999). Regulatory factors link the apposing membranes prior to SNARE complex formation. They come in several flavors (Whyte and Munro, 2002) (Bonifacino and Glick, 2004) and assemble with the aid of Rab family GTPases to promote the initial association of two membranes (Segev, 2001) (Jahn et al., 2003). For example, after two membranes fuse and the *cis*-SNARE complex is dissociated by NSF/ζ-SNAP, the SNAREs need to be kept inactive until the next round of fusion. Cytosolic factors such as GATE-16 and LMA1 bind the individual v- and t-SNAREs and help to keep them separate (Elazar et al., 2003). GATE-16 is part of the non-essential ubiquitin-fold family involved in transport (Gerst, 2003), which directly binds ER-to-Golgi SNAREs (Sagiv et al., 2000). In a recent work it was found that GATE-16 is recruited to uncomplexed GOS-28 (a Golgi SNARE) and prevents association with syntaxin-5 (Muller et al., 2002). LMA1 for Low M_r activity 1, is a dimer composed of thioredoxin and the I_2^B protease inhibitor (Gerst, 2003). LMA-1 is recruited to membranes by NSF, and can be found in complexes containing the t-SNARE after NSF has acted and been released. In addition to its function in homotypic prevacuolar fusion, LMA-1 also facilitates heterotypic yeast ER-to-Golgi transport (Barlowe, 1997). In some cases, *trans*-SNARE complex assembly seems to be arrested at an intermediate stage, with accessory proteins preventing the complete “zipping up” of the four-helix bundle until a fusion signal is received (Chen and Scheller, 2001). The best candidate for such an accessory protein is the putative Ca^{2+} sensor synaptotagmin, which interacts with SNAREs and promotes synaptic vesicle fusion in response to Ca^{2+} influx (Jahn et al., 2003). Synaptotagmin is a family of single

transmembrane lipid-binding proteins exclusively expressed in higher eukaryotes. They act both as negative and positive regulators of fusion *in vitro* and *in vivo* (Chapman, 2002) (Sudhof, 2002). A group of SNARE-interacting proteins is the SM family, whose founding members are yeast Sec1p—the product of the first gene identified by Novick *et al.* (Novick and Schekman, 1979) —and neuronal Munc-18. The SM proteins are essential and each membrane fusion step requires a specific SM protein (Toonen and Verhage, 2003) (Gallwitz and Jahn, 2003). For instance, the SM protein involved in ER-to-Golgi transport in *S. cerevisiae* is Sly1. It binds to preassembled SNARE complexes containing the Sed5 t-SNARE and the Bet1, Sec22 and Bos1 SNAREs (Peng and Gallwitz, 2002). However, the function of SM proteins is still enigmatic. These proteins bind to syntaxins, but the mode of binding is not conserved, and various SM proteins either stimulate or inhibit SNARE complex assembly.

AAA ATPases mediate the disassembly of the four-helix *cis*-SNARE (Vale, 2000) and may be necessary for the activation of individual SNAREs *in vivo* (Hanson et al., 1995) (Hayashi et al., 1995). Studies on homotypic vacuolar fusion *in vitro* have revealed that AAA-type ATPase (e.g. Sec18) priming activity is necessary before tethering to allow for the dissociation of *cis*-SNARE complexes and subsequent *trans*-complex formation (Mayer et al., 1996) (Wickner and Haas, 2000).

A common feature of many proteins that function in vesicle tethering and docking is their propensity to form highly extended, coiled-coil structures (Pfeffer, 1996) (Warren and Malhotra, 1998) (Orci et al., 1998). The best characterized tethering factor is p115, a peripheral-Golgi membrane protein in mammalian cells. p115 is homologous to the yeast protein Uso1 which is required for ER-to-Golgi transport (Sapperstein et al., 1995) (Nakajima et al., 1991) (Barroso et al., 1995). Uso1 is needed to allow the formation of SNARE complexes involved in ER-to-Golgi transport (Sapperstein et al., 1996), consistent with the idea that it acts before membrane fusion. Tethering requires both functional Ypt1, the GTPase of the Rab family that is needed for this transport step (Novick and Zerial, 1997), and the peripheral-membrane protein, Sec35 (VanRheenen et al., 1998), but not functional v- or t-SNAREs (Cao et al., 1998). p115 binds to the Golgi proteins GM130 and giantin. Giantin is proposed to drive transport vesicle capture by latching onto p115 molecules protruding outwards from the Golgi membrane surface (Pfeffer, 1999). A large macromolecular complex named TRAPP (for transport protein

particle) is also required for ER-to-Golgi transport in yeast (Sacher et al., 1998). TRAPP is a large complex, of approximate relative molecular mass 800 kD, that contains about ten polypeptides. TRAPP co-localizes with the relevant t-SNARE on the *cis*-Golgi and is needed for vesicle docking *in vitro*.

Rabs, known as Ypt proteins in yeast, are GTPases that regulate the formation of SNARE complexes *in vivo* (Lian et al., 1994) (Sogaard et al., 1994) (Lupashin and Waters, 1997). They are prenylated at their carboxyl termini, which leads to their membrane association. Rab GTPases interconvert between inactive, GDP-bound forms and active, GTP-bound forms. GTP hydrolysis is not coupled to fusion; rather, Rab conformation, which depends on the guanine nucleotide to which a Rab is bound, regulates the recruitment of docking factors from the cytosol onto membranes. In this way, Rab GTPases regulate vesicle docking. In some heterotypic transfers, the Rab is localized on the transport vesicle (Goud, 1988); in others, they might be found at the target membrane (Siniossoglou et al., 2000) (Wang et al., 2000). Transport vesicles might form bearing an active Rab protein, in a process coupled to cargo selection (Carroll et al., 2001); alternatively, Rabs might subsequently be loaded onto vesicles (or be activated there) and then be maintained in their active conformations. In some cases, a Rab appears to be activated at the target membrane and will probably be maintained in adequate active amounts to avoid an accumulation of unfused vesicles (Siniossoglou et al., 2000) (Wang et al., 2000). To ensure that Rab proteins remain active on transport vesicles, the transport machinery makes use of a set of Rab-interacting proteins that lock the Rabs in their active conformations (Novick and Zerial, 1997) (Schimmoller et al., 1998). After a vesicle fusion event, Rab-GTP is hydrolyzed to Rab-GDP, yielding a substrate for GDI capture. GDI stands for Rab-GDP Dissociation Inhibitor, which has a strong binding preference for GDP-bound Rabs. It is a cytosolic protein that returns Rabs to their membrane of origin (Pfeffer et al., 1995). Complexes of prenylated Rabs bound to GDI have all the information needed to deliver a Rab to a target membrane (Soldati et al., 1994) (Ullrich et al., 1994). Once on the proper membrane, Rabs are converted to their active, GTP-bound conformations and can then bind to effectors in a saturable manner (Soldati et al., 1994) (Ullrich et al., 1994) (Ayad et al., 1997). The process might first be catalyzed by an enzymatic activity that triggers the dissociation of Rab GTPases from the GDI protein, in the context of a given compartment (Dirac-

Svejstrup et al., 1997). In addition to being involved in the regulation of fusion events, Rabs control motor-based movement as well. An interaction between Rab6 and the $p150^{Glued}$ subunit of the dynactin complex has been shown that may be involved in Golgi-to-ER trafficking (Short et al., 2002). Rab1 and Rab2 are the predominant Rabs involved in ER-to-Golgi trafficking; however their role in regulation of molecular motors is not well studied (Murshid and Presley, 2004). Rab GTPases are also known to collect integral and peripheral membrane proteins into a specific domain (or scaffold) on an organelle (Zerial and McBride, 2001), thus defining the identity of compartments (Pfeffer, 2001). For example, Rab1–GTP has been shown to interact with GM130–GRASP65, a Golgi scaffold complex (Moyer et al., 2001) (Weide et al., 2001). Rab1 also binds to p115, a protein that interacts with the Golgi scaffold (Allan et al., 2000). In this manner, Rab1 can facilitate the delivery of transport vesicles to the Golgi, which enables the subsequent SNARE complex formation that drives vesicle fusion. Thus, Rab1 provides a key link between vesicles leaving the ER and their destination, the Golgi complex.

1.4. Current models of membrane traffic

Although many mechanisms of the anterograde ER-to-Golgi and retrograde Golgi-to-ER trafficking pathways have been unraveled, these pathways remain only partially understood. Numerous models have been proposed and new ones are continuously emerging to explain how the cell can maintain the organelles contents intact, while at the same time ensuring continuous transport events between these different compartments. One of the major debates in the field is whether transport is a maturation process or through stable compartments (figure 7). In fact, it is still not known whether the ERGIC is formed of transport intermediates shuttling between the ER and the Golgi, or whether transport intermediates fuse with and bud off stationary ERGIC clusters during their transit in the early secretory pathway (Farquhar, 1985; Pelham, 1989; Bannykh and Balch, 1997; Glick and Malhotra, 1998; Lippincott-Schwartz et al., 2000; Stephens and Pepperkok, 2001; Beznoussenko and Mironov, 2002; Storrie and Nilsson, 2002). These two major hypotheses are the result of genetic, *in vitro*, biochemical and microscopy data.

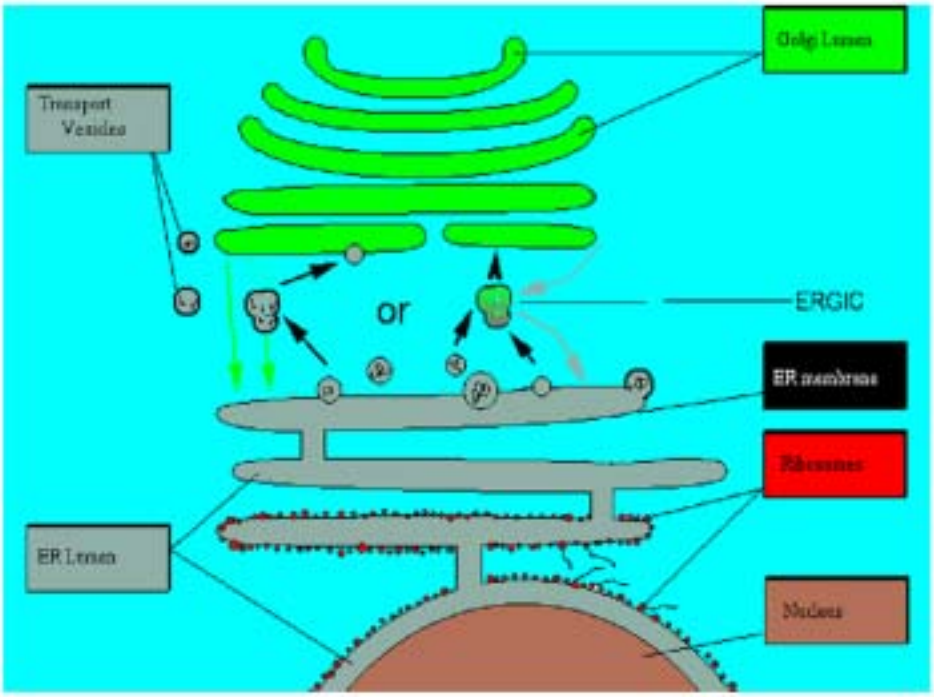

Figure 7: Stability and maturation models in the early secretory pathway.
The stable compartment model (left side): vesicles exiting the ER fuse with pre-existing ERGIC clusters. From the ERGIC, new vesicles targeted to the Golgi or to the ER are formed. The maturation model (right side): vesicles exiting the ER fuse together to form the ERGIC elements. ERGIC clusters fuse with each other to form the *cis*-Golgi cisterna, which will then mature to a medial and *trans*-Golgi cisternae. Balck arrows: anterograde movement, green and grey arrows: retrograde movement.

In the stable compartment model, the COPII machinery concentrates cargo that is exiting the ER in ERES. These sites generate COPII-coated vesicles that fuse with pre-existing ERGIC clusters. In the ERGIC, COPII is exchanged by COPI (Stephens et al., 2000) and cargo is further directed to the Golgi in COPI-coated vesicles leaving intact ERGIC clusters behind. From the ERGIC, COPI-coated vesicles loaded with ERGIC-to-ER targeted proteins detach and move in the retrograde direction also leaving intact ERGIC clusters behind. Both anterograde and retrograde carriers fuse with a pre-existing Golgi and with the ER, respectively (figure 7). The stable compartment model is based on biochemical, immunofluorescence and electron microscopy data. Biochemical data assessed ERGIC-53's localization in the early secretory pathway under different conditions (Klumperman et al., 1998) (Schweizer et al., 1988). Using sucrose gradients at 37°C or 15°C it was demonstrated that ERGIC-53 peaks in ER and ERGIC fractions (Klumperman et al., 1998). Immunofluorescence data showed that ERGIC-53 recycling back to the ER from ERGIC in cells rewarmed from 15°C to 37°C was via tubules that excluded anterograde cargo and were not directed to the Golgi apparatus (Klumperman et al., 1998). These results were further confirmed by immuno-electron microscopy

where ERGIC clusters were found to concentrate closer to the Golgi at 15°C and to move back when cells were rewarmed to 37°C. Thus, using these techniques and different block/recovery conditions, ERGIC-53 was never seen to concentrate in the Golgi, excluding the possibility of its recycling via this organelle and favoring the stable compartment model (Klumperman et al., 1998).

Immunofluorescence data revealed that ERGIC-53, ERGIC's marker protein, is partially co-localizing with COPII (Hammond and Glick, 2000) and COPI subunits as well as Golgi markers (Donaldson et al., 1990) (Lippincott-Schwartz et al., 1990). Using low temperatures (15°C) or different drugs (nocodazole and brefeldin A) showed that ERGIC-53 mislocalizes similarly to some Golgi proteins (Donaldson et al., 1990) and COPII coat (Hammond and Glick, 2000) and is positive for anterograde (Scales et al., 1997) (Presley et al., 1997) as well as recycling cargo (Tang et al., 1995). Electron microscopy data (Bannykh and Balch, 1997) (Horstmann et al., 2002) using two different techniques confirmed that ERGIC clusters are positive for cargo moving from the ER to the Golgi and that the cargo intermediates are first positive for COPII and then for COPI. Live imaging data using VSV-G-GFP (Presley et al., 1997) revealed that when blocked in the ERGIC at 15°C and followed during rewarming, cargo positive clusters move vectorially to the Golgi (Presley et al., 1997). Again these clusters are first positive for COPII components then COPI and movement is microtubule-dependent (Scales et al., 1997). Recent data using correlative video-light electron microscopy and tomography have described four types of saccular carriers mediating ER-to-Golgi transport two of them recruiting COPI complex (Mironov et al., 2003). Glick's laboratory has used a COPII component together with a Golgi marker in *Pichia pastoris* (Bevis et al., 2002) to show that in dividing cells the Golgi marker appears after ERES have emerged. All these data have concluded to a maturation process in the early secretory pathway where specialized COPII-coated domains in the ER trap cargo directly or indirectly through specific interactions with the COPII coat (Aridor et al., 1998). The buds transform into COPII-coated vesicles (Bannykh et al., 1996), without the involvement of COPI (Pelham, 1994). COPII-coated vesicles continue to mature to a COPI-containing ERGIC cluster, which becomes larger and eventually binds to microtubules and uses the dynein/dynactin complex to leave the ERES. The ERES remains after the ERGIC cluster has left and synthesis of a new ERGIC cluster commences (Murshid and Presley, 2004).

In this model it is also considered that *in vivo* COPII-coated regions of ER membrane could directly transform into ERGIC (Stephens and Pepperkok, 2001) and that COPI could play a direct role in this transformation (Lippincott-Schwartz et al., 1998). The ERGIC clusters fuse with one another and migrate anterogradely to form the *cis*-Golgi cisterna (figure 7). Nevertheless, ERGIC maturation to the Golgi was not really investigated. Data with fixed cells have the disadvantage to miss the dynamics, and results with living cells looked at anterograde cargo only and did not analyze an ERGIC marker.

2. Live imaging

Data from genetics, *in vitro* experiments, biochemistry and fixed cells are very valuable and allowed the comprehension of many mechanisms. But, they do not resolve all the issues. In fact, the use of genetics permits to compare a mutant phenotype to wild type; while *in vitro* data does not necessarily reflect what is going on inside cells, biochemical analyses require cell harvest and lysis, and analysis of fixed cells allows capturing single time events only. Thus, results using these different techniques cannot catch fast events nor assess small differences in time and space, which require live imaging.

2.1. Overview

Depending on the addressed question, investigating different mechanisms in living organisms necessitates the use of several procedures. In some organisms like *C. elegans* or *D. melanogaster* where mainly organogenesis is studied, it is rather easy to examine live dynamics using bright filed microscopy and contrast techniques. However in some other thicker organisms like the zebra fish, or when defined events as following the movement of single proteins have to be dealt with, stainings are required. Only few of these stainings could be applied to bright field microscopy. So, the use of fluorescence became a key to analyze virtually any kind of event. Reliable protein labeling requires expertise in protein chemistry, and successful microinjection of labeled products into cells with minimal damage. Moreover, it is difficult to target fluorescently labeled proteins directly to specific sites within a cell, because the distribution and

targeting of most proteins is regulated by their *in vivo* translation and post-translational modifications. By contrast, *de novo* synthesis is much more likely to result in native patterns of protein localization. As a result, proteins can be expressed within cells as fusions to fluorescent proteins or to small tags that can react with specialized fluorophores. Although more traditional methods such as protein microinjection are not without their advantages, the methods for fluorescently labeling proteins by genetic fusion are opening new windows for our understanding of cellular function. Different fluorescent microscopes could be used for time-lapse imaging as far as the cells remain alive for the whole experiment and that fluorescent light does not induce photo-toxicity thus inhibiting dynamics. A suitable and stable environment has to be provided, ensuring a constant temperature and a stably buffered culture medium.

2.2. Fluorophores

2.2.1. Fluorescent proteins

The discovery and development of fluorescent proteins from marine organisms are revolutionizing the study of cell behavior by providing convenient markers for gene expression and protein targeting in intact cells and organisms (van Roessel and Brand, 2002) (Zhang et al., 2002). The most widely used of these fluorescent proteins is the green fluorescent protein (GFP) from the jellyfish *Aequorea victoria* (Shimomura et al., 1962). As *Aequorea* GFP is spontaneously fluorescent through the autocatalytic synthesis of a chromophore, chimeric GFP fusions offer the great advantage that they can be expressed *in situ* by gene transfer into cells. The use of GFP as a minimally invasive tool for studying protein dynamics and function has been stimulated by the engineering of mutant GFPs with improved brightness, photo-stability and expression properties (Zhang et al., 2002) (Tsien, 1998) (Lippincott-Schwartz and Patterson, 2003). Cells that express proteins tagged with these GFPs can be imaged with low light intensities over many hours and so can provide useful information about changes in the steady-state distribution of a protein over time. A large number of GFP variants, which have different spectral properties: blue, cyan and yellowish-green emissions, are available (Chalfie et al., 1994). But none exhibits emission maxima longer than 529 nm

(Shimomura et al., 1962). The finding of novel 'GFP-like proteins' from *Anthozoa* (coral animals), have significantly expanded the range of colors available for cell biological applications. As a result, the family of 'GFP-like proteins' deposited in sequence databases now includes approximately 30 significantly different members (Matz et al., 1999) (Labas et al., 2002). Proteins that fluoresce at red or far-red wavelengths (red fluorescent proteins, RFPs or DsRed) are of specific interest, as eukaryotic cells and tissues display reduced auto-fluorescence at these longer wavelengths. Also, RFPs can be used in combination with other fluorescent proteins that fluoresce at shorter wavelengths for both multicolor labeling and fluorescence resonance energy transfer (FRET) experiments. Despite only a modest degree of sequence similarity, these GFP-like proteins probably share a η-can fold structure that is central to the fluorescence. They can be attached to virtually any protein of interest and still fold into a fluorescent molecule. These fusions can be confined to particular sites within the cell by appropriate targeting signals. They can be used to localize previously uncharacterized proteins (Gonzalez and Bejarano, 2000) or to visualize and track known proteins to further understand cellular events (Lippincott-Schwartz et al., 2000). After protein synthesis, many GFP variants mature quite slowly, involving a multi-step folding process that consists of cyclization, dehydration and oxidation. The red chromophore of DsRed also undergoes these maturation steps, but requires an additional autocatalytic modification of its GFP-like chromophore (Gross et al., 2000); incomplete maturation gives rise to residual green fluorescence, which might be a disadvantage for separation from green signals. Two recently developed varieties of DsRed, known as T1 (Bevis and Glick, 2002) and E57 (Terskikh et al., 2002), display improved maturation, making them preferable for use in multicolor experiments. Conversely, a long-lived green state can be advantageous if the intention is to analyze the history of the synthesis of a protein in a cell. A new mutant of DsRed, E5, is particularly useful for this because it changes its color from green to red over a predictable time course (Terskikh et al., 2000). This feature makes it possible to use the ratio of green-to-red emission as a measure of the time that has elapsed since the initiation of protein synthesis. Therefore, E5 functions as a fluorescent timer that yields both temporal and spatial information about target protein age.

2.2.2. Organic fluorophores

A disadvantage of the known fluorescent proteins is that they are relatively large (~27 kDa in monomeric form) tags for protein labeling. So far, the most promising results for smaller protein labels have come from the use of small organic fluorophores such as fluorescein and rhodamine (<1 kDa), which can be placed at specific sites in proteins using elaborate protein chemistry labeling techniques. An important benefit of using small organic fluorophores is that it minimizes possible steric hindrance problems that can interfere with protein function. If membrane permeabilization or microinjection is possible, then this approach also allows fine control of the quantity of introduced fluorescently labeled proteins. Recently, two innovative techniques have been developed for labeling specific recombinant proteins with small organic fluorophores within live cells (Griffin et al., 1998) (Keppler et al., 2003): the bi-arsenic fluorophore labeling of proteins that have been genetically altered to contain tetracysteine motifs, and the labeling of proteins fused to O6-alkylguanine-DNA alkyltransferase with enzymatic substrate derivatives. In the first technique, Tsien and colleagues made use of the well-known affinity of arsenoxides for closely spaced cysteine pairs (Griffin et al., 1998) (Griffin et al., 2000). Two arsenoxide groups were introduced into fluorescein to form FlAsH, which binds with high affinity to tetra-cysteines containing the rare sequence CCXXCC. Therefore, a host protein of interest can be genetically fused to a short peptide of 6–20 amino acids containing the CCXXCC motif, and this construct can then be produced inside cells. The FlAsH label is membrane-permeant and non-fluorescent, acquiring fluorescence only on binding to the CCXXCC motif. Importantly, this property of the compound significantly decreases the background signal generated by unbound fluorophores. Various derivatives of FlAsH can be designed by chemical modification of the original compound (Zhang et al., 2002). For example, a red analogue of FlAsH has been synthesized using the red fluorophore resorufin, and is termed ReAsH. The benefits of the FlAsH/ReAsH technique for studying protein aging over any time frame is highly versatile compared with the green-to-red shifting E5 protein that matures in a fixed time frame. Among the other potential applications of these fluorophores, new derivatives can be synthesized to incorporate other functionalities, such as photosensitizing groups, into recombinant proteins. A second technique uses

the enzymatic activity of human O6-alkylguanine-DNA alkyltransferase (hAGT). hAGT irreversibly transfers the substrate alkyl group (an O6-benzylguanine (BG) derivative) to one of its cysteine residues (Keppler et al., 2003). The mutant W160hAGT demonstrates increased activity against BG derivatives. Following the expression of a chimeric fusion of W160hAGT and a protein of interest, a membrane-permeable derivative of BG containing fluorescein, BGFL (O6-benzylguanine fluorescein), is added. Once inside the cells, BGFL is acted on by the W160hAGT containing protein, which leads to specific substrate labeling with fluorescein. Although this method seems to produce reliable labeling, there are two drawbacks. First, hAGT, at 207 amino acids in length, might be a too large fusion tag for many applications. Second, experiments on mammalian cells would need to be performed using AGT-deficient cell lines to avoid labeling of the endogenous AGT.

Other approaches have used the selective binding of a chemical ligand to its receptor protein to study pH regulation in different compartments along the secretory pathway (Farinas and Verkman, 1999) (Wu et al., 2001a). For example, synthesized membrane-permeable conjugates of a hapten and fluorescent pH probes were trapped by a single-chain antibody that had been expressed in the lumen of the organelles (Farinas and Verkman, 1999). In another approach, biotin conjugates of fluorescent pH probes were targeted to the secretory compartments by the localized expression of chicken avidin (Wu et al., 2001a), which binds biotin tightly. However, further development of these chemical probes that are genetically targetable will need the exchange of more information and ideas between chemists and biologists.

2.2.3. Quantum dots

In addition to small organic fluorophores, semiconductor nanocrystals (quantum dots) represent a promising new fluorescent label, owing to their photo-stability and wide range of excitation and emission wavelengths (Chan et al., 2002). Quantum dots are semiconductor nanocrystalline particles, typically measuring 2–10 nm in size (roughly the size of typical proteins). They provide several important advantages over organic fluorophores and fluorescent proteins, including narrow, symmetrical and tunable emission spectra that can be varied according to the size and material composition of

the particles. This property allows flexible and close spacing of different quantum dots without substantial spectral overlap. In addition, their absorption spectra are broad, which makes it possible to excite all quantum dot color variants simultaneously using a single excitation wavelength, thereby minimizing sample auto-fluorescence. Last, they have exceptional photo-stability. Despite their advantages over organic fluorophores and fluorescent proteins, the use of quantum dots has so far been limited by their lack of biocompatibility. Indeed, quantum dots are initially synthesized with hydrophobic organic ligands at their surface. For use in aqueous biological conditions, however, these organophilic species must be exchanged for ones that are more polar to prevent their aggregation and non-specific adsorption in biological samples. New advances in surface coating chemistry, have helped to overcome these problems to allow long-term, multi-color imaging of live cells (Wu et al., 2003) (Jaiswal et al., 2003) (Dubertret et al., 2002). Recent advances in nanomaterials have allowed quantum dots to be conjugated to bio-recognition molecules (Wu et al., 2003) (Jaiswal et al., 2003), such as streptavidin and antibodies; these conjugates have been used on both fixed cells and tissue sections. More recently, quantum dots encapsulated in phospholipid micelles were used (Dubertret et al., 2002).

2.3. Techniques

Live imaging is used in different areas ranging from space investigation to medical diagnosis. The methods employed are different but the aim is the same: monitor all the changes over time. In cell biology, widespread applications of fluorescent-based methods are revealing new aspects of protein dynamics and the biological processes that they regulate. They could be used for different purposes including the assessment of recycling and diffusion rates (FRAP), the study of the continuity or discontinuity of membranes (FLIP), the comparison of the dynamics of different fluorescent proteins (multi-color imaging), the analysis of molecular interactions (FRET) (Wouters et al., 2001), the tracking of single cell biochemical reactions (fluorescence correlation spectroscopy) (Elson and Magde, 1974), the analysis of cytoskeletal dynamics (FSM, fluorescence speckle microscopy) (Waterman-Storer and Danuser, 2002), etc. In this section some of these techniques will be discussed.

2.3.1. Photobleaching

Photobleaching, fluorescence depletion within a selected region, is the photo-induced alteration of a fluorophore that extinguishes its fluorescence. As photoactivation (see below), it is used to fluorescently highlight specific populations of molecules that could subsequently be followed as they re-equilibrate in the cell. The extent and rate at which this occurs can be quantified and used with computer-modeling approaches to describe the kinetic parameters of a protein. There are different photobleaching procedures: FRAP iFRAP, FLAP, FLIP and pattern photobleaching.

Fluorescence Recovery After Photobleaching (FRAP) was developed over two decades ago to study the diffusive properties of molecules in living cells (Axelrod et al., 1976) (Elson et al., 1976) (Jacobson et al., 1976) (Schlessinger et al., 1976) (Sheetz et al., 1980). It has experienced a resurgence following the introduction of GFP and the development of commercially available confocal-microscope-based photobleaching methods (Lippincott-Schwartz et al., 2001) (Klonis et al., 2002) (Reits and Neefjes, 2001). In this technique, a region of interest is selectively photobleached with a high-intensity laser and the recovery that occurs as molecules move into the bleached region is monitored over time with low intensity laser light. Two types of confocal microscopes could be used: a laser scanning or an acousto-optical tunable filter (AOTF), which allows rapid (microsecond to millisecond) attenuation of the laser as it scans a field. The resolution of the bleach can be improved by using two-photon excitation that is restricted to a smaller volume (Helmchen and Denk, 2002). Depending on the protein studied, fluorescence recovery can result from protein diffusion, binding/dissociation or transport processes. Studies of the diffusion properties of molecules have important implications for understanding how proteins are retained in different membrane-bound compartments, and what mechanisms coordinate the processing and transport functions of membranes.

Inverse FRAP (iFRAP) is performed as a normal FRAP experiment with the exception that the molecules outside a region of interest are photobleached and the loss of fluorescence from the non-photobleached region is monitored over time. As opposed to the rate of recovery studied using a FRAP experiment, iFRAP offers a way to monitor

the rate of movement out of a region. Because this method indirectly highlights a pool of molecules by decreasing the background fluorescence, it has been used to follow Golgi to plasma membrane transport carriers as they moved from the Golgi and fused with the plasma membrane (Hirschberg et al., 1998) (Nichols et al., 2001).

Fluorescence Localization After Photobleaching (FLAP) (Dunn et al., 2002) also indirectly highlights a pool of molecules. For a FLAP experiment, the same protein of interest is tagged with two different fluorophores that co-localize when expressed in cells. By photobleaching one of these fluorophores, a selected pool can be highlighted and followed over time (Lippincott-Schwartz et al., 2003).

The continuity of a cell compartment can be monitored using a technique called Fluorescence Loss In Photobleaching (FLIP). In a FLIP experiment, a fluorescent cell is repeatedly photobleached within a small region while the whole cell is repeatedly imaged. Any regions of the cell that are connected to the area being bleached will gradually lose fluorescence due to lateral movement of mobile proteins into this area. By contrast, the fluorescence in unconnected regions will not be affected. In addition to assessing continuity between areas of the cell, FLIP can be used to assess whether a protein moves uniformly across a particular cell compartment or undergoes interactions that impede its motion (Phair and Misteli, 2000) (Zaal et al., 1999) (Cole et al., 1996). Furthermore, it can be used to reveal faint fluorescence in unconnected compartments that normally cannot be seen against the bright fluorescence that arises in other parts of the cell (Nehls et al., 2000).

Cellular structures frequently have amorphous shapes, vary from cell to cell and undergo dynamic changes, all factors that make quantitative structural measurements extremely difficult or impossible. To circumvent this problem, spatially controlled photobleaching on a confocal microscope can also be used to introduce artificial landmarks in homogeneously fluorescent structures in an approach called pattern photobleaching. Again, this is possible when the fluorescent marker tightly binds to the structure of interest.

2.3.2. Photoactivation

Photoactivation is the photo-induced activation of an inert molecule to an active state by means of a brief pulse of high intensity irradiation. It is generally associated with the ultraviolet light-induced release of a caging group from a 'caged' compound (Politz, 1999). Studies for development and discovery of new fluorescent protein variants (Zhang et al., 2002) (Tsien, 1998) (Lippincott-Schwartz et al., 2003) yielded several molecules or techniques for optically highlighting proteins. But each had drawbacks for use in living cells, such as modest activation (Yokoe and Meyer, 1996) (Marchant et al., 2001) low stability (Lukyanov et al., 2000) or a requirement for low oxygen conditions (Elowitz et al., 1997) (Sawin and Nurse, 1997). Recently, three photoactivatable fluorescent proteins called photoactivatable GFP (PA-GFP) (Patterson and Lippincott-Schwartz, 2002), Kaede (Ando et al., 2002) and kindling fluorescent protein 1 (KFP1) (Chudakov et al., 2003), have been reported to offer improvements over the earlier versions. They undergo photochemical modification in or near the chromophore. The PA-GFP (Patterson and Lippincott-Schwartz, 2002) was developed with the aim of optimizing the photo-conversion properties of *Aequorea* wtGFP (Yokoe and Meyer, 1996), which produces only a ~threefold increase in fluorescence by 488 nm excitation. Mutation of threonine 203 to histidine in wtGFP to produce PA-GFP decreases the initial absorbance in the minor peak region (~475 nm) and leads to ~100-fold increase after photoactivation (Patterson and Lippincott-Schwartz, 2002). Alternatively, for the Kaede protein, isolated from *Trachyphyllia geoffroyi*, photoactivation results in a 2,000-fold increase in its red-to-green fluorescence ratio (Ando et al., 2002). KFP1 is an A148G mutant of asFP595 (where 'FP' is fluorescent protein) from the sea anemone, *Anemonia sulcata*. It gives a 30-fold increase in red fluorescence after photoactivation (Chudakov et al., 2003). All of these molecules share the common characteristic of displaying low levels of fluorescence before photoactivation and higher levels after photoactivation.

In a typical experiment, a cell or organism that is expressing the photoactivatable fluorescent protein is imaged at one wavelength prior to, and at various intervals after, photoactivation of a selected region with a different wavelength. However, the properties of each protein, including the wavelengths used for imaging and photoactivation, offer distinct advantages and disadvantages. For example, PA-GFP and Kaede both require ~400 nm light for photoactivation, whereas KFP1 uses green light (532 nm), which is probably better for use with living cells. Kaede uses both the red and green fluorescence

bands, which could make multicolor experiments problematic. On the other hand, the green fluorescence of Kaede is bright enough to visualize the localization of the non-photoactivated proteins easily, whereas visualizing PA-GFP and KFP1 is trickier due to their low fluorescence before photoactivation. The self-association properties of Kaede and KFP1 into tetrameric forms limit their usefulness as protein fusion tags because tetramerization might perturb parent protein localization and trafficking. The recent engineering of the DsRed protein into a monomeric form (Campbell et al., 2002) is encouraging for the possibility of the eventual disruption of Kaede and KFP1 into monomers. Variants that are derived from *A. victoria*, such as PA-GFP, self-associate to a lesser degree, and even those interactions can be disrupted by one of three further point mutations (Zacharias et al., 2002). The ability to 'switch on' the fluorescence of the photoactivatable proteins makes them excellent tools for exploring protein behavior in living cells. As the fluorescence of these proteins comes only after photoactivation, newly synthesized non-photoactivated pools are unobserved and do not complicate experimental results. This signal independence from new protein synthesis could allow the study of protein degradation of tagged molecules by 'optical pulse labeling' and monitoring of the fluorescence over time. Photoactivation of these proteins is generally rapid and gives stable fluorescence signals. Therefore, they can be used to examine various kinetic properties of tagged proteins, such as their diffusion coefficient D_{eff}, mobile fraction $M_{f,}$ compartmental residency time and exchange.

2.3.3. Four-dimensional imaging

In some cases, time-lapse microscopy of single optical sections (2D time-lapse recording) can yield the best results — for example, when the structure of interest is flat and when there are no marked deformations along the z axis during the experiment. But when highly dynamic and spatially complex structures, such as live cells and organisms, are imaged, a more complete representation and a full understanding of cellular dynamics are often difficult to obtain from a single z slice. New microscopes and image-processing softwares make it possible to rapidly record three-dimensional images over time (four-dimensional (4D) imaging) (Hiraoka et al., 1989) (Swedlow et al., 1993) (Thomas et al., 1996) (Rizzuto et al., 1998) (Swedlow and Platani, 2002) (Mohler, 1999).

4D experiments often run for hours or days to record a biological process. Therefore, automatic 4D recording with application protocols on 4D microscopes that can auto-focus, track cell movements and revisit multiple-stage locations to follow several cells in parallel can markedly increase throughput and reproducibility of 4D imaging. Two alternative microscopy techniques are routinely used for the acquisition of 4D images with optimized z resolution; z stepping (the movement from one optical section to the next) is achieved by either moving the specimen with a z-scanning stage, or by moving the microscope objective with a high-precision motor (piezo-stepper). First, wide-field fluorescence deconvolution microscopes homogeneously illuminate the whole specimen and grab the entire image simultaneously on a charge-coupled device (CCD) camera. Image stacks are then processed using iterative algorithms that assign out-of focus light back to the fluorescent object it came from in the correct focal plane. In this manner, deconvolution can yield high-resolution 3D information from wide-field images (Swedlow and Platani, 2002) (McNally et al., 1999). By contrast, confocal laser-scanning microscopes excite the fluorophore by moving a focused laser beam line-by-line over the specimen and record each image pixel sequentially on a point detector, the photomultiplier tube. A confocal aperture in front of the detector rejects out-of-focus light before it reaches the detector and confocal stacks therefore immediately yield 3D images with good axial resolution (Inoue, 1995). Deconvolution and confocal microscopes both have their specific advantages and disadvantages, which depend on the precise biological application (Gerlich and Ellenberg, 2003).

4D imaging allows precise quantitative analysis and enhances visual exploration of data by allowing cellular structures to be interactively displayed from many angles. It has become a key tool for understanding the complex organization of biological processes in live specimens. A realistic view of animated 3D-image sequences from interactively defined viewing directions can be achieved by using computer rendering and display in virtual reality viewers (Mohler, 1999) (Gerlich et al., 2001) (Thomas and White, 1998) (Marshall et al., 2001). Two alternative rendering methods are volume rendering and surface reconstruction (Gerlich et al., 2003). Although volume-rendering techniques achieve a satisfactory display of biological structures, these methods are limited to pure visualization and do not deliver any quantitative information. Generally, surface reconstruction achieves a more detailed display of small structures than volume

rendering. Importantly, only the object definition of reconstructed surfaces can be used to generate absolute quantitative data, such as the volume of a structure or the concentration of the fluorophore inside the structure. Such data allows changes in volume and/or concentration for specific cellular structures over time to be measured, which can be very useful to study organelle morphogenesis (Gerlich et al., 2001) (Savino et al., 2001). Alternatively, 4D data can be projected in the x–y plane, neglecting the z dimension (Manders et al., 1999) (Platani et al., 2002) (He et al., 2000). Although this allows a more intuitive access to the data by viewing it as a simple 2D movie, it sacrifices spatial information. Different algorithms are available for such projections: for example, maximum intensity projection produces images that have a particularly high contrast of small structures. However, it does not quantitatively represent fluorescence concentrations and cannot be used for further analysis. Instead, mean-intensity projection should be used for quantification, although it does not produce such crisp images.

2.4. Quantification

Biological results are often supplemented with mathematical validations. It is very challenging to fit biological findings to a mathematical calculation. And this gets more difficult as variables are added. When quantifying live imaging data, the additional variable is time. This gives at least a three variable equation: movement in the x, y directions over time. Mathematical analyses of such data are especially defying. Quantitative imaging requires that cells and sub-cellular structures are loaded with amounts of fluorescence labeled proteins that elicit only a minimal perturbation of normal cell processes, while maintaining a favorable signal-to noise ratio. In this context, the integrity of the labeled protein is crucial. It is also essential that the fluorophores fluoresce at a high efficiency and that the act of labeling does not disrupt the biochemical function or cellular localization of the host protein. There are different ways to do mathematical analyses of live imaging data. The least demanding is to calculate a statistical significance of certain dynamics compared to a control. Another way is to manually track movement and classify it within intervals. Although time consuming, such a quantification is feasible (Dahm et al., 2001). It is better estimated by automatic

particle tracking. But this technique does not evaluate surfaces and volumes, which can only be extracted from 4D data.

2.4.1. Image processing

As for any digital fluorescence microscope image, potential error sources that might impair visualization and bias quantification of images need to be considered. A first step in image analysis is the removal of any signal that does not originate from the specimen (‘noise’). Noise is generated by fluctuations in illumination (laser/arc-lamp intensity) and, to a lesser degree, by thermal fluctuations inside CCD cameras or photomultiplier tubes (‘dark/shot noise’). Any noise source leads to increased unspecific signal and makes the identification of specific fluorescent structures more difficult. Many noise-reducing image processing filters are now available that efficiently reduce shot noise, which typically occurs in random single pixels across the image (Gerlich et al., 2003). For example, anisotropy diffusion filters take into account local image characteristics and therefore selectively remove shot noise without degrading the image. In addition to noise, unspecific background signals — for example, from auto-fluorescence of the culture medium — impair image analysis. So, even after noise filtering, the background of the image at regions outside the fluorescent structure is generally not zero. To quantitatively relate pixel intensity to fluorophore concentration, the background signal has to be removed from the image. This can be achieved by subtracting the mean background intensity, determined in a region outside the fluorescent structure, from all pixels. Many different segmentation techniques are available for 2D images (Gerlich et al., 2003) that achieve better definition of biological objects than simple thresholding.

2.4.2. Kinetic modeling

Changes of protein concentration over time are important for many cell-biological processes, and recent work has measured such changes during transport (Hirschberg et al., 1998). To this end, the authors have used selective photobleaching on a confocal microscope to analyze aspects of protein dynamics such as diffusion, assembly/disassembly of protein complexes in cells, the exchange of cytosolic proteins

on and off organelles, and the lifetime and fate of membrane-bound transport intermediates (Hirschberg et al., 1998) (Phair and Misteli, 2000) (Wu et al., 2001b) (Presley et al., 2002) (figure 8). This type of analysis often requires measuring the fluorescence signal of GFP in a specific structure or area, to compare it with fluorescent intensities of other structures or areas. Once the quantities of fluorescent molecules in different sites or states are known, computer modeling can then be used to determine the parameter values (that is, the rate constants for binding interactions and exchange times) of the processes of interest (Phair and Misteli, 2001). In experiments in which the protein of interest moves freely, the fluorescence will recover to the initial prebleach value and the shape of the recovery curve (figure 8) can be described mathematically with a single component recovery (single) (Kao et al., 1993) (Verkman, 2002) (Siggia et al., 2000). Determining the effective D_{eff} and M_f of a protein from such data is based on previous analysis of FRAP kinetics (Axelrod et al., 1976). If the shape of the curve is complex (that is, it requires a multi-component diffusion equation (Gordon et al., 1995) (Periasamy and Verkman, 1998) (Marguet et al., 1999)), then multiple populations of the molecule with differing diffusion rates are present (complex, figure 8). This can occur when a molecule undergoes binding and release from intracellular components or exists as a monomer and multimeric forms (Phair and Misteli, 2001). Alternatively, the protein might not be diffusing but might be undergoing movement driven by molecular motors or membrane tension flow. A simple test for determining whether a fluorescent protein moves by diffusive movement or facilitated transport is to vary the size of the bleached area or beam radius, ϖ. The recovery will change with an ϖ^2 dependence for diffusive movement only (Wu et al., 1978) (figure 8). Accurate analysis of FRAP data requires that the bleach event is much shorter than the recovery time and preferably as short as possible. Moreover, the recovery event must be monitored until a recovery plateau is achieved, which is much greater than the half-time for recovery.

Recent applications in which kinetic modeling has been used include protein transport through membrane trafficking pathways (Hirschberg et al., 1998) (Zaal et al., 1999) (Nichols et al., 2001) and membrane coat protein dynamics (Presley et al., 2002). These data concluded that trafficking in the early secretory pathway fits to a second order model where VSV-G-GFP exits the ER very quickly and moves through the Golgi with virtually no inhibition (Hirschberg et al., 1998). The results were surprising since it is

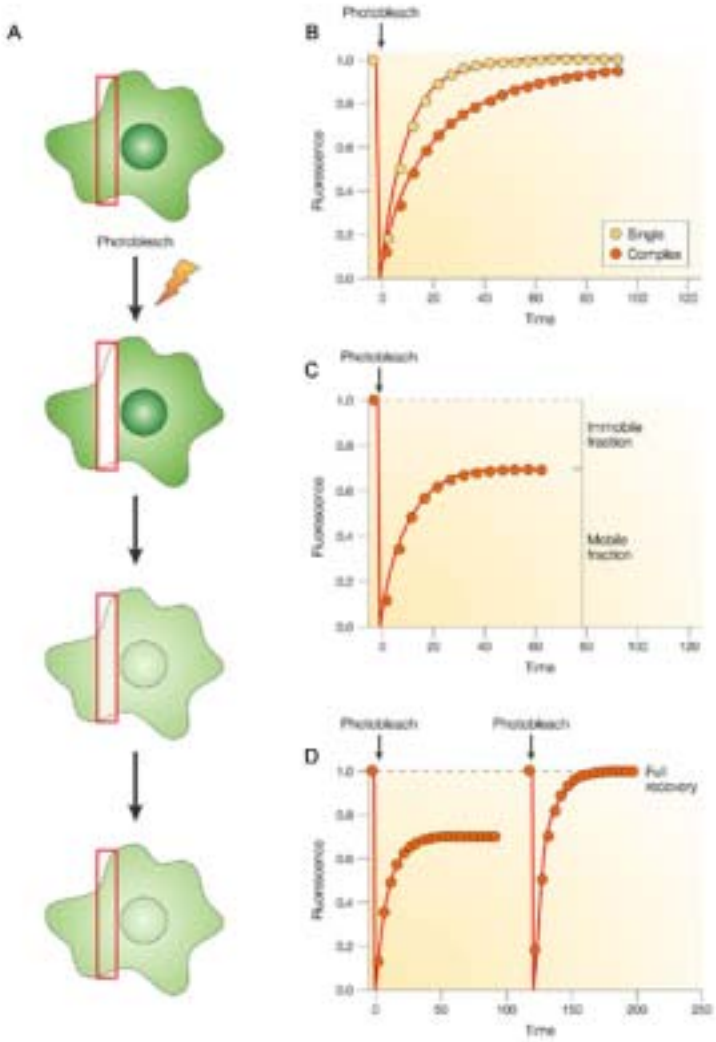

Figure 8: Fluorescence recovery after photobleaching (FRAP) and kinetic modelling. (A) A cell expressing fluorescent molecules is imaged with low light levels before and after photobleaching the strip outlined in red. Recovery of fluorescent molecules from the surrounding area into the photobleached region is monitored over time. Analysis usually includes compensation for the reduction in whole-cell fluorescence. (B) Fluorescence recovery into the photobleached region can be quantified in a FRAP curve. The plots depict the recovery for a single species (simulated by a single exponential curve shown in yellow circles) or the kinetics for two equal populations recovering at two different rates (simulated by a double exponential curve shown in orange circles). The kinetics for recovery of the latter takes longer to a plateau. (C) The level of fluorescence recovery in the photobleached region reveals the mobile and immobile fractions of the fluorophore in the cell. (D) A simple test for photo-induced immobile fractions is to perform a second FRAP experiment in the same region of interest. In the example here, the mobile fraction of the initial FRAP experiment is ~ 70%. The level of recovery can be determined by normalizing the fluorescent signal in the region and repeating the FRAP experiment. In the absence of photodamage, full recovery should be observed. Reproduced from Lippincott-Schwartz *et al.* 2003.

established biochemically that VSV-G is modified during its transit through the Golgi (Zilberstein et al., 1980). Such quantification is essentially based on general dynamics and not on single molecule movement; although this was attempted by using

correlations between fluorescence and protein molecules. In fact, the number of VSV-G-GFP molecules expressed in a single cell was estimated by comparing the total cellular pixel intensity value in digitized images to a standard curve generated with solutions of known concentrations of recombinant purified GFP (Hirschberg et al., 1998).

2.4.3. Concentrations and volumes

Approximation of the real concentration of fluorescently labeled molecules can only be derived from 3D analysis. For that, mean intensity projections can be useful to measure relative fluorophore concentrations and their dynamic changes over time (Gerlich et al., 2001). Measuring the volume of cellular compartments and the absolute concentration of molecules within these compartments over time in live cells would be ideally suited for analysis of many biological processes by kinetic modeling. Traditionally, the volume of cellular structures is often inferred from area measurements in single optical sections or in projections of image stacks. However, this does not take into account the shape or orientation of a given structure. Moreover, when movies are analyzed, flattening or expansion along the optical axis during the experiment can impair volume measurements. Volume measurements require boundary detection of cellular structures (Gerlich et al., 2003) (Monier et al., 2000). When combined with surface reconstruction, the volume of visualized cellular structures can be measured directly. Surface measurements of membrane-bound organelles are more problematic than volume or fluorescence concentration measurements because light microscopes generally do not resolve small membrane invaginations or protrusions. Therefore, surface measurements in light microscopy images, although possible using 4D reconstructed surface models will generally under-estimate the real surface size.

2.4.4. Single particle tracking

It is actually difficult to accurately determine kinetic parameters using multiple-molecule techniques (such as FRAP) because the reactions of individual molecules occur stochastically inside a cell. In addition, it is hard to spot local and temporal heterogeneities in the dynamic movement of molecules using multiple-molecule

techniques. Single molecule techniques can therefore be used to avoid such difficulties. Tracking can be done by manually identifying and tracing moving objects in data sets (Marshall et al., 1997), but it is often very time-consuming to gather and analyze enough data to obtain statistically significant results in this way. This is more optimally achieved by automated single particle tracking, which has the ultimate level of sensitivity. It allows the visualization of dynamic behavior (such as the assembly and disassembly of protein oligomers, (Sako et al., 2000) (Iino et al., 2001)) and reaction kinetics (such as receptor-ligand interactions, (Ueda et al., 2001)) of individual biological molecules inside living cells. It was first used as a powerful method to study purified bio-molecules *in vitro*, because the data obtained are not obscured by the averaging that is inherent in conventional biochemical experiments (Weiss, 2000) (Ishijima and Yanagida, 2001) (Xie, 2001). Recently, this advantage has been extended to studies using living cells (Hinterdorfer et al., 2001) (Sako and Uyemura, 2002), in which it has been possible to quantify the dynamic and kinetic parameters of single-molecule reactions *in vivo*. These measurements have the advantage to provide information about the fluctuations and distributions. They hence require statistical data so that the observed behavior of minor, unusual molecules is not overestimated. However, monitoring many single molecules for statistical analysis is a laborious task. This is because automatic image processing is difficult for single-molecule experiments in living cells due to a limited signal-to-noise ratio and a non-homogeneous background. In addition, as signals cannot be obtained from invisible molecules, the appropriate controls, which depend on the purpose of the experiment, should be used. An example is the interaction of a fluorescent protein with its endogenous partner. Since the endogenous protein does not fluoresce its kinetics cannot be measured although it has an effect on the fluorescent protein fluctuations and distributions. Controls in which the kinetics of the fluorescent protein at different expression levels are measured are a good way to estimate the effect of the interaction with the endogenous partner. Automated single-particle tracking of cellular structures involves three steps of image processing. First, objects have to be identified by using segmentation algorithms. Second, the corresponding objects are detected in successive frames by using a tracking algorithm, which produces trajectories that can be graphically visualized (Platani et al., 2002) (Tvarusko et al., 1999). Finally, the trajectories can be further analyzed to determine properties such as the mean and maximum velocities, the

accelerations, and the mean square displacement or diffusion coefficients (Platani et al., 2002) (Tvarusko et al., 1999) (Thomann et al., 2002). The tracking algorithm outcome could be a vector, which is an estimation of the optical flow between frames (Fisher et al., 1981) (Nomura et al., 1991) (Siegert et al., 1994). In this case the method is called vector field (Nomura et al., 1991). When the vector value is multiplied by the fluorescence intensity, the mass of moving proteins could be assessed. The advantage of computing vectors, is the possibility to additionally consider angles and directionalities of movement (Fisher et al., 1981). A difficulty in quantitative motion analysis of cellular structures is caused by global movements or deformations of the whole specimen during the acquisition period. Such global movements must be separated from the specific local movements of the structures of interest. This can be achieved by measuring only the relative movements of individual objects (Marshall et al., 1997). A more refined correction for global movements uses registration algorithms that can correct for translation, rotation and even global deformations (Fieres et al., 2001). When using the vector field method, different filters are applied to exclude noise vectors resulting from bleaching or unspecific fluorescence. For instance a speed range filter delimits an interval of moving entities. An intensity filter minimizes bleaching and edge effects. Masking certain parts of the cell where pixel values are saturated, and thus induce high noise, is also a good alternative.

Single-molecule visualization of fluorophores could be carried out using Total Internal Reflection Fluorescence Microscopy (TIR-FM) (Funatsu et al., 1995) or epi-fluorescence microscopy (Funatsu et al., 1995) (Sase et al., 1995). TIR-FM is a widely used technique for single molecule detection both *in vitro* and *in vivo* (Ishijima and Yanagida, 2001), (Sako and Uyemura, 2002). TIR-FM, which was originally developed to observe the interface between two media with different diffractive indices (Axelrod et al., 1984), uses an electromagnetic field called the ‘evanescent field’ to excite fluorophores. As the evanescent field diminishes exponentially with distance from the interface, the excitation depth in TIR-FM is limited to a very narrow range — typically one hundred to several hundreds of nanometers. However, using such a narrow excitation depth is the most effective way to overcome the background noise problem, which is often the greatest problem of single molecule imaging. Objective-type TIR-FM (Tokunaga et al., 1997), in which the excitation laser beam illuminates the specimen

through an objective lens, is particularly useful for imaging living cells. The top surface of the specimen is free in this type of TIR-FM, so it can be combined with high resolution differential interference contrast microscopy, which requires an oil immersion condenser, and allows the cells to be easily accessed for changes of the surrounding medium, microinjection or micromanipulation. To observe single molecules deep inside cells in three dimensions, conventional epi-fluorescence microscopy using a laser for excitation (Schutz et al., 2000) and real-time confocal microscopy (Tadakuma et al., 2001) are applicable. The latter is thought to produce better results than TIR-FM for single molecule imaging in dense solutions. Only sparsely labeled samples (<10 particles/μm2) can be visualized as single molecules using TIR-FM, epi-fluorescence microscopy or confocal fluorescence microscopy owing to the low spatial resolution.

2.5. Contribution to understanding the early secretory pathway

The battery of fluorescent proteins and imaging tools that allow monitoring protein dynamics in living cells provide numerous new insights into the behavior of proteins, organelles and cells. In so doing, they lead in a new era of cell biology in which kinetic microscopy methods are used to decipher pathways and mechanisms of biological processes. Live cell imaging has been extensively used to address different questions that further elucidated the early secretory pathway dynamics. It allowed the dissection of many processes and an improved understanding of the subtle mechanisms taking place. Several markers of the early secretory pathway have been tagged with GFP and/or one of its family members to understand compartmentalization and trafficking.

2.5.1. Compartmentalization

FRAP has unveiled important characteristics of the ER lumen, which is enriched in molecules that are involved in protein biogenesis, folding and assembly. Under normal conditions, both membrane-associated and luminal proteins can diffuse freely within the ER (Nehls et al., 2000) (Dayel et al., 1999). Indeed, the measured D_{eff} for many transmembrane proteins localized in the ER have values ranging from 0.2 to 0.5 μm^2 sec^{-1} with little or no immobile fractions (Cole et al., 1996) (Nehls et al., 2000). This

indicated that these proteins have unhindered lateral mobility in the membranes of this compartment. The many kinds of proteins freely mobile within the ER lumen and membranes include both cargo proteins that exit from the ER (Nehls et al., 2000) and resident proteins that are retained in the ER (Pelham, 1996). By contrast, large assemblies of membrane proteins in the ER (for example, CLIMP63, translocons, TAP transporters and nuclear pores) diffuse more slowly or have large immobile fractions (Klopfenstein et al., 1998) (Marguet et al., 1999) (Nikonov et al., 2002) (Barbour and Edidin, 1992). Under conditions of cell stress such as heat shock, change in osmolarity, calcium depletion, a glycosylation block or the production of unfolded proteins (Nehls et al., 2000) (Subramanian and Meyer, 1997) (Nikonov et al., 2002), there are marked changes in the mobility of proteins and luminal continuity. It was thus concluded that the ER lumen is not a stable environment, but undergoes significant global changes in response to cell stress, which could affect its numerous cellular roles. Work by Salmon and collaborators has directly visualized the extension of ER tubules towards but not into the actin cortex at the cell periphery (Waterman-Storer and Salmon, 1998) and thus supported data from previous work in fixed cells (Terasaki et al., 1984) (Patel et al., 1998) concluding that the ER in the cell periphery is in a dynamic equilibrium between fission and homotypic fusion.

Work from Lippincott-Schwartz and co-workers (Cole et al., 1996) and Nilsson and co-workers (Storrie et al., 1998) addressing the ERES fate, have shown that in cells in which microtubules are depolymerized (immobilizing material exiting the ER at the exit point), a fixed number of “exit sites” can be identified (usually about 150/cell) at which cargo proteins accumulate and form Golgi “ministacks” (Cole et al., 1996). Glick and co-workers and Balch and co-workers found GFP-labeled COPII on punctate structures throughout the cytoplasm (Aridor et al., 2001) (Hammond and Glick, 2000), which corresponded to these exit sites and provided evidence of tubular clusters repeatedly leaving the same sites. This provided strong additional support to the notion that the ER has stable specialized exit areas found both adjacent to the central Golgi apparatus (Jamieson and Palade, 1967) and throughout the cell (Cole et al., 1996).

Different laboratories using several live cell imaging techniques have addressed the question of whether the Golgi reconstitutes *de novo* from ER membranes. Nilsson and co-workers (Storrie et al., 1998) and Lippincott-Schwartz and co-workers (Ward et

al., 2001) expressed a dominant negative Sar1p mutant, which prevents the assembly of the COPII complex at ERES leading to a block in ER exit. They found that Golgi resident proteins accumulated in the ER rather than in ministacks (Storrie et al., 1998) (Ward et al., 2001). Moreover, Lippincott-Schwartz and co-workers found that at least one of the Golgi "scaffold" proteins (Shorter and Warren, 2002) (Seemann et al., 2000) as well as membrane-bound and peripherally associated Golgi-resident proteins can rapidly exchange between the Golgi and the cytosol in photobleach experiments. These proteins are rapidly distributed between the central Golgi and ministacks after microtubule disruption with nocodazole (Ward et al., 2001). Conversely, if the Golgi pool of protein was rendered invisible by photobleaching at the beginning of nocodazole treatment, ministack formation was not prevented (Zaal et al., 1999). All these experiments suggested a highly dynamic Golgi apparatus, the identity of which depends on continuous protein exchange with the cytoplasm and ongoing membrane input/output pathways.

2.5.2. Trafficking

Several techniques have revealed that trafficking between the ER and the Golgi is a highly dynamic process. Therefore, the use of live cell imaging was especially informative. Initial work from the Kreis and Lippincott-Schwartz laboratories produced two milestone papers in this field (Scales et al., 1997) (Presley et al., 1997). Both have used VSV-G-GFP to pinpoint anterograde ER-to-Golgi movement. Presley *et al.* have revealed that transport between the ER and the Golgi is via large pleiomorphic structures that move vectorially toward the Golgi area (Presley et al., 1997). Scales *et al.* have identified the same transport intermediates and found that when these intermediates were still nascent immobile spots, they were initially COPII coated and then appeared to exchange the COPII coat for COPI before moving along microtubules to the Golgi apparatus (Scales et al., 1997). These findings were further supported by direct visualization in living cells of COPII, COPI, and VSV-G (Stephens et al., 2000).

Recent data using correlative video–light electron microscopy, where controlled release of procollagen from the ER was followed, showed that ER to Golgi transport is probably more complex than what was described so far (Mironov et al., 2003). Double-

labeling experiments revealed that the large supramolecular cargo procollagen and the small freely diffusible cargo VSV-G concentrate into distinct domains of the same ERES and converge following exit (Mironov et al., 2003). Analysis of export containers, at various time points after the release of cargo from the ER uncovered four types of saccular structures. Type I carriers were characterized as distended ER domains close to ERES. Type II carriers were seen as long flattened saccules, emanating from, but still in continuity with, the ER. Rarely seen type III structures were thin radially oriented distensions devoid of ribosomes and translocating to the Golgi. Type III structures were only seen in tangential thick sections and serial reconstructions. Finally, type IV carriers were more complex structures often appearing as partially stacked arrangements of multiple saccular membranes (Mironov et al., 2003). Type I and type II carriers are either COPII positive or not, depending on the cargo (Palmer and Stephens, 2004). This work advocates that export is initiated by en bloc protrusion of a region of the ER directly adjacent to that coated with COPII.

Dissection of COPII, COPI and Arf1, the components of the membrane-trafficking machinery (Wu et al., 2001b) (Presley et al., 2002) (Stephens et al., 2000) (Bonifacino and Lippincott-Schwartz, 2003), has shown that they undergo continuous binding to and dissociation from membranes irrespective of vesicle budding. Other components such as SNAREs (Chao et al., 1999), motor proteins (Ma and Chisholm, 2002) and tethering factors (Marra et al., 2001), were also analyzed by live imaging techniques. But up to now, it is not completely understood what the meaning of these dynamics is. The COPI-dependent and -independent traffic routes were examined by live imaging, too (Sciaky et al., 1997), (Shima et al., 1999) (White et al., 1999) (Girod et al., 1999). Sciaky *et al.* (Sciaky et al., 1997) and White *et al.* (White et al., 1999) were able to directly image the trafficking of GFP constructs of KDEL-receptor, Rab6 and cholera toxin that utilize the Golgi-to-ER retrograde pathway, and reported tubular transport intermediates. Trafficking of KDEL receptor from the Golgi to the ER could be blocked by microinjection of antibodies against COPI, while trafficking of Rab6 and cholera toxin was not affected (White et al., 1999). Live cell imaging techniques were also used as a compelling approach to characterize the dynamics of VIP36, a protein the localization of which has been controversial for a long time (Fiedler and Simons, 1994) (Fullekrug et al., 1999). Using the manual tracking of movement and classification, Dahm *et al.* (Dahm et al.,

2001) have been able to unravel the localization and the recycling pathway that VIP36 follows. They found that VIP36 and VSV-G move together to the Golgi where they separate, with VIP36 moving retrogradely while VSV-G moving forward. They have thus concluded that VIP36 functions in the early secretory pathway. All the information collected using this powerful procedure gave a more precise overall view of the early secretory pathway, although many of the unraveled mechanisms are controversial and thus need to be further investigated.

3. Aim of the thesis

The early secretory pathway of mammalian cells is constituted of three organelles: the ER, the ER-Golgi-intermediate compartment (ERGIC), and the Golgi. These three compartments are not directly connected, but they continuously cooperate with each other to generate functional proteins at the correct time and place on the one hand, and to maintain their integrity on the other hand. Many molecular mechanisms underlying the functions of each organelle have been unraveled, as were the transport steps between and through these compartments and the machineries involved. Nevertheless, the morphological nature of the intermediates implicated in fulfilling the transport is still highly debated. Indeed, it is still not clearly established whether the transport intermediates are the organelles themselves or whether the compartments of the early secretory pathway are connected by transport carriers. Conclusions based on data generated by means of various techniques from several laboratories are inconsistent. A key question that has to be raised in order to investigate this issue is whether the ER-Golgi-intermediate compartment (ERGIC) is a stable station or just a collection of clusters moving forward and backward in the early secretory pathway.

In the current work, this question is scrutinized in order to shed more light on the highly debated controversy. For that, I tagged ERGIC-53, the bona fide marker of the ERGIC, with GFP and the resulting chimera is used to track ERGIC clusters under different conditions in living mammalian cells. To start, I characterized the ERGIC dynamics by single-color time-lapse microscopy. Once these dynamics accurately established, I compared them to the movement of an extensively used membrane-associated anterograde marker, VSV-G-GFP. The approach applied is an unbiased

automated single-particle tracking method. Direct analysis of the movement of GFP-ERGIC-53 and a luminal anterograde marker protein, ssDsRed, by means of dual-color live imaging followed by manual tracking, gave an additional clarification regarding sorting events in the ERGIC. The results of this work elucidate the nature of the ERGIC in the trafficking crossroads of the early secretory pathway in mammalian cells. With this data the stability of the ERGIC and its involvement in sorting of anterograde and retrograde moving proteins is highlighted. As a consequence, these data open future directions to investigate the mechanistical functions of the ERGIC in the early secretory pathway.

4. References

Allan, B. B., Moyer, B. D., and Balch, W. E. (2000). Rab1 recruitment of p115 into a cis-SNARE complex: programming budding COPII vesicles for fusion. Science *289*, 444-448.

Allan, V. (1996). Motor proteins: a dynamic duo. Curr Biol *6*, 630-633.

Andersson, H., Kappeler, F., and Hauri, H. P. (1999). Protein targeting to endoplasmic reticulum by dilysine signals involves direct retention in addition to retrieval. J Biol Chem *274*, 15080-15084.

Ando, R., Hama, H., Yamamoto-Hino, M., Mizuno, H., and Miyawaki, A. (2002). An optical marker based on the UV-induced green-to-red photoconversion of a fluorescent protein. Proc Natl Acad Sci U S A *99*, 12651-12656.

Antonny, B., and Schekman, R. (2001). ER export: public transportation by the COPII coach. Curr Opin Cell Biol *13*, 438-443.

Appenzeller, C., Andersson, H., Kappeler, F., and Hauri, H. P. (1999). The lectin ERGIC-53 is a cargo transport receptor for glycoproteins. Nat Cell Biol *1*, 330-334.

Appenzeller-Herzog, C., Roche, A. C., Nufer, O., and Hauri, H. P. (2004). pH-induced conversion of the transport lectin ERGIC-53 triggers glycoprotein release. J Biol Chem.

Aridor, M., Fish, K. N., Bannykh, S., Weissman, J., Roberts, T. H., Lippincott-Schwartz, J., and Balch, W. E. (2001). The Sar1 GTPase coordinates biosynthetic cargo selection with endoplasmic reticulum export site assembly. J Cell Biol *152*, 213-229.

Aridor, M., Weissman, J., Bannykh, S., Nuoffer, C., and Balch, W. E. (1998). Cargo selection by the COPII budding machinery during export from the ER. J Cell Biol *141*, 61-70.

Axelrod, D., Burghardt, T. P., and Thompson, N. L. (1984). Total internal reflection fluorescence. Annu Rev Biophys Bioeng *13*, 247-268.

Axelrod, D., Koppel, D. E., Schlessinger, J., Elson, E., and Webb, W. W. (1976). Mobility measurement by analysis of fluorescence photobleaching recovery kinetics. Biophys J *16*, 1055-1069.

Ayad, N., Hull, M., and Mellman, I. (1997). Mitotic phosphorylation of rab4 prevents binding to a specific receptor on endosome membranes. Embo J *16*, 4497-4507.

Balch, W. E., Dunphy, W. G., Braell, W. A., and Rothman, J. E. (1984). Reconstitution of the transport of protein between successive compartments of the Golgi measured by the coupled incorporation of N-acetylglucosamine. Cell *39*, 405-416.

Balch, W. E., McCaffery, J. M., Plutner, H., and Farquhar, M. G. (1994). Vesicular stomatitis virus glycoprotein is sorted and concentrated during export from the endoplasmic reticulum. Cell *76*, 841-852.

Bannykh, S. I., and Balch, W. E. (1997). Membrane dynamics at the endoplasmic reticulum-Golgi interface. J Cell Biol *138*, 1-4.

Bannykh, S. I., Rowe, T., and Balch, W. E. (1996). The organization of endoplasmic reticulum export complexes. J Cell Biol *135*, 19-35.

Barbour, S., and Edidin, M. (1992). Cell-specific constraints to the lateral diffusion of a membrane glycoprotein. J Cell Physiol *150*, 526-533.

Barlowe, C. (1997). Coupled ER to Golgi transport reconstituted with purified cytosolic proteins. J Cell Biol *139*, 1097-1108.

Barlowe, C. (2000). Traffic COPs of the early secretory pathway. Traffic *1*, 371-377.

Barlowe, C., Orci, L., Yeung, T., Hosobuchi, M., Hamamoto, S., Salama, N., Rexach, M. F., Ravazzola, M., Amherdt, M., and Schekman, R. (1994). COPII: a membrane coat formed by Sec proteins that drive vesicle budding from the endoplasmic reticulum. Cell *77*, 895-907.

Barroso, M., Nelson, D. S., and Sztul, E. (1995). Transcytosis-associated protein (TAP)/p115 is a general fusion factor required for binding of vesicles to acceptor membranes. Proc Natl Acad Sci U S A *92*, 527-531.

Beckers, C. J. M., Block, M. R., Glick, B. S., Rothman, J. E., and Balch, W. E. (1989). Vesicular transport between the endoplasmic reticulum and the Gilgi stack requires the NEM-sensitive fusion protein. Nature *339*, 397-400.

Bednarek, S. Y., Ravazzola, M., Hosobuchi, M., Amherdt, M., Perrelet, A., Schekman, R., and Orci, L. (1995). COPI- and COPII-coated vesicles bud directly from the endoplasmic reticulum in yeast. Cell *83*, 1183-1196.

Bennett, M. K., and Scheller, R. H. (1993). The molecular machinery for secretion is conserved from yeast to neurons. Proc Natl Acad Sci U S A *90*, 2559-2563.

Bevis, B. J., and Glick, B. S. (2002). Rapidly maturing variants of the Discosoma red fluorescent protein (DsRed). Nat Biotechnol *20*, 83-87.

Bevis, B. J., Hammond, A. T., Reinke, C. A., and Glick, B. S. (2002). De novo formation of transitional ER sites and Golgi structures in Pichia pastoris. Nat Cell Biol *4*, 750-756.

Beznoussenko, G. V., and Mironov, A. A. (2002). Models of intracellular transport and evolution of the Golgi complex. Anat Rec *268*, 226-238.

Bi, X., Corpina, R. A., and Goldberg, J. (2002). Structure of the Sec23/24-Sar1 pre-budding complex of the COPII vesicle coat. Nature *419*, 271-277.

Blobel, G., and Dobberstein, B. (1975a). Transfer of proteins across membranes. I. Presence of proteolytically processed and unprocessed nascent immunoglobulin light chains on membrane-bound ribosomes of murine myeloma. J Cell Biol *67*, 835-851.

Blobel, G., and Dobberstein, B. (1975b). Transfer to proteins across membranes. II. Reconstitution of functional rough microsomes from heterologous components. J Cell Biol *67*, 852-862.

Block, M. R., Glick, B. S., Wilcox, C. A., Wieland, F. T., and Rothman, J. E. (1988). Purification of an N-ethylmaleimide-sensitive protein catalyzing vesicular transport. Proc Natl Acad Sci USA *85*, 7852-7856.

Bock, J. B., Matern, H. T., Peden, A. A., and Scheller, R. H. (2001). A genomic perspective on membrane compartment organization. Nature *409*, 839-841.

Boehm, J., Letourneur, F., Ballensiefen, W., Ossipov, D., Demolliere, C., and Schmitt, H. D. (1997). Sec12p requires Rer1p for sorting to coatomer (COPI)-coated vesicles and retrieval to the ER. J Cell Sci *110 (Pt 8)*, 991-1003.

Bonifacino, J. S., and Glick, B. S. (2004). The mechanisms of vesicle budding and fusion. Cell *116*, 153-166.

Bonifacino, J. S., and Lippincott-Schwartz, J. (2003). Coat proteins: shaping membrane transport. Nat Rev Mol Cell Biol *4*, 409-414.

Bremser, M., Nickel, W., Schweikert, M., Ravazzola, M., Amherdt, M., Hughes, C. A., Sollner, T. H., Rothman, J. E., and Wieland, F. T. (1999). Coupling of coat assembly and vesicle budding to packaging of putative cargo receptors. Cell *96*, 495-506.

Briley, G. P., Hissong, M. A., Chiu, M. L., and Lee, D. C. (1997). The carboxyl-terminal valine residues of proTGF alpha are required for its efficient maturation and intracellular routing. Mol Biol Cell *8*, 1619-1631.

Burkhardt, J. K., Echeverri, C. J., Nilsson, T., and Vallee, R. B. (1997). Overexpression of the dynamitin (p50) subunit of the dynactin complex disrupts dynein-dependent maintenance of membrane organelle distribution. J Cell Biol *139*, 469-484.

Campbell, R. E., Tour, O., Palmer, A. E., Steinbach, P. A., Baird, G. S., Zacharias, D. A., and Tsien, R. Y. (2002). A monomeric red fluorescent protein. Proc Natl Acad Sci U S A *99*, 7877-7882.

Cao, X., Ballew, N., and Barlowe, C. (1998). Initial docking of ER-derived vesicles requires Uso1p and Ypt1p but is independent of SNARE proteins. Embo J *17*, 2156-2165.

Caro, L. G., and Palade, G. E. (1964). Protein Synthesis, Storage, and Discharge in the Pancreatic Exocrine Cell. An Autoradiographic Study. J Cell Biol *20*, 473-495.

Carroll, K. S., Hanna, J., Simon, I., Krise, J., Barbero, P., and Pfeffer, S. R. (2001). Role of Rab9 GTPase in facilitating receptor recruitment by TIP47. Science *292*, 1373-1376.

Chalfie, M., Tu, Y., Euskirchen, G., Ward, W. W., and Prasher, D. C. (1994). Green fluorescent protein as a marker for gene expression. Science *263*, 802-805.

Chan, W. C., Maxwell, D. J., Gao, X., Bailey, R. E., Han, M., and Nie, S. (2002). Luminescent quantum dots for multiplexed biological detection and imaging. Curr Opin Biotechnol *13*, 40-46.

Chao, D. S., Hay, J. C., Winnick, S., Prekeris, R., Klumperman, J., and Scheller, R. H. (1999). SNARE membrane trafficking dynamics in vivo. J Cell Biol *144*, 869-881.

Chapman, E. R. (2002). Synaptotagmin: a Ca(2+) sensor that triggers exocytosis? Nat Rev Mol Cell Biol *3*, 498-508.

Chardin, P., and McCormick, F. (1999). Brefeldin A: the advantage of being uncompetitive. Cell *97*, 153-155.

Chardin, P., Paris, S., Antonny, B., Robineau, S., Beraud-Dufour, S., Jackson, C. L., and Chabre, M. (1996). A human exchange factor for ARF contains Sec7- and pleckstrin-homology domains. Nature *384*, 481-484.

Chen, Y. A., and Scheller, R. H. (2001). SNARE-mediated membrane fusion. Nat Rev Mol Cell Biol *2*, 98-106.

Chudakov, D. M., Belousov, V. V., Zaraisky, A. G., Novoselov, V. V., Staroverov, D. B., Zorov, D. B., Lukyanov, S., and Lukyanov, K. A. (2003). Kindling fluorescent proteins for precise in vivo photolabeling. Nat Biotechnol *21*, 191-194.

Clary, D. O., Griff, I. C., and Rothman, J. E. (1990). SNAPs, a family of NSF attachment proteins involved in intracellular membrane fusion in animals and yeast. Cell *61*, 709-721.

Cole, N. B., Ellenberg, J., Song, J., DiEuliis, D., and Lippincott-Schwartz, J. (1998). Retrograde transport of Golgi-localized proteins to the ER. J Cell Biol *140*, 1-15.

Cole, N. B., Smith, C. L., Sciaky, N., Terasaki, M., Edidin, M., and Lippincott-Schwartz, J. (1996). Diffusional mobility of Golgi proteins in membranes of living cells. Science *273*, 797-801.

Cosson, P., Lefkir, Y., Demolliere, C., and Letourneur, F. (1998). New COP1-binding motifs involved in ER retrieval. Embo J *17*, 6863-6870.

Cosson, P., and Letourneur, F. (1994). Coatomer interaction with di-lysine endoplasmic reticulum retention motifs. Science *263*, 1929-1631.

Dahm, T., White, J., Grill, S., Fullekrug, J., and Stelzer, E. H. (2001). Quantitative ER <--> Golgi transport kinetics and protein separation upon Golgi exit revealed by vesicular integral membrane protein 36 dynamics in live cells. Mol Biol Cell *12*, 1481-1498.

Dayel, M. J., Hom, E. F., and Verkman, A. S. (1999). Diffusion of green fluorescent protein in the aqueous-phase lumen of endoplasmic reticulum. Biophys J *76*, 2843-2851.

De Matteis, M. A., and Morrow, J. S. (2000). Spectrin tethers and mesh in the biosynthetic pathway. J Cell Sci *113 (Pt 13)*, 2331-2343.

Deacon, S. W., Serpinskaya, A. S., Vaughan, P. S., Lopez Fanarraga, M., Vernos, I., Vaughan, K. T., and Gelfand, V. I. (2003). Dynactin is required for bidirectional organelle transport. J Cell Biol *160*, 297-301.

Diaz, R., Mayorga, L. S., Weidman, P. J., Rothman, J. E., and Stahl, P. (1989). Vesicle fusion following receptor-mediated endocytosis requires a protein active in Golgi transport. Nature *339*, 398-400.

Dietrich, L. E., Boeddinghaus, C., LaGrassa, T. J., and Ungermann, C. (2003). Control of eukaryotic membrane fusion by N-terminal domains of SNARE proteins. Biochim Biophys Acta *1641*, 111-119.

Dirac-Svejstrup, A. B., Sumizawa, T., and Pfeffer, S. R. (1997). Identification of a GDI displacement factor that releases endosomal Rab GTPases from Rab-GDI. Embo J *16*, 465-472.

Dominguez, M., Dejgaard, K., Fullekrug, J., Dahan, S., Fazel, A., Paccaud, J. P., Thomas, D. Y., Bergeron, J. J., and Nilsson, T. (1998). gp25L/emp24/p24 protein family members of the cis-Golgi network bind both COP I and II coatomer. J Cell Biol *140*, 751-765.

Donaldson, J. G., Cassel, D., Kahn, R. A., and Klausner, R. D. (1992a). ADP-ribosylation factor, a small GTP-binding protein, is required for binding of the coatomer protein beta-COP to Golgi membranes. Proc Natl Acad Sci U S A *89*, 6408-6412.

Donaldson, J. G., Finazzi, D., and Klausner, R. D. (1992b). Brefeldin A inhibits Golgi membrane-catalysed exchange of guanine nucleotide onto ARF protein. Nature *360*, 350-352.

Donaldson, J. G., Kahn, R. A., Lippincott-Schwartz, J., and Klausner, R. D. (1991). Binding of ARF and ß-COP to Golgi membranes: possible regulation by a trimeric G protein. Science *254*, 1197-1199.

Donaldson, J. G., Lippincott-Schwartz, J., Bloom, G. S., Kreis, T. E., and Klausner, R. D. (1990). Dissociation of a110 kD peripheral membrane protein from the Golgi apparatus is an early event in brefeldin A action. J Cell Biol *111*, 2295-2306.

Dubertret, B., Skourides, P., Norris, D. J., Noireaux, V., Brivanlou, A. H., and Libchaber, A. (2002). In vivo imaging of quantum dots encapsulated in phospholipid micelles. Science *298*, 1759-1762.

Dunn, G. A., Dobbie, I. M., Monypenny, J., Holt, M. R., and Zicha, D. (2002). Fluorescence localization after photobleaching (FLAP): a new method for studying protein dynamics in living cells. J Microsc *205*, 109-112.

Eakle, K. A., Bernstein, M., and Emr, S. D. (1988). Characterization of a component of the yeast secretion machinery: identification of the SEC18 gene product. Mol Cell Biol *8*, 4098-4109.

Elazar, Z., Scherz-Shouval, R., and Shorer, H. (2003). Involvement of LMA1 and GATE-16 family members in intracellular membrane dynamics. Biochim Biophys Acta *1641*, 145-156.

Ellgaard, L., and Helenius, A. (2003). Quality control in the endoplasmic reticulum. Nat Rev Mol Cell Biol *4*, 181-191.

Elowitz, M. B., Surette, M. G., Wolf, P. E., Stock, J., and Leibler, S. (1997). Photoactivation turns green fluorescent protein red. Curr Biol *7*, 809-812.

Elson, E. L., and Magde, D. (1974). Fluorescence correlation spectroscopy. I. Conceptual basis and theory. Biopolymers *13*, 1-27.

Elson, E. L., Schlessinger, J., Koppel, D. E., Axelrod, D., and Webb, W. W. (1976). Measurement of lateral transport on cell surfaces. Prog Clin Biol Res *9*, 137-147.

Eugster, A., Frigerio, G., Dale, M., and Duden, R. (2004). The {alpha}- and {beta}'-COP WD40 Domains Mediate Cargo-selective Interactions with Distinct Di-lysine Motifs. Mol Biol Cell *15*, 1011-1023.

Farinas, J., and Verkman, A. S. (1999). Receptor-mediated targeting of fluorescent probes in living cells. J Biol Chem *274*, 7603-7606.

Farquhar, M. G. (1985). Progress in unraveling pathways of Golgi traffic. Annu Rev Cell Biol *1*, 447-488.

Fasshauer, D., Bruns, D., Shen, B., Jahn, R., and Brunger, A. T. (1997). A structural change occurs upon binding of syntaxin to SNAP-25. J Biol Chem *272*, 4582-4590.

Fasshauer, D., Sutton, R. B., Brunger, A. T., and Jahn, R. (1998). Conserved structural features of the synaptic fusion complex: SNARE proteins reclassified as Q- and R-SNAREs. Proc Natl Acad Sci U S A *95*, 15781-15786.

Feiguin, F., Ferreira, A., Kosik, K. S., and Caceres, A. (1994). Kinesin-mediated organelle translocation revealed by specific cellular manipulations. J Cell Biol *127*, 1021-1039.

Ferro-Novick, S., and Jahn, R. (1994). Vesicle fusion from yeast to man. Nature *370*, 191-193.

Fiedler, K., and Simons, K. (1994). A putative novel class of animal lectins in the secretory pathway homologous to leguminous lectins. Cell *77*, 625-626.

Fiedler, K., and Simons, K. (1996). Characterization of VIP36, an animal lectin homologous to leguminous lectins. J Cell Sci *109*, 271-276.

Fiedler, K., Veit, M., Stamnes, M. A., and Rothman, J. E. (1996). Bimodal interaction of coatomer with the p24 family of putative cargo receptors. Science *273*, 1396-1399.

Fieres, j., Mattes, J., and Eils, R. (2001). Pattern recognition. In Lecture Notes in Computer Science, B. Radig, and S. Florczyk, eds. (Springer Verlag), pp. 76-83.

Fisher, P. R., Smith, E., and Williams, K. L. (1981). An extracellular chemical signal controlling phototactic behavior by D. discoideum slugs. Cell *23*, 799-807.

Fullekrug, J., Scheiffele, P., and Simons, K. (1999). VIP36 localisation to the early secretory pathway. J Cell Sci *112 (Pt 17)*, 2813-2821.

Funatsu, T., Harada, Y., Tokunaga, M., Saito, K., and Yanagida, T. (1995). Imaging of single fluorescent molecules and individual ATP turnovers by single myosin molecules in aqueous solution. Nature *374*, 555-559.

Gallwitz, D., and Jahn, R. (2003). The riddle of the Sec1/Munc-18 proteins - new twists added to their interactions with SNAREs. Trends Biochem Sci *28*, 113-116.

Gerlich, D., Beaudouin, J., Gebhard, M., Ellenberg, J., and Eils, R. (2001). Four-dimensional imaging and quantitative reconstruction to analyse complex spatiotemporal processes in live cells. Nat Cell Biol *3*, 852-855.

Gerlich, D., and Ellenberg, J. (2003). 4D imaging to assay complex dynamics in live specimens. Nat Cell Biol *Suppl*, S14-19.

Gerlich, D., Mattes, J., and Eils, R. (2003). Quantitative motion analysis and visualization of cellular structures. Methods *29*, 3-13.

Gerst, J. E. (1999). SNAREs and SNARE regulators in membrane fusion and exocytosis. Cell Mol Life Sci *55*, 707-734.

Gerst, J. E. (2003). SNARE regulators: matchmakers and matchbreakers. Biochim Biophys Acta *1641*, 99-110.

Gething, M.-J., K. McCammon, and J. Sambrook (1986a). Expression of wild-type and mutant forms of influenza hemagglutinin: the role of folding in intracellular transport. Cell *46*, 939 - 950.

Gething, M.-J., R.W. Doms, D. York and J. White (1986b). Studies on the mechanism of membrane fusion: Site specific mutagenesis of the hemagglutinin of Influenza virus. J Cell Biol *102*, 11.

Gill, S. R., Schroer, T. A., Szilak, I., Steuer, E. R., Sheetz, M. P., and Cleveland, D. W. (1991). Dynactin, a conserved, ubiquitously expressed component of an activator of vesicle motility mediated by cytoplasmic dynein. J Cell Biol *115*, 1639-1650.

Girod, A., Storrie, B., Simpson, J. C., Johannes, L., Goud, B., Roberts, L. M., Lord, J. M., Nilsson, T., and Pepperkok, R. (1999). Evidence for a COP-I-independent transport route from the Golgi complex to the endoplasmic reticulum. Nat Cell Biol *1*, 423-430.

Glick, B. S., and Malhotra, V. (1998). The curious status of the Golgi apparatus. Cell *95*, 883-889.

Glick, B. S., and Rothman, J. E. (1987). Possible role for fatty acyl-coenzyme A in intracellular protein transport. Nature *326*, 309-312.

Godi, A., Santone, I., Pertile, P., Devarajan, P., Stabach, P. R., Morrow, J. S., Di Tullio, G., Polishchuk, R., Petrucci, T. C., Luini, A., and De Matteis, M. A. (1998). ADP ribosylation factor regulates spectrin binding to the Golgi complex. Proc Natl Acad Sci U S A *95*, 8607-8612.

Gonzalez, C., and Bejarano, L. A. (2000). Protein traps: using intracellular localization for cloning. Trends Cell Biol *10*, 162-165.

Gordon, G. W., Chazotte, B., Wang, X. F., and Herman, B. (1995). Analysis of simulated and experimental fluorescence recovery after photobleaching. Data for two diffusing components. Biophys J *68*, 766-778.

Goud, B., A. Salminen, N.C. Walworth, & P. Novick (1988). A GTP-binding protein required for secretion rapidly associates with secretory vesicles and the plasma membrane yeast. Cell *53*, 753-768.

Griff, I. C., Schekman, R., Rothman, J. E., and Kaiser, C. A. (1992). The yeast SEC17 gene product is functionally equivalent to mammalian alpha-SNAP protein. J Biol Chem *267*, 12106-12115.

Griffin, B. A., Adams, S. R., Jones, J., and Tsien, R. Y. (2000). Fluorescent labeling of recombinant proteins in living cells with FlAsH. Methods Enzymol *327*, 565-578.

Griffin, B. A., Adams, S. R., and Tsien, R. Y. (1998). Specific covalent labeling of recombinant protein molecules inside live cells. Science *281*, 269-272.

Gross, L. A., Baird, G. S., Hoffman, R. C., Baldridge, K. K., and Tsien, R. Y. (2000). The structure of the chromophore within DsRed, a red fluorescent protein from coral. Proc Natl Acad Sci U S A *97*, 11990-11995.

Guo, Q., Penman, M., Trigatti, B. L., and Krieger, M. (1996). A single point mutation in epsilon-COP results in temperature-sensitive, lethal defects in membrane transport in a Chinese hamster ovary cell mutant. J Biol Chem *271*, 11191-11196.

Hammond, A. T., and Glick, B. S. (2000). Dynamics of transitional endoplasmic reticulum sites in vertebrate cells. Mol Biol Cell *11*, 3013-3030.

Hammond, C., and Helenius, A. (1994). Folding of VSV G protein: sequential interaction with BiP and calnexin. Science *266*, 456-458.

Hanson, P. I., Otto, H., Barton, N., and Jahn, R. (1995). The N-ethylmaleimide-sensitive fusion protein and alpha-SNAP induce a conformational change in syntaxin. J Biol Chem *270*, 16955-16961.

Hanson, P. I., Roth, R., Morisaki, H., Jahn, R., and Heuser, J. E. (1997). Structure and conformational changes in NSF and its membrane receptor complexes visualized by quick-freeze/deep-etch electron microscopy. Cell *90*, 523-535.

Harada, A., Takei, Y., Kanai, Y., Tanaka, Y., Nonaka, S., and Hirokawa, N. (1998). Golgi vesiculation and lysosome dispersion in cells lacking cytoplasmic dynein. J Cell Biol *141*, 51-59.

Hara-Kuge, S., Kuge, O., Orci, L., Amherdt, M., Ravazzola, M., Wieland, F. T., and Rothman, J. E. (1994). En bloc incorporation of coatomer subunits during the assembly of COP-coated vesicles. J Cell Biol *124*, 883-892.

Harter, C., and Wieland, F. (1996). The secretory pathway: mechanisms of protein sorting and transport. Biochim Biophys Acta *1286*, 75-93.

Hauri, H. P., Kappeler, F., Andersson, H., and Appenzeller, C. (2000). ERGIC-53 and traffic in the secretory pathway. J Cell Sci *113*, 587-596.

Hauri, H. P., and Schweizer, A. (1992). The endoplasmic reticulum-Golgi intermediate compartment. Curr Opin Cell Biol *4*, 600-608.

Hayashi, T., Yamasaki, S., Nauenburg, S., Binz, T., and Niemann, H. (1995). Disassembly of the reconstituted synaptic vesicle membrane fusion complex in vitro. Embo J *14*, 2317-2325.

He, X., Asthana, S., and Sorger, P. K. (2000). Transient sister chromatid separation and elastic deformation of chromosomes during mitosis in budding yeast. Cell *101*, 763-775.

Helmchen, F., and Denk, W. (2002). New developments in multiphoton microscopy. Curr Opin Neurobiol *12*, 593-601.

Helms, J. B., and Rothman, J. E. (1992). Inhibition by brefeldin A of a Golgi membrane enzyme that catalyzes exchange of guanine nucleotide bound to ARF. Nature *360*, 352-354.

Hinterdorfer, P., Schutz, G., Kienberger, F., and Schindler, H. (2001). Detection and characterization of single biomolecules at surfaces. J Biotechnol *82*, 25-35.

Hiraoka, Y., Minden, J. S., Swedlow, J. R., Sedat, J. W., and Agard, D. A. (1989). Focal points for chromosome condensation and decondensation revealed by three-dimensional in vivo time-lapse microscopy. Nature *342*, 293-296.

Hirschberg, K., Miller, C. M., Ellenberg, J., Presley, J. F., Siggia, E. D., Phair, R. D., and Lippincott-Schwartz, J. (1998). Kinetic analysis of secretory protein traffic and characterization of golgi to plasma membrane transport intermediates in living cells. J Cell Biol *143*, 1485-1503.

Hobbie, L., Fisher, A. S., Lee, S., Flint, A., and Krieger, M. (1994). Isolation of three classes of conditional lethal Chinese hamster ovary cell mutants with temperature-dependent defects in low density lipoprotein receptor stability and intracellular membrane transport. J Biol Chem *269*, 20958-20970.

Holleran, E. A., and Holzbaur, E. L. F. (1998). Speculating about spectrin: new insights into the Golgi-associated cytoskeleton. trends in cell biology *8*, 26-29.

Holleran, E. A., Ligon, L. A., Tokito, M., Stankewich, M. C., Morrow, J. S., and Holzbaur, E. L. (2001). beta III spectrin binds to the Arp1 subunit of dynactin. J Biol Chem *276*, 36598-36605.

Horstmann, H., Ng, C. P., Tang, B. L., and Hong, W. (2002). Ultrastructural characterization of endoplasmic reticulum - Golgi transport containers (EGTC). J Cell Sci *115*, 4263-4273.

Hu, C., Ahmed, M., Melia, T. J., Sollner, T. H., Mayer, T., and Rothman, J. E. (2003). Fusion of cells by flipped SNAREs. Science *300*, 1745-1749.

Huang, M., Weissman, J. T., Beraud-Dufour, S., Luan, P., Wang, C., Chen, W., Aridor, M., Wilson, I. A., and Balch, W. E. (2001). Crystal structure of Sar1-GDP at 1.7 A resolution and the role of the NH2 terminus in ER export. J Cell Biol *155*, 937-948.

Iino, R., Koyama, I., and Kusumi, A. (2001). Single molecule imaging of green fluorescent proteins in living cells: E-cadherin forms oligomers on the free cell surface. Biophys J *80*, 2667-2677.

Inoue, S. (1995). In Handbook in biological confocal microscopy, J. Pawley, ed. (New York, Plenum Press), pp. 1-14.

Iodice, L., Sarnataro, S., and Bonatti, S. (2001). The carboxyl-terminal valine is required for transport of glycoprotein CD8 alpha from the endoplasmic reticulum to the intermediate compartment. J Biol Chem *276*, 28920-28926.

Ishijima, A., and Yanagida, T. (2001). Single molecule nanobioscience. Trends Biochem Sci *26*, 438-444.

Itin, C., Roche, A. C., Monsigny, M., and Hauri, H.-P. (1996). ERGIC-53 is a functional mannose-selective and calcium-dependent human homologue of leguminous lectins. Mol Biol Cell *7*, 483-493.

Jacobson, K., Derzko, Z., Wu, E. S., Hou, Y., and Poste, G. (1976). Measurement of the lateral mobility of cell surface components in single, living cells by fluorescence recovery after photobleaching. J Supramol Struct *5*, 565(417)-576(428).

Jahn, R., Lang, T., and Sudhof, T. C. (2003). Membrane fusion. Cell *112*, 519-533.

Jaiswal, J. K., Mattoussi, H., Mauro, J. M., and Simon, S. M. (2003). Long-term multiple color imaging of live cells using quantum dot bioconjugates. Nat Biotechnol *21*, 47-51.

Jamieson, J. D., and Palade, G. E. (1967). Intracellular transport of secretory proteins in the pancreatic exocrine cell. I. Role of the peripheral elements of the Golgi complex. J Cell Biol *34*, 577–596.

Johannes, L., and Goud, B. (1998). Surfing on a retrograde wave: how does Shiga toxin reach the endoplasmic reticulum? Trends Cell Biol *8*, 158-162.

Johnson, A. E., and van Waes, M. A. (1999). The translocon: a dynamic gateway at the ER membrane. Annu Rev Cell Dev Biol *15*, 799-842.

Kahn, R. A., Kern, F. G., Clark, J., Gelman, E. P., and Rulka, C. (1991). Human ADP-ribosylation factors. J Biol Chem *266*, 2606-2614.

Kao, H. P., Abney, J. R., and Verkman, A. S. (1993). Determinants of the translational mobility of a small solute in cell cytoplasm. J Cell Biol *120*, 175-184.

Kappeler, F., Klopfenstein, D. R., Foguet, M., Paccaud, J. P., and Hauri, H. P. (1997). The recycling of ERGIC-53 in the early secretory pathway. ERGIC-53 carries a cytosolic endoplasmic reticulum-exit determinant interacting with COPII. J Biol Chem *272*, 31801-31808.

Keppler, A., Gendreizig, S., Gronemeyer, T., Pick, H., Vogel, H., and Johnsson, K. (2003). A general method for the covalent labeling of fusion proteins with small molecules in vivo. Nat Biotechnol *21*, 86-89.

Klausner, R. D., Donaldson, J. G., and Lippincott-Schwartz, J. (1992). Brefeldin A: Insights into the control of membrane traffic and organelle structure. J Cell Biol *116*, 1071-1080.

Klonis, N., Rug, M., Harper, I., Wickham, M., Cowman, A., and Tilley, L. (2002). Fluorescence photobleaching analysis for the study of cellular dynamics. Eur Biophys J *31*, 36-51.

Klopfenstein, D. R., Kappeler, F., and Hauri, H. P. (1998). A novel direct interaction of endoplasmic reticulum with microtubules. Embo J *17*, 6168-6177.

Klumperman, J., Schweizer, A., Clausen, H., Tang, B. L., Hong, W., Oorschot, V., and Hauri, H. P. (1998). The recycling pathway of protein ERGIC-53 and dynamics of the ER-Golgi intermediate compartment. J Cell Sci *111*, 3411-3425.

Kreis, T. E., and H. F. Lodish (1986). Oligomerization is essential for transport of vesicular stomatitis viral glycoprotein to the cell surface. Cell *46*, 929 - 937.

Labas, Y. A., Gurskaya, N. G., Yanushevich, Y. G., Fradkov, A. F., Lukyanov, K. A., Lukyanov, S. A., and Matz, M. V. (2002). Diversity and evolution of the green fluorescent protein family. Proc Natl Acad Sci U S A *99*, 4256-4261.

Lanoix, J., Ouwendijk, J., Lin, C. C., Stark, A., Love, H. D., Ostermann, J., and Nilsson, T. (1999). GTP hydrolysis by arf-1 mediates sorting and concentration of Golgi resident enzymes into functional COP I vesicles. Embo J *18*, 4935-4948.

Lederkremer, G. Z., Cheng, Y., Petre, B. M., Vogan, E., Springer, S., Schekman, R., Walz, T., and Kirchhausen, T. (2001). Structure of the Sec23p/24p and Sec13p/31p complexes of COPII. Proc Natl Acad Sci U S A *98*, 10704-10709.

Letourneur, F., and Cosson, P. (1998). Targeting to the endoplasmic reticulum in yeast cells by determinants present in transmembrane domains. J Biol Chem *273*, 33273-33278.

Letourneur, F., Gaynor, E. C., Hennecke, S., Demolliere, C., Duden, R., Emr, S. D., Riezman, H., and Cosson, P. (1994). Coatomer is essential for retrieval of dilysine-tagged proteins to the endoplasmic reticulum. Cell *79*, 1199-1207.

Lewis, M. J., and Pelham, H. R. (1992). Ligand-induced redistribution of a human KDEL receptor from the Golgi complex to the endoplasmic reticulum. Cell *68*, 353-364.

Lewis, M. J., and Pelham, H. R. (1996). SNARE-mediated retrograde traffic from the Golgi complex to the endoplasmic reticulum. Cell *85*, 205-215.

Lian, J. P., Stone, S., Jiang, Y., Lyons, P., and Ferro-Novick, S. (1994). Ypt1p implicated in v-SNARE activation. Nature *372*, 698-701.

Lin, R. C., and Scheller, R. H. (1997). Structural organization of the synaptic exocytosis core complex. Neuron *19*, 1087-1094.

Lin, R. C., and Scheller, R. H. (2000). Mechanisms of synaptic vesicle exocytosis. Annu Rev Cell Dev Biol *16*, 19-49.

Lippincott-Schwartz, J., Altan-Bonnet, N., and Patterson, G. H. (2003). Photobleaching and photoactivation: following protein dynamics in living cells. Nat Cell Biol *Suppl*, S7-14.

Lippincott-Schwartz, J., Cole, N., and Presley, J. (1998). Unravelling Golgi membrane traffic with green fluorescent protein chimeras. Trends Cell Biol *8*, 16-20.

Lippincott-Schwartz, J., Cole, N. B., Marotta, A., Conrad, P. A., and Bloom, G. S. (1995). Kinesin is the motor for microtubule-mediated Golgi-to-ER membrane traffic. J Cell Biol *128*, 293-306.

Lippincott-Schwartz, J., Donaldson, J. G., Schweitzer, A., Berger, E. G., Hauri, H.-P., Yuan, L. C., and Klausner, R. D. (1990). Microtubule-dependent retrograde transport of

proteins into the ER in the presence of brefeldin A suggests an ER recycling pathway. Cell *60*, 821-836.

Lippincott-Schwartz, J., and Patterson, G. H. (2003). Development and use of fluorescent protein markers in living cells. Science *300*, 87-91.

Lippincott-Schwartz, J., Roberts, T. H., and Hirschberg, K. (2000). Secretory protein trafficking and organelle dynamics in living cells. Annu Rev Cell Dev Biol *16*, 557-589.

Lippincott-Schwartz, J., Snapp, E., and Kenworthy, A. (2001). Studying protein dynamics in living cells. Nat Rev Mol Cell Biol *2*, 444-456.

Lippincott-Schwartz, J., Yuan, L. C., Bonifacino, J. S., and Klausner, R. D. (1989). Rapid redistribution of Golgi proteins into ER in cells treated with brefeldin A: evidence for membrane cycling from Golgi to ER. Cell *56*, 801-813.

Lowe, M., and Kreis, T. E. (1995). In vitro assembly and disassembly of coatomer. J Biol Chem *270*, 31364-31371.

Lukyanov, K. A., Fradkov, A. F., Gurskaya, N. G., Matz, M. V., Labas, Y. A., Savitsky, A. P., Markelov, M. L., Zaraisky, A. G., Zhao, X., Fang, Y.*, et al.* (2000). Natural animal coloration can Be determined by a nonfluorescent green fluorescent protein homolog. J Biol Chem *275*, 25879-25882.

Lupas, A. N., and Martin, J. (2002). AAA proteins. Curr Opin Struct Biol *12*, 746-753.

Lupashin, V. V., and Waters, M. G. (1997). t-SNARE activation through transient interaction with a rab-like guanosine triphosphatase. Science *276*, 1255-1258.

Ma, S., and Chisholm, R. L. (2002). Cytoplasmic dynein-associated structures move bidirectionally in vivo. J Cell Sci *115*, 1453-1460.

Malhotra, V., Orci, L., Glick, B. S., Block, M. R., and Rothman, J. E. (1988). Role of an N-ethylmaleimide sensitive transport component in promoting fusion of transport vesicles with cisternae of the Golgi stack. Cell *54*, 221-227.

Malsam, J., Gommel, D., Wieland, F. T., and Nickel, W. (1999). A role for ADP ribosylation factor in the control of cargo uptake during COPI-coated vesicle biogenesis. FEBS Lett *462*, 267-272.

Manders, E. M., Kimura, H., and Cook, P. R. (1999). Direct imaging of DNA in living cells reveals the dynamics of chromosome formation. J Cell Biol *144*, 813-821.

Marchant, J. S., Stutzmann, G. E., Leissring, M. A., LaFerla, F. M., and Parker, I. (2001). Multiphoton-evoked color change of DsRed as an optical highlighter for cellular and subcellular labeling. Nat Biotechnol *19*, 645-649.

Marguet, D., Spiliotis, E. T., Pentcheva, T., Lebowitz, M., Schneck, J., and Edidin, M. (1999). Lateral diffusion of GFP-tagged H2Ld molecules and of GFP-TAP1 reports on the assembly and retention of these molecules in the endoplasmic reticulum. Immunity *11*, 231-240.

Marra, P., Maffucci, T., Daniele, T., Tullio, G. D., Ikehara, Y., Chan, E. K., Luini, A., Beznoussenko, G., Mironov, A., and De Matteis, M. A. (2001). The GM130 and GRASP65 Golgi proteins cycle through and define a subdomain of the intermediate compartment. Nat Cell Biol *3*, 1101-1113.

Marshall, W. F., Marko, J. F., Agard, D. A., and Sedat, J. W. (2001). Chromosome elasticity and mitotic polar ejection force measured in living Drosophila embryos by four-dimensional microscopy-based motion analysis. Curr Biol *11*, 569-578.

Marshall, W. F., Straight, A., Marko, J. F., Swedlow, J., Dernburg, A., Belmont, A., Murray, A. W., Agard, D. A., and Sedat, J. W. (1997). Interphase chromosomes undergo constrained diffusional motion in living cells. Curr Biol *7*, 930-939.

Martinez-Menarguez, J. A., Geuze, H. J., Slot, J. W., and Klumperman, J. (1999). Vesicular tubular clusters between the ER and Golgi mediate concentration of soluble secretory proteins by exclusion from COPI-coated vesicles. Cell *98*, 81-90.

Matsuoka, K., Orci, L., Amherdt, M., Bednarek, S. Y., Hamamoto, S., Schekman, R., and Yeung, T. (1998). COPII-coated vesicle formation reconstituted with purified coat proteins and chemically defined liposomes. Cell *93*, 263-275.

Matz, M. V., Fradkov, A. F., Labas, Y. A., Savitsky, A. P., Zaraisky, A. G., Markelov, M. L., and Lukyanov, S. A. (1999). Fluorescent proteins from nonbioluminescent Anthozoa species. Nat Biotechnol *17*, 969-973.

May, A. P., Misura, K. M., Whiteheart, S. W., and Weis, W. I. (1999). Crystal structure of the amino-terminal domain of N-ethylmaleimide-sensitive fusion protein. Nat Cell Biol *1*, 175-182.

Mayer, A., Wickner, W., and Haas, A. (1996). Sec18p (NSF)-driven release of Sec17p (alpha-SNAP) can precede docking and fusion of yeast vacuoles. Cell *85*, 83-94.

McNally, J. G., Karpova, T., Cooper, J., and Conchello, J. A. (1999). Three-dimensional imaging by deconvolution microscopy. Methods *19*, 373-385.

McNew, J. A., Parlati, F., Fukuda, R., Johnston, R. J., Paz, K., Paumet, F., Sollner, T. H., and Rothman, J. E. (2000). Compartmental specificity of cellular membrane fusion encoded in SNARE proteins. Nature *407*, 153-159.

Mezzacasa, A., and Helenius, A. (2002). The transitional ER defines a boundary for quality control in the secretion of tsO45 VSV glycoprotein. Traffic *3*, 833-849.

Miller, E. A., Beilharz, T. H., Malkus, P. N., Lee, M. C., Hamamoto, S., Orci, L., and Schekman, R. (2003). Multiple cargo binding sites on the COPII subunit Sec24p ensure capture of diverse membrane proteins into transport vesicles. Cell *114*, 497-509.

Mironov, A. A., Mironov, A. A., Jr., Beznoussenko, G. V., Trucco, A., Lupetti, P., Smith, J. D., Geerts, W. J., Koster, A. J., Burger, K. N., Martone, M. E.*, et al.* (2003). ER-to-Golgi carriers arise through direct en bloc protrusion and multistage maturation of specialized ER exit domains. Dev Cell *5*, 583-594.

Misura, K. M., Bock, J. B., Gonzalez, L. C., Jr., Scheller, R. H., and Weis, W. I. (2002). Three-dimensional structure of the amino-terminal domain of syntaxin 6, a SNAP-25 C homolog. Proc Natl Acad Sci U S A *99*, 9184-9189.

Mohler, W. A. (1999). Visual reality: using computer reconstruction and animation to magnify the microscopist's perception. Mol Biol Cell *10*, 3061-3065.

Monier, K., Armas, J. C., Etteldorf, S., Ghazal, P., and Sullivan, K. F. (2000). Annexation of the interchromosomal space during viral infection. Nat Cell Biol *2*, 661-665.

Mossessova, E., Bickford, L. C., and Goldberg, J. (2003). SNARE selectivity of the COPII coat. Cell *114*, 483-495.

Moyer, B. D., Allan, B. B., and Balch, W. E. (2001). Rab1 interaction with a GM130 effector complex regulates COPII vesicle cis--Golgi tethering. Traffic *2*, 268-276.

Muller, J. M., Shorter, J., Newman, R., Deinhardt, K., Sagiv, Y., Elazar, Z., Warren, G., and Shima, D. T. (2002). Sequential SNARE disassembly and GATE-16-GOS-28 complex assembly mediated by distinct NSF activities drives Golgi membrane fusion. J Cell Biol *157*, 1161-1173.

Muniz, M., Nuoffer, C., Hauri, H. P., and Riezman, H. (2000). The Emp24 complex recruits a specific cargo molecule into endoplasmic reticulum-derived vesicles. J Cell Biol *148*, 925-930.

Murshid, A., and Presley, J. F. (2004). ER-to-Golgi transport and cytoskeletal interactions in animal cells. Cell Mol Life Sci *61*, 133-145.

Nakajima, H., Hirata, A., Ogawa, Y., Yonehara, T., Yoda, K., and Yamasaki, M. (1991). A cytoskeleton-related gene, uso1, is required for intracellular protein transport in Saccharomyces cerevisiae. J Cell Biol *113*, 245-260.

Nakano, A., and Muramatsu, M. (1989). A novel GTP-binding protein, Sar1p, is involved in transport from the endoplasmic reticulum to the Golgi apparatus. J Cell Biol *109*, 2677-2691.

Nehls, S., Snapp, E. L., Cole, N. B., Zaal, K. J., Kenworthy, A. K., Roberts, T. H., Ellenberg, J., Presley, J. F., Siggia, E., and Lippincott-Schwartz, J. (2000). Dynamics and retention of misfolded proteins in native ER membranes. Nat Cell Biol *2*, 288-295.

Nichols, B. J., Kenworthy, A. K., Polishchuk, R. S., Lodge, R., Roberts, T. H., Hirschberg, K., Phair, R. D., and Lippincott-Schwartz, J. (2001). Rapid cycling of lipid raft markers between the cell surface and Golgi complex. J Cell Biol *153*, 529-541.

Nichols, W. C., Seligsohn, U., Zivelin, A., Terry, V. H., Hertel, C. E., Wheatley, M. A., Moussalli, M. J., Hauri, H. P., Ciavarella, N., Kaufman, R. J., and Ginsburg, D. (1998). Mutations in the ER-Golgi intermediate compartment protein ERGIC-53 cause combined deficiency of coagulation factors V and VIII. Cell *93*, 61-70.

Nikonov, A. V., Snapp, E., Lippincott-Schwartz, J., and Kreibich, G. (2002). Active translocon complexes labeled with GFP-Dad1 diffuse slowly as large polysome arrays in the endoplasmic reticulum. J Cell Biol *158*, 497-506.

Nishimura, N., and Balch, W. E. (1997). A di-acidic signal required for selective export from the endoplasmic reticulum. Science *277*, 556-558.

Nomura, A., Miike, H., and Koga, K. (1991). Field theory approach for determining optical flow. Pattern Recognition Letters *12*, 183-190.

Novick, P., C. Field, and R. Schekman (1980). Cell Identification of 23 complementation groups required for post-translational events in the yeast secretory pathway. Cell *21*, 205 - 215.

Novick, P., and Schekman, R. (1979). Secretion and cell-surface growth are blocked in a temperature-sensitive mutant of Saccharomyces cerevisiae. Proc Natl Acad Sci U S A *76*, 1858-1862.

Novick, P., and Zerial, M. (1997). The diversity of Rab proteins in vesicle transport. Curr Opin Cell Biol *9*, 496-504.

Nufer, O., Guldbrandsen, S., Degen, M., Kappeler, F., Paccaud, J. P., Tani, K., and Hauri, H. P. (2002). Role of cytoplasmic C-terminal amino acids of membrane proteins in ER export. J Cell Sci *115*, 619-628.

Orci, L., Perrelet, A., and Rothman, J. E. (1998). Vesicles on strings: morphological evidence for processive transport within the Golgi stack. Proc Natl Acad Sci U S A *95*, 2279-2283.

Orci, L., Stamnes, M., Ravazzola, M., Amherdt, M., Perrelet, A., Sollner, T. H., and Rothman, J. E. (1997). Bidirectional transport by distinct populations of COPI-coated vesicles. Cell *90*, 335-349.

Palfrey, H. C., and Artalejo, C. R. (2003). Secretion: kiss and run caught on film. Curr Biol *13*, R397-399.

Palmer, D. J., Helms, J. B., Beckers, C. J., Orci, L., and Rothman, J. E. (1993). Binding of coatomer to Golgi membranes requires ADP-ribosylation factor. J Biol Chem *268*, 12083-12089.

Palmer, K. J., and Stephens, D. J. (2004). Biogenesis of ER-to-Golgi transport carriers: complex roles of COPII in ER export. Trends Cell Biol *14*, 57-61.

Palokangas, H., Ying, M., Vaananen, K., and Saraste, J. (1998). Retrograde transport from the pre-Golgi intermediate compartment and the Golgi complex is affected by the vacuolar H+-ATPase inhibitor bafilomycin A1. Mol Biol Cell *9*, 3561-3578.

Parlati, F., Varlamov, O., Paz, K., McNew, J. A., Hurtado, D., Sollner, T. H., and Rothman, J. E. (2002). Distinct SNARE complexes mediating membrane fusion in Golgi transport based on combinatorial specificity. Proc Natl Acad Sci U S A *99*, 5424-5429.

Paschal, B. M., and Vallee, R. B. (1987). Retrograde transport by the microtubule-associated protein MAP 1C. Nature *330*, 181-183.

Patel, S. K., Indig, F. E., Olivieri, N., Levine, N. D., and Latterich, M. (1998). Organelle membrane fusion: a novel function for the syntaxin homolog Ufe1p in ER membrane fusion. Cell *92*, 611-620.

Patterson, G. H., and Lippincott-Schwartz, J. (2002). A photoactivatable GFP for selective photolabeling of proteins and cells. Science *297*, 1873-1877.

Pelham, H. R. (1989). Control of protein exit from the endoplasmic reticulum. Annu Rev Cell Biol *5*, 1-23.

Pelham, H. R. (1994). About turn for the COPs? Cell *79*, 1125-1127.

Pelham, H. R. (1996). The dynamic organisation of the secretory pathway. Cell Struct Funct *21*, 413-419.

Peng, R., and Gallwitz, D. (2002). Sly1 protein bound to Golgi syntaxin Sed5p allows assembly and contributes to specificity of SNARE fusion complexes. J Cell Biol *157*, 645-655.

Pepperkok, R., Whitney, J. A., Gomez, M., and Kreis, T. E. (2000). COPI vesicles accumulating in the presence of a GTP restricted arf1 mutant are depleted of anterograde and retrograde cargo. J Cell Sci *113 (Pt 1)*, 135-144.

Periasamy, N., and Verkman, A. S. (1998). Analysis of fluorophore diffusion by continuous distributions of diffusion coefficients: application to photobleaching measurements of multicomponent and anomalous diffusion. Biophys J *75*, 557-567.

Petersen, O. H., Tepikin, A., and Park, M. K. (2001). The endoplasmic reticulum: one continuous or several separate Ca(2+) stores? Trends Neurosci *24*, 271-276.

Peyroche, A., Antonny, B., Robineau, S., Acker, J., Cherfils, J., and Jackson, C. L. (1999). Brefeldin A acts to stabilize an abortive ARF-GDP-Sec7 domain protein complex: involvement of specific residues of the Sec7 domain. Mol Cell *3*, 275-285.

Pfeffer, S. R. (1996). Transport vesicle docking: SNAREs and associates. Annu Rev Cell Dev Biol *12*, 441-461.

Pfeffer, S. R. (1999). Transport-vesicle targeting: tethers before SNAREs. Nat Cell Biol *1*, E17-22.

Pfeffer, S. R. (2001). Rab GTPases: specifying and deciphering organelle identity and function. Trends Cell Biol *11*, 487-491.

Pfeffer, S. R., Dirac-Svejstrup, A. B., and Soldati, T. (1995). Rab GDP dissociation inhibitor: putting rab GTPases in the right place. J Biol Chem *270*, 17057-17059.

Phair, R. D., and Misteli, T. (2000). High mobility of proteins in the mammalian cell nucleus. Nature *404*, 604-609.

Phair, R. D., and Misteli, T. (2001). Kinetic modelling approaches to in vivo imaging. Nat Rev Mol Cell Biol *2*, 898-907.

Platani, M., Goldberg, I., Lamond, A. I., and Swedlow, J. R. (2002). Cajal body dynamics and association with chromatin are ATP-dependent. Nat Cell Biol *4*, 502-508.

Politz, J. C. (1999). Use of caged fluorochromes to track macromolecular movement in living cells. Trends Cell Biol *9*, 284-287.

Porter, K. R., Claude, A., and Fullam, E. (1945). A study of tissue culture cells by electron microscopy. Methods and preliminary observations. J Exp Med *81*, 233–241.

Presley, J. F., Cole, N. B., Schroer, T. A., Hirschberg, K., Zaal, K. J., and Lippincott-Schwartz, J. (1997). ER-to-Golgi transport visualized in living cells. Nature *389*, 81-85.

Presley, J. F., Ward, T. H., Pfeifer, A. C., Siggia, E. D., Phair, R. D., and Lippincott-Schwartz, J. (2002). Dissection of COPI and Arf1 dynamics in vivo and role in Golgi membrane transport. Nature *417*, 187-193.

Puertollano, R., Randazzo, P. A., Presley, J. F., Hartnell, L. M., and Bonifacino, J. S. (2001). The GGAs promote ARF-dependent recruitment of clathrin to the TGN. Cell *105*, 93-102.

Rambourg, A., and Clermont, Y. (1990). Three-dimensional electron microscopy: structure of the Golgi apparatus. Eur J Cell Biol *51*, 189-200.

Rein, U., Andag, U., Duden, R., Schmitt, H. D., and Spang, A. (2002). ARF-GAP-mediated interaction between the ER-Golgi v-SNAREs and the COPI coat. J Cell Biol *157*, 395-404.

Reits, E. A., and Neefjes, J. J. (2001). From fixed to FRAP: measuring protein mobility and activity in living cells. Nat Cell Biol *3*, E145-147.

Rice, L. M., and Brunger, A. T. (1999). Crystal structure of the vesicular transport protein Sec17: implications for SNAP function in SNARE complex disassembly. Mol Cell *4*, 85-95.

Rizzuto, R., Carrington, W., and Tuft, R. A. (1998). Digital imaging microscopy of living cells. Trends Cell Biol *8*, 288-292.

Roghi, C., and Allan, V. J. (1999). Dynamic association of cytoplasmic dynein heavy chain 1a with the Golgi apparatus and intermediate compartment. J Cell Sci *112 (Pt 24)*, 4673-4685.

Roth, J. (2002). Protein N-glycosylation along the secretory pathway: relationship to organelle topography and function, protein quality control, and cell interactions. Chem Rev *102*, 285-303.

Rothman, J. E. (1994). Mechanisms of intracellular protein transport. Nature *372*, 55-63.

Rothman, J. E., and Wieland, F. T. (1996). Protein sorting by transport vesicles. Science *272*, 227-234.

Sacher, M., Jiang, Y., Barrowman, J., Scarpa, A., Burston, J., Zhang, L., Schieltz, D., Yates, J. R., 3rd, Abeliovich, H., and Ferro-Novick, S. (1998). TRAPP, a highly conserved novel complex on the cis-Golgi that mediates vesicle docking and fusion. Embo J *17*, 2494-2503.

Sagiv, Y., Legesse-Miller, A., Porat, A., and Elazar, Z. (2000). GATE-16, a membrane transport modulator, interacts with NSF and the Golgi v-SNARE GOS-28. Embo J *19*, 1494-1504.

Sako, Y., Minoghchi, S., and Yanagida, T. (2000). Single-molecule imaging of EGFR signalling on the surface of living cells. Nat Cell Biol *2*, 168-172.

Sako, Y., and Uyemura, T. (2002). Total internal reflection fluorescence microscopy for single-molecule imaging in living cells. Cell Struct Funct *27*, 357-365.

Sandvig, K., and van Deurs, B. (1996). Endocytosis, intracellular transport, and cytotoxic action of Shiga toxin and ricin. Physiol Rev *76*, 949-966.

Sapperstein, S. K., Lupashin, V. V., Schmitt, H. D., and Waters, M. G. (1996). Assembly of the ER to Golgi SNARE complex requires Uso1p. J Cell Biol *132*, 755-767.

Sapperstein, S. K., Walter, D. M., Grosvenor, A. R., Heuser, J. E., and Waters, M. G. (1995). p115 is a general vesicular transport factor related to the yeast endoplasmic reticulum to Golgi transport factor Uso1p. Proc Natl Acad Sci U S A *92*, 522-526.

Sase, I., Miyata, H., Corrie, J. E., Craik, J. S., and Kinosita, K., Jr. (1995). Real time imaging of single fluorophores on moving actin with an epifluorescence microscope. Biophys J *69*, 323-328.

Sato, K., Sato, M., and Nakano, A. (1997). Rer1p as common machinery for the endoplasmic reticulum localization of membrane proteins. Proc Natl Acad Sci U S A *94*, 9693-9698.

Savino, T. M., Gebrane-Younes, J., De Mey, J., Sibarita, J. B., and Hernandez-Verdun, D. (2001). Nucleolar assembly of the rRNA processing machinery in living cells. J Cell Biol *153*, 1097-1110.

Sawin, K. E., and Nurse, P. (1997). Photoactivation of green fluorescent protein. Curr Biol *7*, R606-607.

Scales, S. J., Gomez, M., and Kreis, T. E. (2000). Coat proteins regulating membrane traffic. Int Rev Cytol *195*, 67-144.

Scales, S. J., Pepperkok, R., and Kreis, T. E. (1997). Visualization of ER-to-Golgi transport in living cells reveals a sequential mode of action for COPII and COPI. Cell *90*, 1137-1148.

Scheel, J., Pepperkok, R., Lowe, M., Griffiths, G., and Kreis, T. E. (1997). Dissociation of coatomer from membranes is required for brefeldin A-induced transfer of Golgi enzymes to the endoplasmic reticulum. J Cell Biol *137*, 319-333.

Schimmoller, F., Simon, I., and Pfeffer, S. R. (1998). Rab GTPases, directors of vesicle docking. J Biol Chem *273*, 22161-22164.

Schlessinger, J., Koppel, D. E., Axelrod, D., Jacobson, K., Webb, W. W., and Elson, E. L. (1976). Lateral transport on cell membranes: mobility of concanavalin A receptors on myoblasts. Proc Natl Acad Sci U S A *73*, 2409-2413.

Schroer, T. A. (1996). structure and function of dynactin. Sem Cell Devel Biol *7*, 321-328.

Schutz, G. J., Kada, G., Pastushenko, V. P., and Schindler, H. (2000). Properties of lipid microdomains in a muscle cell membrane visualized by single molecule microscopy. Embo J *19*, 892-901.

Schweizer, A., Fransen, J. A. M., Baechi, T., Ginsel, L., and Hauri, H.-P. (1988). Identification, by a monoclonal antibody, of a 53-kD protein associated with a tubular-vesicular compartment at the *cis*-side of the Golgi apparatus. J Cell Biol *107*, 1643-1653.

Sciaky, N., Presley, J., Smith, C., Zaal, K. J., Cole, N., Moreira, J. E., Terasaki, M., Siggia, E., and Lippincott-Schwartz, J. (1997). Golgi tubule traffic and the effects of brefeldin A visualized in living cells. J Cell Biol *139*, 1137-1155.

Seemann, J., Jokitalo, E., Pypaert, M., and Warren, G. (2000). Matrix proteins can generate the higher order architecture of the Golgi apparatus. Nature *407*, 1022-1026.

Segev, N. (2001). Ypt/rab gtpases: regulators of protein trafficking. Sci STKE *2001*, RE11.

Serafini, T., Orci, L., Amherdt, M., Brunner, M., Kahn, R. A., and Rothman, J. E. (1991). ADP-ribosylation factor is a subunit of the coat of Golgi-derived COP- coated vesicles: a novel role for a GTP-binding protein. Cell *67*, 239-253.

Sheetz, M. P., Schindler, M., and Koppel, D. E. (1980). Lateral mobility of integral membrane proteins is increased in spherocytic erythrocytes. Nature *285*, 510-511.

Shima, D. T., Scales, S. J., Kreis, T. E., and Pepperkok, R. (1999). Segregation of COPI-rich and anterograde-cargo-rich domains in endoplasmic-reticulum-to-Golgi transport complexes. Curr Biol *9*, 821-824.

Shimomura, O., Johnson, F. H., and Saiga, Y. (1962). Extraction, purification and properties of aequorin, a bioluminescent protein from the luminous hydromedusan, Aequorea. J Cell Comp Physiol *59*, 223-239.

Shimoni, Y., Kurihara, T., Ravazzola, M., Amherdt, M., Orci, L., and Schekman, R. (2000). Lst1p and Sec24p cooperate in sorting of the plasma membrane ATPase into COPII vesicles in Saccharomyces cerevisiae. J Cell Biol *151*, 973-984.

Short, B., Preisinger, C., Schaletzky, J., Kopajtich, R., and Barr, F. A. (2002). The Rab6 GTPase regulates recruitment of the dynactin complex to Golgi membranes. Curr Biol *12*, 1792-1795.

Shorter, J., and Warren, G. (2002). Golgi architecture and inheritance. Annu Rev Cell Dev Biol *18*, 379-420.

Siegert, F., Weijer, C. J., Nomura, A., and Miike, H. (1994). A gradient method for the quantitative analysis of cell movement and tissue flow and its application to the analysis of multicellular Dictyostelium development. J Cell Sci *107 (Pt 1)*, 97-104.

Siggia, E. D., Lippincott-Schwartz, J., and Bekiranov, S. (2000). Diffusion in inhomogeneous media: theory and simulations applied to whole cell photobleach recovery. Biophys J *79*, 1761-1770.

Siniossoglou, S., Peak-Chew, S. Y., and Pelham, H. R. (2000). Ric1p and Rgp1p form a complex that catalyses nucleotide exchange on Ypt6p. Embo J *19*, 4885-4894.

Sogaard, M., Tani, K., Ye, R. R., Geromanos, S., Tempst, P., Kirchhausen, T., Rothman, J. E., and Sollner, T. (1994). A rab protein is required for the assembly of SNARE complexes in the docking of transport vesicles. Cell *78*, 937-948.

Soldati, T., Shapiro, A. D., Svejstrup, A. B., and Pfeffer, S. R. (1994). Membrane targeting of the small GTPase Rab9 is accompanied by nucleotide exchange. Nature *369*, 76-78.

Sollner, T., Whiteheart, S. W., Brunner, M., Erdjument-Bromage, H., Geromanos, S., Tempst, P., and Rothman, J. E. (1993). SNAP receptors implicated in vesicle targeting and fusion. Nature *362*, 318-324.

Sonnichsen, B., Fullekrug, J., Nguyen Van, P., Diekmann, W., Robinson, D. G., and Mieskes, G. (1994). Retention and retrieval: both mechanisms cooperate to maintain calreticulin in the endoplasmic reticulum. J Cell Sci *107 (Pt 10)*, 2705-2717.

Springer, S., and Schekman, R. (1998). Nucleation of COPII vesicular coat complex by endoplasmic reticulum to Golgi vesicle SNAREs. Science *281*, 698-700.

Stephens, D. J., Lin-Marq, N., Pagano, A., Pepperkok, R., and Paccaud, J. P. (2000). COPI-coated ER-to-Golgi transport complexes segregate from COPII in close proximity to ER exit sites. J Cell Sci *113*, 2177-2185.

Stephens, D. J., and Pepperkok, R. (2001). Illuminating the secretory pathway: when do we need vesicles? J Cell Sci *114*, 1053-1059.

Stephens, D. J., and Pepperkok, R. (2002). Imaging of procollagen transport reveals COPI-dependent cargo sorting during ER-to-Golgi transport in mammalian cells. J Cell Sci *115*, 1149-1160.

Storrie, B., and Nilsson, T. (2002). The Golgi apparatus: balancing new with old. Traffic *3*, 521-529.

Storrie, B., Pepperkok, R., and Nilsson, T. (2000). Breaking the COPI monopoly on Golgi recycling. Trends Cell Biol *10*, 385-391.

Storrie, B., White, J., Rottger, S., Stelzer, E. H., Suganuma, T., and Nilsson, T. (1998). Recycling of golgi-resident glycosyltransferases through the ER reveals a novel pathway and provides an explanation for nocodazole-induced Golgi scattering. J Cell Biol *143*, 1505-1521.

Subramanian, K., and Meyer, T. (1997). Calcium-induced restructuring of nuclear envelope and endoplasmic reticulum calcium stores. Cell *89*, 963-971.

Sudhof, T. C. (2002). Synaptotagmins: why so many? J Biol Chem *277*, 7629-7632.

Sutton, R. B., Fasshauer, D., Jahn, R., and Brunger, A. T. (1998). Crystal structure of a SNARE complex involved in synaptic exocytosis at 2.4 A resolution. Nature *395*, 347-353.

Swedlow, J. R., and Platani, M. (2002). Live cell imaging using wide-field microscopy and deconvolution. Cell Struct Funct *27*, 335-341.

Swedlow, J. R., Sedat, J. W., and Agard, D. A. (1993). Multiple chromosomal populations of topoisomerase II detected in vivo by time-lapse, three-dimensional wide-field microscopy. Cell *73*, 97-108.

Szule, J. A., and Coorssen, J. R. (2003). Revisiting the role of SNAREs in exocytosis and membrane fusion. Biochim Biophys Acta *1641*, 121-135.

Tadakuma, H., Yamaguchi, J., Ishihama, Y., and Funatsu, T. (2001). Imaging of single fluorescent molecules using video-rate confocal microscopy. Biochem Biophys Res Commun *287*, 323-327.

Tanaka, K., and Fukudome, H. (1991). Three-dimensional organization of the Golgi complex observed by scanning electron microscopy. J Electron Microsc Tech *17*, 15-23.

Tang, B. L., Low, S. H., Hauri, H. P., and Hong, W. (1995). Segregation of ERGIC53 and the mammalian KDEL receptor upon exit from the 15 degrees C compartment. Eur J Cell Biol *68*, 398-410.

Tanigawa, G., Orci, L., Amherdt, M., Ravazzola, M., Helms, J. B., and Rothman, J. E. (1993). Hydrolysis of bound GTP by ARF protein triggers uncoating of Golgi-derived COP-coated vesicles. J Cell Biol *123*, 1365-1371.

Terasaki, M., and Jaffe, L. A. (1991). Organization of the sea urchin egg endoplasmic reticulum and its reorganization at fertilization. J Cell Biol *114*, 929-940.

Terasaki, M., Song, J., Wong, J. R., Weiss, M. J., and Chen, L. B. (1984). Localization of endoplasmic reticulum in living and glutaraldehyde-fixed cells with fluorescent dyes. Cell *38*, 101-108.

Terskikh, A., Fradkov, A., Ermakova, G., Zaraisky, A., Tan, P., Kajava, A. V., Zhao, X., Lukyanov, S., Matz, M., Kim, S.*, et al.* (2000). "Fluorescent timer": protein that changes color with time. Science *290*, 1585-1588.

Terskikh, A. V., Fradkov, A. F., Zaraisky, A. G., Kajava, A. V., and Angres, B. (2002). Analysis of DsRed Mutants. Space around the fluorophore accelerates fluorescence development. J Biol Chem *277*, 7633-7636.

Thomann, D., Rines, D. R., Sorger, P. K., and Danuser, G. (2002). Automatic fluorescent tag detection in 3D with super-resolution: application to the analysis of chromosome movement. J Microsc *208*, 49-64.

Thomas, C., DeVries, P., Hardin, J., and White, J. (1996). Four-dimensional imaging: computer visualization of 3D movements in living specimens. Science *273*, 603-607.

Thomas, C. F., and White, J. G. (1998). Four-dimensional imaging: the exploration of space and time. Trends Biotechnol *16*, 175-182.

Thyberg, J., and Moskalewski, S. (1985). Microtubules and the organization of the Golgi complex. Exp Cell Res *159*, 1-16.

Tokunaga, M., Kitamura, K., Saito, K., Iwane, A. H., and Yanagida, T. (1997). Single molecule imaging of fluorophores and enzymatic reactions achieved by objective-type total internal reflection fluorescence microscopy. Biochem Biophys Res Commun *235*, 47-53.

Toonen, R. F., and Verhage, M. (2003). Vesicle trafficking: pleasure and pain from SM genes. Trends Cell Biol *13*, 177-186.

Tsien, R. Y. (1998). The green fluorescent protein. Annu Rev Biochem *67*, 509-544.

Turner, K. M., Burgoyne, R. D., and Morgan, A. (1999). Protein phosphorylation and the regulation of synaptic membrane traffic. Trends Neurosci *22*, 459-464.

Tvarusko, W., Bentele, M., Misteli, T., Rudolf, R., Kaether, C., Spector, D. L., Gerdes, H. H., and Eils, R. (1999). Time-resolved analysis and visualization of dynamic processes in living cells. Proc Natl Acad Sci U S A *96*, 7950-7955.

Ueda, M., Sako, Y., Tanaka, T., Devreotes, P., and Yanagida, T. (2001). Single-molecule analysis of chemotactic signaling in Dictyostelium cells. Science *294*, 864-867.

Ullrich, O., Horiuchi, H., Bucci, C., and Zerial, M. (1994). Membrane association of Rab5 mediated by GDP-dissociation inhibitor and accompanied by GDP/GTP exchange. Nature *368*, 157-160.

Urena, J. M., Merlos-Suarez, A., Baselga, J., and Arribas, J. (1999). The cytoplasmic carboxy-terminal amino acid determines the subcellular localization of proTGF-(alpha) and membrane type matrix metalloprotease (MT1-MMP). J Cell Sci *112 (Pt 6)*, 773-784.

Vaisberg, E. A., Grissom, P. M., and McIntosh, J. R. (1996). Mammalian cells express three distinct dynein heavy chains that are localized to different cytoplasmic organelles. J Cell Biol *133*, 831-842.

Vale, R. D. (2000). AAA proteins. Lords of the ring. J Cell Biol *150*, F13-19.

van Roessel, P., and Brand, A. H. (2002). Imaging into the future: visualizing gene expression and protein interactions with fluorescent proteins. Nat Cell Biol *4*, E15-20.

VanRheenen, S. M., Cao, X., Lupashin, V. V., Barlowe, C., and Waters, M. G. (1998). Sec35p, a novel peripheral membrane protein, is required for ER to Golgi vesicle docking. J Cell Biol *141*, 1107-1119.

Vasudevan, C., Han, W., Tan, Y., Nie, Y., Li, D., Shome, K., Watkins, S. C., Levitan, E. S., and Romero, G. (1998). The distribution and translocation of the G protein ADP-ribosylation factor 1 in live cells is determined by its GTPase activity. J Cell Sci *111 (Pt 9)*, 1277-1285.

Verkman, A. S. (2002). Solute and macromolecule diffusion in cellular aqueous compartments. Trends Biochem Sci *27*, 27-33.

Volchuk, A., Amherdt, M., Ravazzola, M., Brugger, B., Rivera, V. M., Clackson, T., Perrelet, A., Sollner, T. H., Rothman, J. E., and Orci, L. (2000). Megavesicles implicated in the rapid transport of intracisternal aggregates across the Golgi stack. Cell *102*, 335-348.

Vollenweider, F., Kappeler, F., Itin, C., and Hauri, H. P. (1998). Mistargeting of the lectin ERGIC-53 to the endoplasmic reticulum of HeLa cells impairs the secretion of a lysosomal enzyme. J Cell Biol *142*, 377-389.

Walch-Solimena, C., Jahn, R., and Sudhof, T. C. (1993). Synaptic vesicle proteins in exocytosis: what do we know? Curr Opin Neurobiol *3*, 329-336.

Wang, W., Sacher, M., and Ferro-Novick, S. (2000). TRAPP stimulates guanine nucleotide exchange on Ypt1p. J Cell Biol *151*, 289-296.

Ward, T. H., Polishchuk, R. S., Caplan, S., Hirschberg, K., and Lippincott-Schwartz, J. (2001). Maintenance of Golgi structure and function depends on the integrity of ER export. J Cell Biol *155*, 557-570.

Warren, G., and Malhotra, V. (1998). The organization of the Golgi complex. Current Opinion in Cell Biology *10*, 493-498.

Waterman-Storer, C. M., and Danuser, G. (2002). New directions for fluorescent speckle microscopy. Curr Biol *12*, R633-640.

Waterman-Storer, C. M., and Salmon, E. D. (1998). Endoplasmic reticulum membrane tubules are distributed by microtubules in living cells using three distinct mechanisms. Curr Biol *8*, 798-806.

Waters, M. G., Serafini, T., and Rothman, J. E. (1991). 'Coatomer': a cytosolic protein complex containing subunits of non-clathrin-coated Golgi transport vesicles. Nature *349*, 248-251.

Weber, T., Zemelman, B. V., McNew, J. A., Westermann, B., Gmachl, M., Parlati, F., Sollner, T. H., and Rothman, J. E. (1998). SNAREpins: minimal machinery for membrane fusion. Cell *92*, 759-772.

Weide, T., Bayer, M., Koster, M., Siebrasse, J. P., Peters, R., and Barnekow, A. (2001). The Golgi matrix protein GM130: a specific interacting partner of the small GTPase rab1b. EMBO Rep *2*, 336-341.

Weimbs, T., Mostov, K., Low, S. H., and Hofmann, K. (1998). A model for structural similarity between different SNARE complexes based on sequence relationships. Trends Cell Biol *8*, 260-262.

Weiss, S. (2000). Measuring conformational dynamics of biomolecules by single molecule fluorescence spectroscopy. Nat Struct Biol *7*, 724-729.

White, J., Johannes, L., Mallard, F., Girod, A., Grill, S., Reinsch, S., Keller, P., Tzschaschel, B., Echard, A., Goud, B., and Stelzer, E. H. (1999). Rab6 coordinates a novel Golgi to ER retrograde transport pathway in live cells. J Cell Biol *147*, 743-760.

Whiteheart, S. W., Schraw, T., and Matveeva, E. A. (2001). N-ethylmaleimide sensitive factor (NSF) structure and function. Int Rev Cytol *207*, 71-112.

Whyte, J. R., and Munro, S. (2002). Vesicle tethering complexes in membrane traffic. J Cell Sci *115*, 2627-2637.

Wickner, W., and Haas, A. (2000). Yeast homotypic vacuole fusion: a window on organelle trafficking mechanisms. Annu Rev Biochem *69*, 247-275.

Wilson, D. W., Wilcox, C. A., Flynn, G. C., Chen, E., Kuang, W.-J., Henzel, W. J., Block, M. R., Ullrich, A., and Rothman, J. E. (1989). A fusion protein required for vesicle-mediated transport in both mammalian cells and yeast. Nature *339*, 355-359.

Wouters, F. S., Verveer, P. J., and Bastiaens, P. I. (2001). Imaging biochemistry inside cells. Trends Cell Biol *11*, 203-211.

Wu, E. S., Jacobson, K., Szoka, F., and Portis, A., Jr. (1978). Lateral diffusion of a hydrophobic peptide, N-4-nitrobenz-2-oxa-1,3-diazole gramicidin S, in phospholipid multibilayers. Biochemistry *17*, 5543-5550.

Wu, M. M., Grabe, M., Adams, S., Tsien, R. Y., Moore, H. P., and Machen, T. E. (2001a). Mechanisms of pH regulation in the regulated secretory pathway. J Biol Chem *276*, 33027-33035.

Wu, X., Liu, H., Liu, J., Haley, K. N., Treadway, J. A., Larson, J. P., Ge, N., Peale, F., and Bruchez, M. P. (2003). Immunofluorescent labeling of cancer marker Her2 and other cellular targets with semiconductor quantum dots. Nat Biotechnol *21*, 41-46.

Wu, X., Zhao, X., Baylor, L., Kaushal, S., Eisenberg, E., and Greene, L. E. (2001b). Clathrin exchange during clathrin-mediated endocytosis. J Cell Biol *155*, 291-300.

Xie, s. (2001). Single-molecule approach to enzymology. Single Mol *2*, 229-236.

Xu, D., Joglekar, A. P., Williams, A. L., and Hay, J. C. (2000). Subunit structure of a mammalian ER/Golgi SNARE complex. J Biol Chem *275*, 39631-39639.

Yokoe, H., and Meyer, T. (1996). Spatial dynamics of GFP-tagged proteins investigated by local fluorescence enhancement. Nat Biotechnol *14*, 1252-1256.

Yoshihisa, T., Barlowe, C., and Schekman, R. (1993). Requirement for a GTPase-activating protein in vesicle budding from the endoplasmic reticulum. Science *259*, 1466-1468.

Yu, R. C., Jahn, R., and Brunger, A. T. (1999). NSF N-terminal domain crystal structure: models of NSF function. Mol Cell *4*, 97-107.

Zaal, K. J., Smith, C. L., Polishchuk, R. S., Altan, N., Cole, N. B., Ellenberg, J., Hirschberg, K., Presley, J. F., Roberts, T. H., Siggia, E.*, et al.* (1999). Golgi membranes are absorbed into and reemerge from the ER during mitosis. Cell *99*, 589-601.

Zacharias, D. A., Violin, J. D., Newton, A. C., and Tsien, R. Y. (2002). Partitioning of lipid-modified monomeric GFPs into membrane microdomains of live cells. Science *296*, 913-916.

Zerial, M., and McBride, H. (2001). Rab proteins as membrane organizers. Nat Rev Mol Cell Biol *2*, 107-117.

Zhang, J., Campbell, R. E., Ting, A. Y., and Tsien, R. Y. (2002). Creating new fluorescent probes for cell biology. Nat Rev Mol Cell Biol *3*, 906-918.

Zilberstein, A., Snider, M. D., Porter, M., and Lodish, H. F. (1980). Mutants of vesicular stomatitis virus blocked at different stages in maturation of the viral glycoprotein. Cell *21*, 417-427.

ER-Golgi intermediate compartment clusters define a stationary sorting compartment

[1]Houchaima Ben-Tekaya, [2]Kota Miura, [2]Rainer Pepperkok and [1]*Hans-Peter Hauri

[1] Department of Pharmacology and Neurobiology, Biozentrum, University of Basel, Klingelbergstrasse 70, CH-4056 Basel, Switzerland

[2] Department of Cell Biology and Biophysics, European Molecular Biology Laboratory Heidelberg, D-69117 Heidelberg, Germany.

Running title: ERGIC clusters define a stationary sorting compartment

*To whom correspondence should be addressed.
Phone: +41 61 267 22 22
Fax: +41 61 267 22 08
e-mail: Hans-Peter.Hauri@unibas.ch

Total characters count (including spaces): 53’793

Summary

The endoplasmic reticulum - Golgi intermediate compartment (ERGIC) defined by the cycling lectin ERGIC-53 consists of tubulovesicular clusters, but it is unknown if these membranes are transport vehicles or stable entities. Here, we show by live imaging that GFP-ERGIC-53 mainly localizes to long-lived stationary and some short-lived highly mobile elements. Unlike the anterograde marker VSV-G-GFP, GFP-ERGIC-53 does not vectorially move to the Golgi upon exit from the ERGIC, as assessed by a novel quantitative vector field method. Dual color imaging of GFP-ERGIC-53 and a secretory protein (signal-sequence-tagged DsRed) reveals that the stationary elements are sites of repeated sorting of retrograde and anterograde cargo, and are interconnected by highly mobile elements. Based on these results, we conclude that the ERGIC is a membrane compartment in the true sense and not simply a collection of mobile carriers mediating protein traffic from endoplasmic reticulum to Golgi.

Introduction

Newly synthesized secretory proteins, also termed cargo, leave the endoplasmic reticulum (ER) in COPII-coated vesicles at the part rough-part smooth transitional elements of the ER (Palade, 1975; Bannykh et al., 1996; Schekman and Orci, 1996). These ER exit sites (ERES) are localized both in the proximity of the Golgi apparatus and more peripherally in the cell. Two major hypotheses explain how cargo is transported from ER to Golgi in higher eukaryotic cells (Farquhar, 1985; Pelham, 1989; Bannykh and Balch, 1997; Glick and Malhotra, 1998; Lippincott-Schwartz et al., 2000; Stephens and Pepperkok, 2001; Beznoussenko and Mironov, 2002; Storrie and Nilsson, 2002). According to the stable compartment model, cargo is packaged into COP II vesicles that fuse with pre-existing tubulovesicular membrane clusters of the ER-Golgi intermediate compartment (ERGIC). Transport vesicles subsequently bud from the ERGIC and fuse with the cis-Golgi. According to the now prevailing maturation model, COP II vesicles fuse with one another to form the ERGIC. The ERGIC clusters then

move as mobile transport complexes to the Golgi and form a new cis-cisterna by homotypic fusion.

The ERGIC (Hauri et al., 2000) consists of a constant average number of tubulovesicular clusters that stain positive for the type I membrane lectin ERGIC-53 and the COPI subunit ß-COP (Schweizer et al., 1988; Bannykh et al., 1996; Klumperman et al., 1998). It is equivalent to the site at which ER-Golgi transport of the anterograde marker membrane protein VSV-G and some other secretory proteins is blocked at 15°C (Schweizer et al., 1990; Lotti et al., 1992; Blum et al., 2000). Morphological and biochemical data indicate that ERGIC-53 recycles from ERGIC to ER (Lippincott-Schwartz et al., 1990; Aridor et al., 1995; Tang et al., 1995; Kappeler et al., 1997) by a route that appears to largely bypass the Golgi apparatus (Klumperman et al., 1998).

The view that ERGIC clusters are transport vehicles rather than stable entities is largely based on studies where transport of VSV-G-GFP through the secretory pathway was visualized in living cells (Presley et al., 1997; Scales et al., 1997; Lippincott-Schwartz et al., 2000). Upon ER exit, VSV-G-GFP becomes concentrated into bright fluorescent dots, localized adjacent to ERES that rapidly move to the Golgi area in a microtubule dependent manner. Nevertheless, nothing in this data set precludes the possibility that the VSV-G-containing transport complexes, despite their considerable size and complexity, originate from a stable ERGIC compartment by a dissociative process. By recording anterograde cargo only, a stable ERGIC may not become apparent. What is needed, therefore, is the visualization of anterograde and retrograde traffic from the ERGIC. If the ERGIC is just a maturing transport complex, anterograde and retrograde sorting would be expected to consume the ERGIC clusters. In the opposite case the sorting event would leave behind an ERGIC structure that persists, at least for a certain time period, and is capable of multiple rounds of sorting.

To test the two hypotheses we have visualized and quantified in living cells the trafficking of the recycling marker ERGIC-53 tagged with green fluorescent protein (GFP-ERGIC-53) and compared it with that of the well established anterograde reporter protein VSV-G-GFP and of a soluble secretory version of DsRed. We find GFP-ERGIC-53 in two distinct structures, long-lived and short-lived. The long-lived structures, corresponding to the previously described tubulovesicular clusters, are localized close to ERES, move little, and can undergo multiple rounds of anterograde and retrograde

sorting as well as cleavage and fusion. The short-lived structures are highly dynamic, move in all directions without preference for the Golgi area and are proposed to connect the stationary elements. These observations support the notion of a stable ERGIC that is highly active in anterograde/retrograde sorting and can horizontally exchange material.

Results

Features of GFP-ERGIC-53 and endogenous ERGIC-53 are indistinguishable

To visualize the ERGIC and retrograde traffic from the ERGIC in living cells we tagged ERGIC-53 with green fluorescent protein (GFP-ERGIC-53) and stably expressed it in HeLa cells. GFP was attached to the N-terminus of ERGIC-53 in order not to interfere with its trafficking that is controlled by multiple position-dependent, C-terminal transport determinants (Kappeler et al., 1997; Nufer et al., 2002; Nufer et al., 2003). In some of the obtained clones GFP-ERGIC-53 was inducible by sodium butyrate, providing a means to study the effect of different expression levels of up to 4-fold compared to endogenous ERGIC-53. All the tested clones, however, gave similar results.

By confocal microscopy GFP-ERGIC-53 localized to the Golgi area, peripheral dots and, less prominently, to the ER (Fig. 1A). This distribution is very similar to that of endogenous ERGIC-53 in non-transfected cells. In the present work we mainly focused on peripheral structures since the labeling in the Golgi area is too dense to distinguish individual ERGIC spots. Like endogenous ERGIC-53, GFP-ERGIC-53 colocalized with the COP I subunit η-COP and there was partial overlap with the distribution of the COP II subunit Sec31 (Fig. 1A;(Klumperman et al., 1998; Shima et al., 1999; Hammond and Glick, 2000)). In transiently transfected COS cells highly over-expressing ERGIC-53, a fraction of the protein is known to escape to the plasma membrane and to be subsequently endocytosed by a signal-mediated process (Hauri et al., 2000). This is not the case, however, in our HeLa clones expressing GFP-ERGIC-53, since no co-labeling with the endosomal marker transferrin receptor (Fig. 1A) or the lysosomal marker Lamp1 (not shown) was observed.

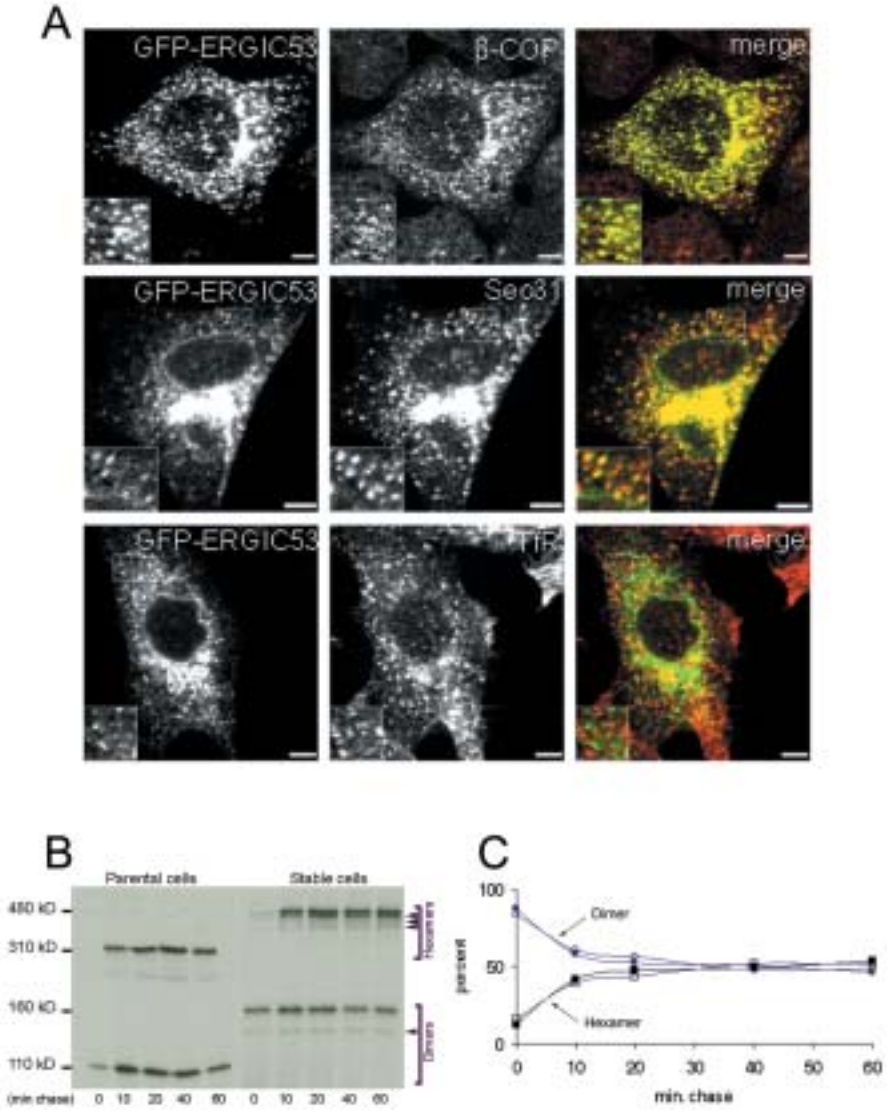

Figure 1: GFP-ERGIC-53 localizes and oligomerizes like endogenous ERGIC-53. (A) HeLa cells stably expressing GFP-ERGIC-53 were treated with sodium butyrate overnight, fixed with para-formaldehyde, and stained for ß-COP, Sec31 or transferrin receptor. Images were taken with a confocal fluorescence microscope. Higher magnifications are also presented (insets). Bar, 5 µm. (B) GFP-ERGIC-53 cells treated with sodium butyrate, or non-transfected cells were pulsed with 35S-methionine and chased for the indicated times. Proteins were immunoprecipitated either with anti-ERGIC-53 for the control cells or with anti-GFP for the stable clone. Immunoprecipitates were analysed by non-reducing SDS-PAGE and visualized by fluorography. During the time course, dimers (lower bands) disappear as hexamers (higher bands) form until a steady state is reached when each species is represented to 50 %. GFP-ERGIC-53 dimers appear as two bands corresponding to homodimers and heterodimers (lower arrowhead) with endogenous ERGIC-53. These dimers are converted to hetero-hexamers (upper arrowheads) and homo-hexamers. (C) Quantification of dimer and hexamer formation during the chase period. 100 % is the sum of homo-dimers and homo-hexamers at a given chase time. Shown is a representative experiment.

To test if GFP-ERGIC-53 oligomerizes correctly into disulfide-linked dimers and hexamers (Schweizer et al., 1988), cells were metabolically labeled with ^{35}S-methionine in a pulse-chase experiment and ERGIC-53 was immunoprecipitated and analyzed by SDS-PAGE under non-reducing conditions. Fig. 1B shows that GFP-ERGIC-53 initially

appears as a 160 kD band corresponding to dimers which is in part converted to a 480 kD species corresponding to hexamers. These high Mr species break down to an 80 kD monomeric form under reducing conditions (not shown). Importantly, the kinetics of conversion of dimeric to hexameric forms is identical to that of endogenous ERGIC-53 (Fig. 1C). Additional bands on the gel run with the samples of the GFP-ERGIC-53-expressing cells are hetero-oligomers formed between GFP-ERGIC-53 and the endogenous protein as anti-GFP co-immunoprecipitated GFP-ERGIC-53 and ERGIC-53 (not shown). This hetero-oligomerization is an additional indication for correct folding of GFP-ERGIC-53.

Fluorescence recovery after photobleaching was then used to test if GFP-ERGIC-53 recycles. When the peripheral cytoplasm was bleached, fluorescent dots reappeared within 3 min (not shown). We did not see massive horizontal transfer of peripheral GFP-ERGIC-53 to refill the bleached area, suggesting that the reappearing dots largely originated from a recycling process involving the ER. The reappearance is not due to new protein synthesis since it also occurred in cycloheximide-treated cells. A similar recovery was observed when the Golgi area was bleached. Collectively, these data suggest that the GFP-tag does not interfere with the folding and recycling of ERGIC-53.

GFP-ERGIC-53 imaging reveals two populations with different dynamics

To explore the dynamics of GFP-ERGIC-53 in living HeLa cells we used bright field and confocal time-lapse imaging with recording intervals of 10 sec (termed “slow imaging”) or 0.2 sec (termed “fast imaging”) to follow long- and short-time events, respectively.

Slow imaging of GFP-ERGIC-53 for 15 min (Fig 2A) and longer (not shown) revealed fluorescent puncta with a diameter of 0.9 to 1.2 µm exhibiting short range movement of 1.2 µm on average with a maximal velocity of 0.2 µm sec^{-1} (supplementary data movie 1). These structures did not move to the Golgi area but rather hovered about in place. We call them “stationary” structures. They correspond to the COP I-positive tubulovesicular clusters of the ERGIC previously identified by immunoelectron microscopy (Klumperman et al., 1998). Some stationary structures persisted during the entire recording time and occasionally fused with one another (Fig 2A arrowheads) or split. Others disappeared or appeared *de novo* in non-labeled areas. The fluorescence

intensity of the spots did not remain constant but fluctuated with time indicating continuous recycling of GFP-ERGIC-53. Recycling was confirmed by the recovery of fluorescence seen after partial bleaching of these spots (not shown). In rare instances some dynamic tubular structures were observed that rapidly disappeared (Fig. 2A, arrows). They probably correspond to the fast moving structures seen with fast imaging (see below).

To test if the appearance and disappearance of the stationary structures correspond to *de novo* formation and consumption events or to movement into or out of the focal plane, we performed 4D imaging (3D over time) using an imaging interval of 10 sec and a step size of 0.8 µm. This approach showed that stationary GFP-ERGIC-53 spots can indeed form de novo or be consumed. Moreover, imaging for more than 30 min confirmed that many structures are long-lived, can undergo several fusion and splitting events, and do not exhibit a preferential movement to the Golgi area (Fig. 2B, supplementary data movie 2). These features were unchanged when cells were imaged in the presence of cycloheximide to block protein synthesis.

Fast imaging (0.2 sec intervals) of GFP-ERGIC-53 revealed, in addition to the stationary structures, short-lived fast-moving structures difficult to track under slow imaging conditions. The short-lived elements moved in all directions and could occasionally be seen to originate from stationary structures (supplementary data movie 3 and Fig. 2C). They had an apparent average diameter of 0.5 µm and moved in a stop-and-go fashion along curvilinear trajectories with speeds ranging from 1 to 7 µm sec^{-1}. Often these structures seemed to cross each other, to move from one stationary structure to another or to cross several of them during their long-range movement of up to 6 µm. They frequently changed shape by becoming slightly elongated (supplementary data movie 3). Tracking several of these structures for up to 70 sec showed that they moved only rarely in the direction of the Golgi area (tracks in Fig. 3C). At 37°C the fast moving structures amounted to about 20% of all GFP-ERGIC-53 spots. Long tubules were infrequently seen. Their number was highly increased, however, when GFP-ERGIC-53 expression was induced by a 40 h sodium butyrate treatment (not shown). Fast movement was absent in cells preincubated on ice for 15 min and imaged at 37°C in the presence of nocodazole suggesting microtubule dependence (not shown).

Collectively, our live imaging approach uncovered that most ERGIC-53 spots in the periphery are stationary and a minor population is highly dynamic.

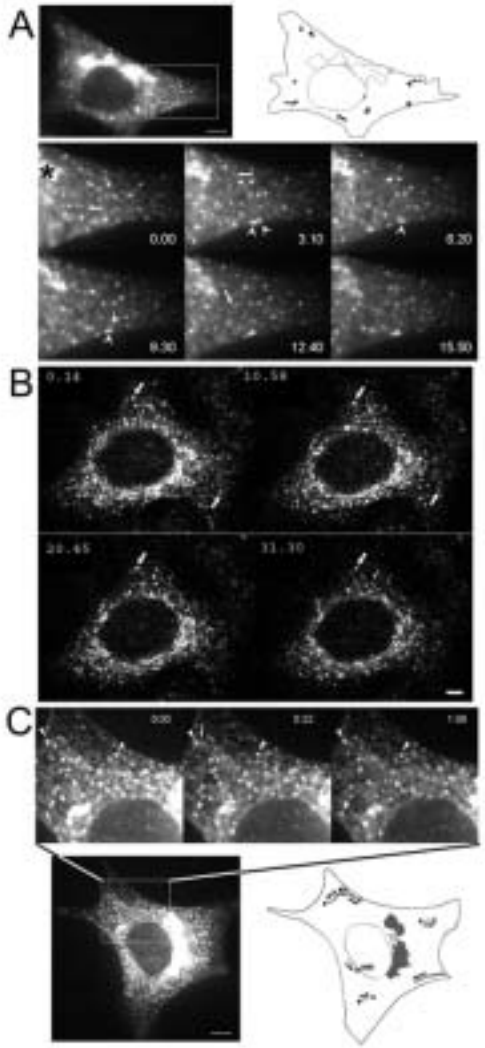

Figure 2: Live imaging of GFP-ERGIC-53 reveals two types of structures with different dynamics. (A) Whole cell and its schematic representation where paths of stationary structures imaged every 10 sec have been traced (see supplementary data movie 1). Note that these structures undergo very short range to no movement. Lower panel: image series of the outlined portion in the upper panel. Arrowheads point two peripheral ERGIC structures fusing with each other. Arrows point to elongated ERGIC structures. (B) Representative images from supplementary data movie 2. GFP-ERGIC-53-expressing HeLa cells were imaged in the xyz directions every 10 sec. Arrows point to long-lasting structures that can persist for up to at least 31 min. (C) Data taken from supplementary data movie 3 imaged with an interval of 0.2 sec. Representative frames show three peripheral ERGIC structures (arrowheads) that hardly move during the entire imaging interval. The arrow points to a peripheral stationary spot shooting out an elongated structure. Lower panel: whole cell and a schematic representation of paths that GFP-ERGIC-53 fast moving structures followed during the imaging time. Note that the movement does not follow a defined direction, and often seems to connect two peripheral stationary structures. Bar, 5 µm; time: min.sec.

Trafficking routes of GFP-ERGIC-53

To explore the dynamics of GFP-ERGIC-53 in more detail we used conditions that reversibly block protein recycling in ER or ERGIC. Incubating the cells with the ER-exit blocking protein kinase inhibitor H89 (Aridor and Balch, 2000) relocalised GFP-ERGIC-53 to the ER (Fig. 3A, supplementary data movie 4) as reported previously for endogenous ERGIC-53 (Lee and Linstedt, 2000). Antibody staining of fixed cells confirmed that during the H89 block GFP-ERGIC-53 and endogenous ERGIC-53 increasingly colocalized with the ER marker CLIMP-63, while the structure of the Golgi defined by giantin remained unchanged (not shown). Addition of H89 rapidly stopped the movement as well as the splitting and fusion activities of the peripheral stationary spots, and, synchronously with the Golgi area, the spots lost fluorescence within 20 min at the expense of an increasingly fluorescent ER (arrow in Fig. 3A, supplementary data movie 4). H89 also stopped the fast moving structures (not shown). Upon removal of H89, GFP-ERGIC-53 reappeared simultaneously in peripheral spots and the Golgi area (Fig. 3B, supplementary data movie 5) while the ER fluorescence decreased concomitantly (compare Fig. 3B recovery 2.0 and 26.1). Of note, the peripheral ERGIC structures did not directionally move to refill the Golgi area (arrow in Fig. 3B). This suggests that ERGIC structures in the periphery and in the Golgi area independently received GFP-ERGIC-53 from the ER. Fast moving ERGIC-53 structures only appeared after almost full recovery of the stationary structures and often derived from them moving in all directions (not shown).

To study trafficking from the ERGIC, low temperature/rewarming experiments were performed. Incubation at 15°C to 16°C is known to reversibly accumulate ERGIC-53 (Lippincott-Schwartz et al., 1990; Klumperman et al., 1998). Upon rewarming from 16°C to 37°C, the stationary peripheral GFP-ERGIC-53 spots rapidly emitted tubules moving with an average velocity of around 1 μm sec^{-1} (Fig. 4, supplementary data movie 6), while the fast moving structures had essentially the same movement as observed at 37°C (not shown). Single stationary structures could repeatedly extend multiple tubules in different directions. The tubules formed and detached within seconds and stayed at peripheral sites for only brief periods before vanishing in the proximity of a stationary structure or disappearing in the cell periphery toward no defined structures. Formation

and translocation of GFP-ERGIC-53-enriched tubules decreased with time until the activity entirely stopped (not shown). Tubule formation in general did not consume the stationary structure. Moreover, the tubules had no apparent preference for moving to the Golgi area.

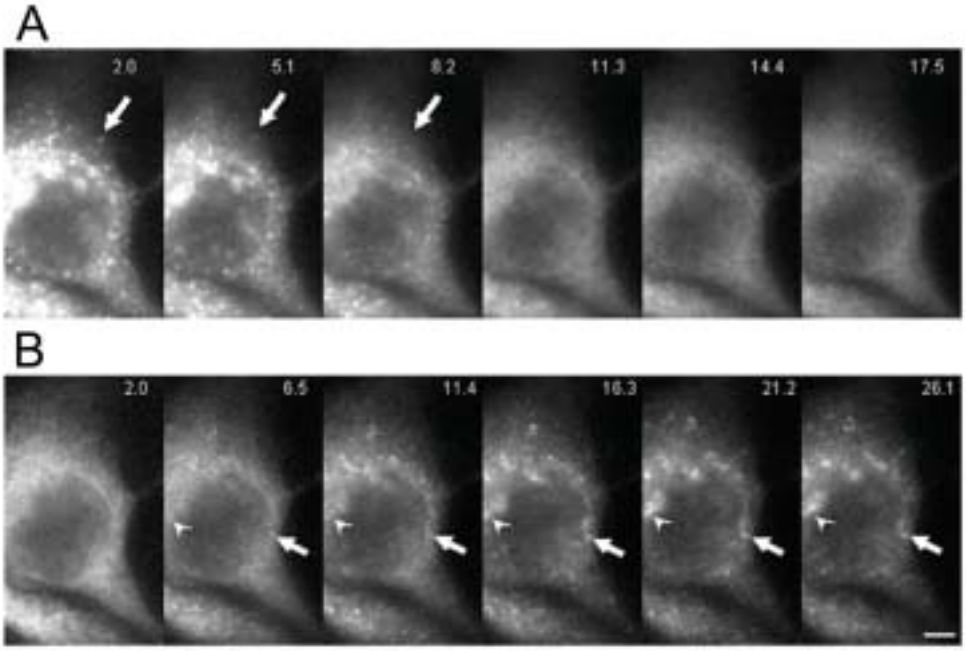

Figure 3: GFP-ERGIC-53 stationary structures in the periphery and in the Golgi area are equivalent. (A) Time points from supplementary data movie 4 showing the relocalisation of GFP-ERGIC-53 to the ER when cells are treated with H89. The arrow points to a peripheral ERGIC structure that loses fluorescence and disappears without moving to the Golgi area. (B) Time series from supplementary data movie 5 showing the recovery of the same cell after H89 washout. The arrow points to a peripheral ERGIC structure that gets brighter during recovery but does not move to the Golgi area (arrowhead) that is refilled at the same time as peripheral ERGIC structures appear. Bar, 5 µm. Time: min.sec.

To further investigate whether these tubular processes were directed to the Golgi area, we photobleached this region in cells rewarmed from 16°C. At early recovery and rewarming times, tubules forming from peripheral spots extended randomly into different directions while the Golgi area was refilled homogeneously and independently of the tubules (not shown). Obviously, the refilling of the Golgi area reflects direct transport of GFP-ERGIC-53 from the ER into ERGIC clusters that are concentrated near the Golgi apparatus and cannot be resolved by light microscopy (Klumperman et al., 1998). After 10 min of recovery, the profile of GFP-ERGIC-53-containing structures, including the Golgi area, was similar to that of the pre-bleached state. Collectively, these experiments suggest that the dynamic tubules indicate the ERGIC to ER recycling route and that the recycling of GFP-ERGIC-53 largely bypasses the Golgi.

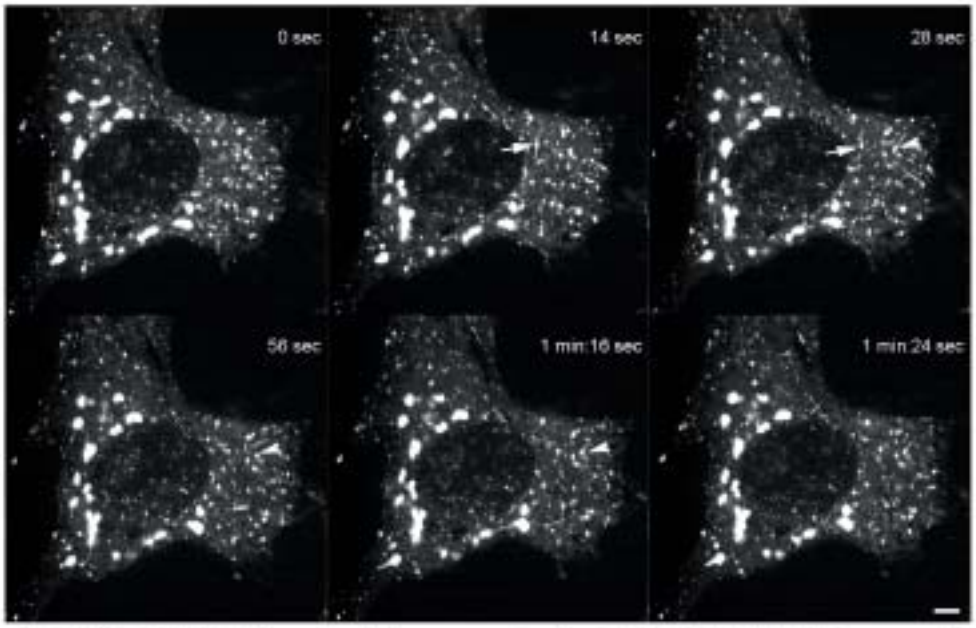

Figure 4: GFP-ERGIC-53 tubule formation during rewarming from 16°C. GFP-ERGIC-53-expressing HeLa cells were incubated 3 h at 16 C, shifted to 37 C for 1 min 53 sec and imaged every 0.6 sec (see supplementary data movie 6). 0 sec indicates the time at which imaging started. Extensive tubular structures appear from peripheral ERGIC spots and move with no preference in different directions. A single ERGIC structure can simultaneously extend tubules in opposite directions without getting consumed (arrow). Several rounds of tubule emission from the same ERGIC spot do not consume it (arrowhead). Bar, 5 µm. Time: min.sec.

GFP-ERGIC-53 and VSV-G-GFP take different routes from the ERGIC

Our conclusion regarding the recycling pathway of GFP-ERGIC-53 is based on visual analysis. To further test this visual impression we sought to quantitatively compare the traffic route of GFP-ERGIC-53 from the ERGIC with that of the well-studied anterograde marker protein VSV-G-GFP. To this end, we measured the directionality of protein flow rate after a low temperature block by a vector field method that is based on the optical flow estimation (Miura and Pepperkok, in preparation). HeLa cells either stably expressing GFP-ERGIC-53 or infected with adenovirus carrying the ts045-VSV-G-GFP DNA were subjected to the low-temperature/rewarming procedure and imaged at different rewarming times for approximately 100 sec. We analyzed moving entities with speed ranges between 200 nm sec^{-1} and 400 nm sec^{-1} from several 10 sec sub-sequences of each movie. There was enough displacement during this short period of time to optimally measure directionality relative to the Golgi. During rewarming from 16°C to 37°C, the movement of GFP-ERGIC-53 had a slight preference away from the Golgi (Fig. 5A). This is consistent with and quantitatively supports our visual impression that GFP-ERGIC-53 does not preferentially move to the Golgi. For VSV-G-GFP,

rewarming from 15°C to 32°C generated a preferential movement toward the Golgi (Fig. 5B). This finding is in accord with previous reports on the dynamics of VSV-G-GFP during rewarming from 15°C (Presley et al., 1997; Scales et al., 1997). Although seemingly small, the differences between toward and away produce a net directional transport of VSV-G to the Golgi as a result of cumulative effects. Collectively, these results show quantitatively that GFP-ERGIC-53 and VSV-G-GFP leave the ERGIC to different directions, consistent with their opposed transport to the ER and to the Golgi, respectively.

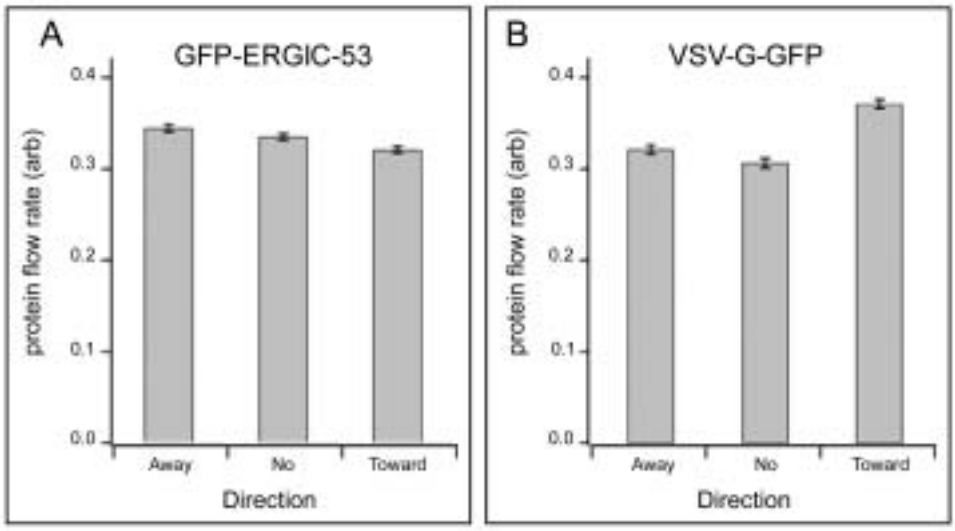

Figure 5: GFP-ERGIC-53 and VSV G-GFP take different routes from ERGIC. Quantification of the flow rate direction of GFP-ERGIC-53 (A) and VSV-G-GFP (B) in cells rewarmed from 16 C to 37 C or 15 C to 32 C, respectively. Plotted is the protein flow rate in arbitrary units (normalized to 1) against the direction of movement. Note that VSV-G-GFP is directed toward the Golgi while GFP-ERGIC-53 is directed away from the Golgi. These differences are statistically significant (t-test, P≤ 0.05). Bars are means + SD (GFP-ERGIC-53: n=67, VSV-G-GFP: n=73); No, non-directional movement.

Sorting of anterograde and retrograde cargo in the ERGIC

To obtain sorting information also on a soluble secretory protein and to directly visualize the sorting of anterograde and retrograde cargo in the same cell we constructed a secretory form of pDsRedT1 (Bevis and Glick, 2002), termed ssDsRed, by attaching an N-terminal signal sequence. ssDsRed was transfected into HeLa cells stably expressing GFP-ERGIC-53 and transport was studied by dual color imaging.

By immunoprecipitation experiments we verified that ssDsRed was indeed secreted into the culture medium (not shown). When transport was blocked at 16°C, ssDsRed displayed an enhanced ER pattern, and some ERGIC-53 spots also co-

labeled with ssDsRed. Rewarming to 37°C led to a gradual decrease of ER fluorescence followed by an increase in peripheral ERGIC structures and subsequently the Golgi area (Fig 6A, supplementary data movie 7). To quantify ssDsRed segregation from peripheral ERGIC clusters we tracked structures co-localizing with GFP-ERGIC-53 in six cells and classified the different initial sorting events during rewarming from 16°C.

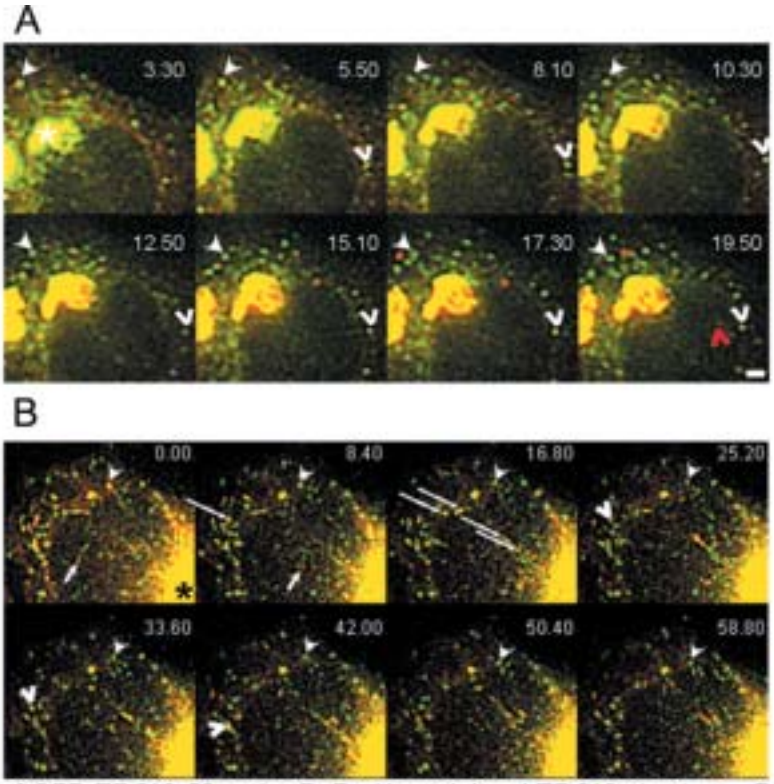

Figure 6: Sorting of GFP-ERGIC-53 and ssDsRed in peripheral ERGIC structures. Data from cells co-expressing GFP-ERGIC-53 and ssDsRed rewarmed from a 3 h 16 C block. (A) Time series (taken every 10 sec) from supplementary data movie 7. 3.30 indicates the time (min: sec) after rewarming to 37 C. The filled arrowhead points to a stationary GFP-ERGIC-53 structure from which ssDsRed segregates Note that even in the proximity of the Golgi the ERGIC stationary structure does not move toward this area. The empty arrowhead points to another stationary structure from which ssDsRed segregates. 11 min 50 sec later, this same structure receives new ssDsRed material that is shot toward the Golgi at time point 19.50 (red arrowhead). Note that the Golgi (asterisk) becomes redder as the rewarming proceeds. Time: min.sec. (B) Cell imaged with an interval of 0.2 sec, 12 min after shifting the temperature from 15 C to 37 C. 0.00 indicates the time at which the imaging started. The filled arrowhead points to a stationary structure that segregates ssDsRed as in A. Some GFP-ERGIC-53 structures are positive for ssDsRed and move together toward the Golgi (arrow) or toward other ERGIC structures (empty arrowhead). Often moving structures carrying both GFP-ERGIC-53 and ssDsRed cross several GFP-ERGIC-53 stationary structures (long arrows). Time: sec.msec. Bar, 5 µm.

According to the two transport models described in Introduction and based on our observations of ERGIC-53's recycling, two major scenarios can be predicted. In the first one, ssDsRed and GFP-ERGIC-53 segregate without disappearance of the GFP-ERGIC-53 spot that remains in place. This would favor the notion that the ERGIC is a stable compartment. In the second scenario, the sorting of ssDsRed consumes the

ERGIC whereby ssDsRed moves to the Golgi and GFP-ERGIC-53 recycles to the ER. In this case the ERGIC would be a transient station supporting the maturation model. Table 1 shows that 55% of the stationary ERGIC structures efficiently sorted ssDsRed and ERGIC-53 in a single step, whereby ssDsRed structures of considerable size left the ERGIC and moved to the Golgi area while the GFP-ERGIC-53 spot remained stationary. In 12% of the cases the sorting was incomplete. In 31% of the cases no sorting was observed, but many of these elements underwent fission and fusion. In only 2% of the cases the sorting resulted in the complete consumption of the yellow ERGIC spot. Thus, in a majority of sorting events the ERGIC remained stationary and was not consumed. Many of the ERGIC structures segregated ssDsRed repeatedly (Fig. 6A empty arrowheads, supplementary data movie 7) indicating anterograde flow through a persisting ERGIC structure. These observations are in accord with the stable compartment model.

Table 1:

Quantification of GFP-ERGIC-53 and ssDsRed initial sorting in the ERGIC of live cells following rewarming from 15°C to 37°C*

Observation	**%**	**Consistent with stable compartment model**
Complete sorting:		
- Export of ssDsRed spot, GFP-ERGIC-53 spot remains stationary	55	yes
- Consumption by sorting	2	no
Incomplete sorting:		
- Export of ssDsRed spot	7	yes
- Export of GFP-ERGIC-53 spot	5	yes
No sorting	31	-

*Recording intervals of 10 sec for 20 min (see Methods).

To make sure we did not miss fast sorting events we studied ssDsRed and GFP-ERGIC-53 segregation by the fast recording procedure. As with the slow recording, ssDsRed segregated from GFP-ERGIC-53 stationary structures (Fig. 6B, filled arrowheads). Of the fast moving structures 29% were positive for both markers and therefore appeared yellow in merged images. When observed for up to 1 min, 77% of these yellow structures showed no sign of sorting and often fused eventually with stationary structures indicating intra-ERGIC transport. 23% of the fast moving yellow structures separated into a red and a green vehicle which moved in opposite directions. Hence, some of the fast moving structures exhibited bi-directional sorting.

Discussion

Although no stable marker for the ERGIC is known, the continuous recycling of ERGIC-53 has allowed us to visualize the ERGIC for prolonged times in living cells and to compare the dynamics of sorting of the retrograde marker protein ERGIC-53 and the anterograde markers VSV-G and ssDsRed. Our findings shed new light on the nature of the ERGIC and on protein trafficking early in the secretory pathway. They support the notion of a stable ERGIC consisting of numerous discontinuous elements that operate in bi-directional sorting. This conclusion is based on three major observations. First, GFP-ERGIC-53 is localized in stationary spots displaying short range non-directional movement. Unlike VSV-G-GFP spots, GFP-ERGIC-53 spots do not show a preferential movement toward the Golgi region and hence do not exhibit typical features of anterograde carriers (ACs). Their short range movement is dependent on intact microtubules as it is lost in nocodazole-treated cells. On the basis of their localization close to ERES defined by Sec31 and the fact that they co-label with anti-ß-COP, the spots correspond to the ERGIC-53-containing tubulovesicular clusters previously identified in fixed cells by immunofluorescence and immunoelectron microscopy (Schweizer et al., 1988; Klumperman et al., 1998). Second, many of the stationary GFP-ERGIC-53 structures are long-lived and persist for more than 30 min, another feature

that is inconsistent with an exclusively AC function. ER to Golgi transport is a rapid event. The ERGIC spots can undergo splitting and occasionally fuse with one another. Some appear *de novo*, others disappear. Interestingly, similar features have been observed for ERES (Stephens et al., 2000; Hammond and Glick, 2000) suggesting that the dynamics of ERES and ERGIC clusters may be regulated in concert. The precise relationship of ERES and ERGIC is currently unclear and remains to be studied in greater detail. Third, the ERGIC spots are not consumed by the sorting of GFP-ERGIC-53 and ssDsRed. They can undergo multiple rounds of sorting of anterograde and retrograde cargo.

Our conclusion regarding the nature of the ERGIC is at variance with that drawn from previous live imaging studies on VSV-G-GFP transport (Presley et al., 1997; Scales et al., 1997). These authors concluded that the ERGIC clusters are transport vehicles for protein delivery to the Golgi, rather than a stable compartment (Lippincott-Schwartz et al., 2000). In accord with these studies we observed that ACs moving to the Golgi are rather large and cannot be small transport vesicles. However, only by visualization of the sorting of anterograde and retrograde traffic from the ERGIC in living cells did the stable nature of this compartment become apparent.

Quantification of the directionality of movement by a fully numerical processing procedure supports our visual impression that GFP-ERGIC-53 largely escapes packaging into ACs. Unlike VSV-G-GFP, GFP-ERGIC-53 shows no preferential movement to the Golgi upon exit from the ERGIC. It rather moves in the opposite direction. Considering the apparently random distribution of ERGIC clusters in the peripheral cytoplasm one would expect no preferred directionality for GFP-ERGIC-53 cycling back to the ER. However, low temperature blocks tend to concentrate the ERGIC clusters closer to the Golgi apparatus (Klumperman et al., 1998). Therefore, the measured net flow for ERGIC-53 results from a combined effect: repositioning of ERGIC clusters and recycling of ERGIC-53. At first glance the measured difference of 13.5% between anterograde and retrograde movements of VSV-G-GFP appears to be small. It should be noted, however, that the quantification time was short (10 sec) and that extrapolation to a longer time results in a net flow to the Golgi within a few minutes. Thus, directed transport is the consequence of a slight preference in movement toward one direction. Overall, this novel vector field method that is based on the optical flow

estimation validates previous conclusions derived from fixed cells (Klumperman et al., 1998) that ERGIC to ER retrograde transport largely bypasses the Golgi. It is also consistent with our ssDsRed/GFP-ERGIC-53 dual imaging data showing preferential sorting of anterograde and retrograde traffic in the ERGIC.

By imaging at high temporal resolution of 5 frames per second (fast imaging) we have uncovered a third pathway not previously described. This pathway is mediated by fast moving carriers (FCs) a fraction of which contains both GFP-ERGIC-53 and ssDsRed. The pathway is highly sensitive to microtubule-disrupting drugs as well as H89 and requires the existence of stationary ERGIC structures as unveiled by H89 wash-out experiments. Because FCs do not exhibit preferential movement to the Golgi area and can occasionally be seen to originate from and fuse with stationary ERGIC structures, we propose that they functionally connect ERGIC clusters by horizontal exchange. Although a majority of the FCs remains unsorted and appears to eventually fuse with a stationary structure, some can separate into a GFP-ERGIC-53-containing and an ssDsRed-containing dot which move in opposite directions. The GFP-ERGIC-53 dot tends to rapidly disappear, whereas the ssDsRed dot moves to the Golgi. This suggests that some FCs are involved in anterograde/retrograde sorting.

Integrating our new data with previously published findings the following picture regarding the organization and traffic routes in the early secretory pathway emerges (Fig. 7). Newly synthesized secretory proteins and ERGIC-53 are transported from the ER to the ERGIC clusters that are lying close to and are (at least functionally) separated from ERES (Mezzacasa and Helenius, 2002). While there is agreement that ER-exit is COP II-dependent, this process may (Horstmann et al., 2002) or may not (Mironov et al., 2003) involve budding of transport vesicles in higher eukaryotes. Once in the ERGIC, anterograde cargo is sorted from ERGIC-53 into rather large ACs by a dissociative process. The size of ACs may vary according to cargo flux and can be considerable under conditions of massive synchronized release of VSV-G from the ER (Horstmann et al., 2002). ACs then rapidly move to the Golgi in a microtubule-dependent way. In contrast, ERGIC-53 is packaged into retrograde carriers (RCs), the size and shape of which can vary too. RCs must also have a considerable size to be visible. When traffic is inhibited at 15°C followed by rewarming to 37°C, RCs emanating from the ERGIC clusters are often tubular. It appears that conditions of massive cargo transport favor the

formation of tubules regardless of the pathway. Like ERGIC to Golgi anterograde transport, efficient ERGIC to ER retrograde transport requires intact microtubules.

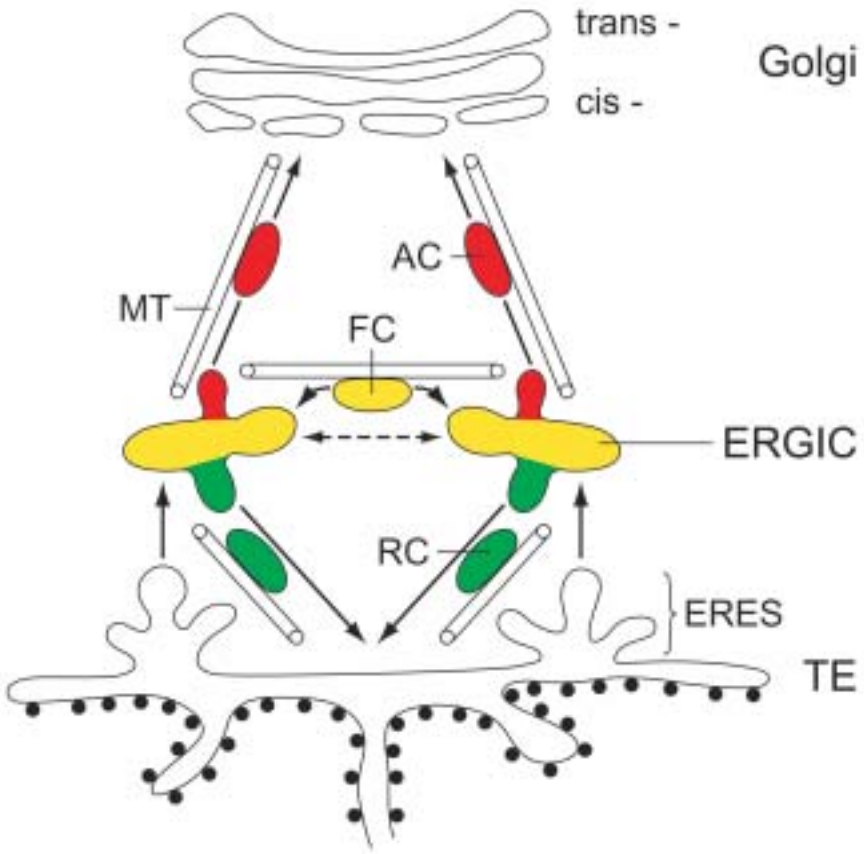

Figure 7: Model of the organization of the early secretory pathway and sorting of anterograde and retrograde traffic in the ERGIC. The cycling protein GFP-ERGIC-53 (green) and anterograde cargo, such as VSV-G-GFP or ssDsRed (red), leave the ER at ER-exit sites (ERES) of the transitional elements of the rough ER (TE) and are transported to the ER-Golgi intermediate compartment (ERGIC) by a microtubule-independent process. The ERGIC is a collection of stationary tubulovesicular clusters exhibiting short range, non-directional, but microtubule-dependent movement. The clusters can split or fuse with one another (dashed arrow). Sorting in the ERGIC leads to anterograde carriers (AC) mediating transport of ssDsRed to the cis-Golgi and to retrograde carriers (RC) mediating transport of GFP-ERGIC-53 back to the ER. Both pathways are dependent on intact microtubules. Individual ERGIC-clusters are connected by fast moving carriers (FC) that carry both markers and are transported along microtubules. M, microtubules.

What is the role of the newly discovered FCs that connect individual stationary ERGIC elements and are only visible at high temporal resolution? FCs may functionally link the ERGIC clusters allowing the exchange of critical components within the discontinuous ERGIC system. Alternatively, FCs may be incompletely sorted ACs that, due to their incomplete sorting, are incompetent to travel to the Golgi. Thereby, the FCs pathway would operate as a backup system in order to prevent anterograde transport of incompletely sorted membranes. Our study does not lend support to the notion of an ERGIC-53-positive late subdomain of ERGIC close to the Golgi as proposed by Marra *et*

al., 2003. Inconsistent with such a view, ERGIC-53 appears with indistinguishable kinetics in clusters close to the Golgi and in the periphery after H89 wash-out, and ACs moving from stationary ERGIC spots to the Golgi do not comprise detectable levels of ERGIC-53. Moreover, GFP-ERGIC-53 spots in the periphery and in the Golgi region are GM-130 negative in these cells (not shown). Our data rather suggest that all ERGIC clusters are qualitatively very similar or identical.

In conclusion, we find that in living cells the ERGIC defined by ERGIC-53 is composed of stationary long-lived structures close to ERES. The ERGIC structures are sites of active sorting of anterograde and retrograde cargo. Both anterograde and retrograde transport from the ERGIC must involve a dissociative process the precise molecular mechanism of which remains to be uncovered. In view of the new finding that the ERGIC is an organelle in the true sense, it is likely to have additional functions that remain to be uncovered.

Experimental procedures

Recombinant DNAs

Standard molecular biology protocols including PCR-based splicing and mutagenesis were used. Oligonucleotides were from Microsynth (Switzerland) and enzymes from New England BioLabs. GFP-ERGIC-53 was constructed in three steps: (1) The first AUG in the GFP coding sequence of the pEGFP-C1 vector (Clontech Laboratories Inc) was removed using the gene splicing by overlap extension procedure. The prolactin signal sequence (PRL) was amplified from a pCB6 vector construct in which it is up-stream an HA tag, and NheI restriction sites were introduced. The resulting PCR product was inserted into either pDsRedT1-N1 vector (Bevis and Glick, 2002) or the modified pEGFP-C1 vector (from step1). (3) GFP-ERGIC-53 was engineered from pBluescript SK-ERGIC-53 construct described in Schindler et al. (Schindler et al., 1993). ERGIC-53's original signal sequence was replaced by an XmaI restriction site and the generated PCR product was inserted into the pEGFPC1 vector containing the pre-prolactin. Throughout this manuscript GFP refers to the enhanced version of GFP. VSV-

G tsO45 C-terminally tagged with GFP (here termed VSV-G-GFP) was as described (Scales et al., 1997). All constructs were verified by sequencing.

Cell culture, pulse-chase and immunoprecipitation

HeLa cells (ATCC) were grown in DMEM supplemented with 10 % fetal bovine serum, non-essential amino acids, fungizone, penicillin and streptomycin. Calcium-phosphate precipitation or Fugene6 (Roche) was used for transient transfections unless stated otherwise. 24 h later, the cells were processed for imaging or for stable transfection. HeLa stable cell lines were produced by selection for G418 resistance (0.6 mg ml^{-1}; Sigma-Aldrich). Single clones were screened for expression with or without sodium butyrate induction (10 mM). Results are from at least two independent clones. HeLa cells grown in 3.5 cm dishes were subjected to pulse-chase using ^{35}S-methionine, followed by immunoprecipitation with mAb G1/93 (Schweizer et al., 1988) or anti-GFP (Boehringer Mannheim, Germany).

Immunofluorescence microscopy

Cells were cultured in 8-well Lab-Teck glass chamber slides (Nalge Nunc International). Cells were fixed with 3 % para-formaldehyde and permeabilized with 0.1 % saponin, 10 mM glycine 0.1 % sodium azide in PBS (solution 1). Non-specific binding was blocked by a 10 min incubation in solution 1 containing 0.3 % BSA. Cells were then incubated with primary antibodies diluted in solution 1 followed by appropriate secondary antibodies for 45 to 90 min. After several washings, the cells were embedded in Mowiol 4-88 (Calbiochem) supplemented with 1.3 mg ml^{-1} DABCO (Sigma-Aldrich). Antibodies used: G1/296 anti-CLIMP63 (Schweizer et al., 1993), G1/221 anti-transferrin receptor (Vollenweider et al., 1998), maD anti-ß-COP (Pepperkok et al., 1993), and anti-Sec31 (Shugrue et al., 1999). Primary antibodies were detected with affinity-purified Alexa® 565 either goat-anti-mouse or goat anti-rabbit (Molecular Probes, USA). Images were obtained using a Leica TCS NT confocal laser scanning microscope, a 63x 1.32 NA

lens, a pinhole diameter of 1 Airy units, and 488 nm laser excitation for GFP and 568 nm for Alexa® 565.

Live cell imaging

HeLa cells were cultured on 18 mm round glass cover-slips and treated with sodium butyrate overnight followed by incubation without sodium butyrate for a few hours. They were then transferred to imaging medium 1 (Ham's F12 supplemented with 20 mM HEPES, pH 7.4) in a Ludin chamber (Life Imaging Services GmbH, Switzerland, www.lis.ch) and imaged with a 63x 1.4 NA Plan-Apochromat oil objective on a Zeiss Axiovert 135M microscope at 37 ∀C. Images were taken with a CCD camera (SensiCam; PCO Computer Optics GmbH) using a filter wheel to switch between excitation and emission wavelengths. The excitation/emission combinations used were at 480/525 for GFP and 565/620 for DsRed (Chroma Technology Corp.). ImagePro® Plus software (Media Cybernetics®) was used for both recording and image processing, which essentially consisted of narrowing the look-up table range and using a High Gauss and sharpening filters. Image J from NIH Image was also used for image processing (http://rsb.info.nih.gov/nih-image/). Speeds and displacements were measured using a macro written in NIH Image by Jens Rietdorf (ALMF, EMBL, Heidelberg). Fast dual recording and 4D imaging was done at the Advanced Light Microscopy Facility (ALMF) EMBL, Heidelberg. The imaging medium was MEM without phenol red, supplemented with 30 mM HEPES, pH 7.4 and 0.5 g l^{-1} sodium bicarbonate. For the dual color fast time-lapse recording a temperature controlled Olympus TILL/Photonics® time lapse microscope, equipped with an emission beam splitter (DualView, OpticalInsights Inc.) which splits the emitted light into two spectrally distinct channels was used. The sample was excited at 488 nm and the fluorescence signal was split into two channels using a dichroid mirror (centered around 560 nm) and two emission filters (BP530/30 and LP590) introduced into the emission beam splitter. A Perkin Elmer spinning disc confocal microscope (UltraVIEWRS) mounted on a ZEISS Axiovert 200 microscope was used for 4D image acquisition. Individual z-stacks at distinct time-points were acquired using a 60X Plan Neofluar objective and subsequently projected for each time-point

separately using a macro written in IDL by Timo Zimmerman (ALMF, EMBL, Heidelberg).

Transport blocks

Cells were incubated in HEPES-buffered medium (20 mM HEPES, pH 7.4). To reversibly block traffic in the ERGIC, cells were incubated in DMEM at 15°C/16°C for 2-3h then rewarmed to 37°C/32°C and imaged. To block ERGIC-53 in the ER, cells were incubated on the temperature controlled microscope stage for 20 min in imaging medium 1 supplemented with 50 - 90 µM H89 (Calbiochem). The drug was removed by flushing fresh medium 1 warmed to 37∀C. Data for quantification of sorting in stationary GFP-ERGIC-53 structures was collected from 6 different cells (each corresponding to a separate experiment) imaged every 10 sec during rewarming. Yellow structures were counted and the first event taking place was scored. To quantify sorting in fast moving structures, cells were imaged every 0.2 sec for 1 min at different rewarming times. The collected RGB movies were extracted into green and red, and all fast moving structures were scored in both channels separately. Their overlap was then assessed over time.

Quantification of directionality

HeLa stable cell lines were pre-treated for 16 h with sodium butyrate, which was removed 6 h prior to imaging. The cells were infected with adenovirus carrying the ts045-VSV-G-GFP DNA as described (Scales et al., 1997) and recorded during recovery from a 15°/16°C block using a temperature controlled spinning disk confocal microscope (ALMF, EMBL, Heidelberg). Protein transport was measured at different rewarming times in 6 cells expressing GFP-ERGIC-53 or VSV-G-GFP using a program written in IGOR Pro (Wavemetrics Inc. OR, USA). The program is based on gradient-based optical flow estimation (Nomura et al., 1991) that measures the speed and direction of moving objects in an image sequence. We scored directions toward a reference point in the Golgi apparatus. Velocity and intensity filters were used to eliminate the apparent vectors generated by noise in the image sequence. The direction corresponds to the

angle between the moving direction and the reference point. The direction is 0° when the spot moves straight to the reference point and 180° or -180° when moving straight away from the reference point. Directions were categorized by angle intervals. Particles moving in the interval of -60° to 60° were designated “toward”, those moving in the interval -120° to 120 ° were designated “away”, and the remaining angle values (-60°to -120°and 60°to 120°) were designated “non-directional”. Protein mass flow rates in each direction were calculated by multiplying fluorescence intensity and speed. The flow rate is thus a measure of transported protein per unit of time. Statistical significance (PÒ 0.05) of the preference in a certain direction among these three categories was probed by t-test.

Acknowledgements

We thank Beat Ludin, Jens Rietdorf and Timo Zimmermann for imaging assistance, Benjamin Glick for providing pDsRedT1, Fred Gorelick for providing antibodies to Sec31, Käthy Bucher, Maria Susanna Balda and Karl Matter for continuous support, and the members of the Hauri and Pepperkok groups for suggestions. The study was supported by the Swiss National Science Foundation (HP.H), the University of Basel (HP.H) and a Quality of Life EU NetworkGrant QCRI-CT-2002-01272 (R.P.)

References

Aridor, M., and Balch, W. E. (2000). Kinase signaling initiates coat complex II (COPII) recruitment and export from the mammalian endoplasmic reticulum. J Biol Chem *275*, 35673-35676.

Aridor, M., Bannykh, S. I., Rowe, T., and Balch, W. E. (1995). Sequential coupling between COPII and COPI vesicle coats in endoplasmic reticulum to Golgi transport. J Cell Biol *131*, 875-893.

Bannykh, S. I., and Balch, W. E. (1997). Membrane dynamics at the endoplasmic reticulum-Golgi interface. J Cell Biol *138*, 1-4.

Bannykh, S. I., Rowe, T., and Balch, W. E. (1996). The organization of endoplasmic reticulum export complexes. J Cell Biol *135*, 19-35.

Bevis, B. J., and Glick, B. S. (2002). Rapidly maturing variants of the Discosoma red fluorescent protein (DsRed). Nat Biotechnol *20*, 83-87.

Beznoussenko, G. V., and Mironov, A. A. (2002). Models of intracellular transport and evolution of the Golgi complex. Anat Rec *268*, 226-238.

Blum, R., Stephens, D. J., and Schulz, I. (2000). Lumenal targeted GFP, used as a marker of soluble cargo, visualises rapid ERGIC to Golgi traffic by a tubulo-vesicular network. J Cell Sci *113 (Pt 18)*, 3151-3159.

Farquhar, M. G. (1985). Progress in unraveling pathways of Golgi traffic. Annu Rev Cell Biol *1*, 447-488.

Glick, B. S., and Malhotra, V. (1998). The curious status of the Golgi apparatus. Cell *95*, 883-889.

Gomez, M., Scales, S. J., Kreis, T. E., and Perez, F. (2000). Membrane recruitment of coatomer and binding to dilysine signals are separate events. J Biol Chem *275*, 29162-29169.

Hammond, A. T., and Glick, B. S. (2000). Dynamics of transitional endoplasmic reticulum sites in vertebrate cells. Mol Biol Cell *11*, 3013-3030.

Hauri, H. P., Kappeler, F., Andersson, H., and Appenzeller, C. (2000). ERGIC-53 and traffic in the secretory pathway. J Cell Sci *113*, 587-596.

Horstmann, H., Ng, C. P., Tang, B. L., and Hong, W. (2002). Ultrastructural characterization of endoplasmic reticulum - Golgi transport containers (EGTC). J Cell Sci *115*, 4263-4273.

Kappeler, F., Klopfenstein, D. R., Foguet, M., Paccaud, J. P., and Hauri, H. P. (1997). The recycling of ERGIC-53 in the early secretory pathway. ERGIC-53 carries a cytosolic endoplasmic reticulum-exit determinant interacting with COPII. J Biol Chem *272*, 31801-31808.

Klumperman, J., Schweizer, A., Clausen, H., Tang, B. L., Hong, W., Oorschot, V., and Hauri, H. P. (1998). The recycling pathway of protein ERGIC-53 and dynamics of the ER-Golgi intermediate compartment. J Cell Sci *111*, 3411-3425.

Lee, T. H., and Linstedt, A. D. (2000). Potential role for protein kinases in regulation of bidirectional endoplasmic reticulum-to-Golgi transport revealed by protein kinase inhibitor H89. Mol Biol Cell *11*, 2577-2590.

Lippincott-Schwartz, J., Donaldson, J. G., Schweitzer, A., Berger, E. G., Hauri, H.-P., Yuan, L. C., and Klausner, R. D. (1990). Microtubule-dependent retrograde transport of proteins into the ER in the presence of brefeldin A suggests an ER recycling pathway. Cell *60*, 821-836.

Lippincott-Schwartz, J., Roberts, T. H., and Hirschberg, K. (2000). Secretory protein trafficking and organelle dynamics in living cells. Annu Rev Cell Dev Biol *16*, 557-589.

Lotti, L. V., Torrisi, M. R., Pascale, M. C., and Bonatti, S. (1992). Immunocytochemical analysis of the transfer of vesicular stomatitis virus G glycoprotein from the intermediate compartment to the Golgi complex. J Cell Biol *118*, 43-50.

Marra, P., Maffucci, T., Daniele, T., Tullio, G. D., Ikehara, Y., Chan, E. K., Luini, A., Beznoussenko, G., Mironov, A., and De Matteis, M. A. (2001). The GM130 and

GRASP65 Golgi proteins cycle through and define a subdomain of the intermediate compartment. Nat Cell Biol *3*, 1101-1113.

Mezzacasa, A., and Helenius, A. (2002). The transitional ER defines a boundary for quality control in the secretion of tsO45 VSV glycoprotein. Traffic *3*, 833-849.

Mironov, A. A., Mironov, A. A., Jr., Beznoussenko, G. V., Trucco, A., Lupetti, P., Smith, J. D., Geerts, W. J., Koster, A. J., Burger, K. N., Martone, M. E.*, et al.* (2003). ER-to-Golgi carriers arise through direct en bloc protrusion and multistage maturation of specialized ER exit domains. Dev Cell *5*, 583-594.

Nomura, A., Miike, H., and Koga, K. (1991). Field theory approach for determining optical flow. Pattern Recognition Letters *12*, 183-190.

Nufer, O., Guldbrandsen, S., Degen, M., Kappeler, F., Paccaud, J. P., Tani, K., and Hauri, H. P. (2002). Role of cytoplasmic C-terminal amino acids of membrane proteins in ER export. J Cell Sci *115*, 619-628.

Nufer, O., Kappeler, F., Guldbrandsen, S., and Hauri, H. P. (2003). ER export of ERGIC-53 is controlled by cooperation of targeting determinants in all three of its domains. J Cell Sci *116*, 4429-4440.

Palade, G. (1975). Intracellular aspects of the process of protein synthesis. Science *189*, 347-358.

Pelham, H. R. (1989). Control of protein exit from the endoplasmic reticulum. Annu Rev Cell Biol *5*, 1-23.

Pepperkok, R., Scheel, J., Horstmann, H., Hauri, H.P., Griffiths, G., and Kreis, T.E. (1993). Beta-COP is essential for biosynthetic membrane transport from the endoplasmic reticulum to the Golgi complex in vivo. Cell *74*, 71-82.

Presley, J. F., Cole, N. B., Schroer, T. A., Hirschberg, K., Zaal, K. J., and Lippincott-Schwartz, J. (1997). ER-to-Golgi transport visualized in living cells. Nature *389*, 81-85.

Scales, S. J., Pepperkok, R., and Kreis, T. E. (1997). Visualization of ER-to-Golgi transport in living cells reveals a sequential mode of action for COPII and COPI. Cell *90*, 1137-1148.

Schekman, R., and Orci, L. (1996). Coat proteins and vesicle budding. Science *271*, 1526-1533.

Schindler, R., Itin, C., Zerial, M., Lottspeich, F., and Hauri, H. P. (1993). ERGIC-53, a membrane protein of the ER-Golgi intermediate compartment, carries an ER retention motif. Eur J Cell Biol *61*, 1-9.

Schweizer, A., Ericsson, M., Bachi, T., Griffiths, G., and Hauri, H. P. (1993). Characterization of a novel 63 kDa membrane protein. Implications for the organization of the ER-to-Golgi pathway. J Cell Sci *104*, 671-683.

Schweizer, A., Fransen, J. A. M., Baechi, T., Ginsel, L., and Hauri, H.-P. (1988). Identification, by a monoclonal antibody, of a 53-kD protein associated with a tubular-vesicular compartment at the *cis*-side of the Golgi apparatus. J Cell Biol *107*, 1643-1653.

Schweizer, A., Fransen, J. A. M., Matter, K., Kreis, T. E., Ginsel, L., and Hauri, H.-P. (1990). Identification of an intermediate compartment involved in protein transport from ER to Golgi apparatus. Eur J Cell Biol *53*, 185-196.

Shima, D. T., Scales, S. J., Kreis, T. E., and Pepperkok, R. (1999). Segregation of COPI-rich and anterograde-cargo-rich domains in endoplasmic-reticulum-to-Golgi transport complexes. Curr Biol *9*, 821-824.

Shugrue, C.A., Kolen, E.R., Peters, H., Czernik, A., Kaiser, C., Matovcik, L., Hubbard, A.L., and Gorelick, F. (1999). Identification of the putative mammalian orthologue of Sec31P, a component of the COPII coat. J. Cell Sci. *112*, 4547-4556.

Stephens, D. J., Lin-Marq, N., Pagano, A., Pepperkok, R., and Paccaud, J. P. (2000). COPI-coated ER-to-Golgi transport complexes segregate from COPII in close proximity to ER exit sites. J Cell Sci *113*, 2177-2185.

Stephens, D. J., and Pepperkok, R. (2001). Illuminating the secretory pathway: when do we need vesicles? J Cell Sci *114*, 1053-1059.

Storrie, B., and Nilsson, T. (2002). The Golgi apparatus: balancing new with old. Traffic *3*, 521-529.

Tang, B. L., Low, S. H., Hauri, H. P., and Hong, W. (1995). Segregation of ERGIC53 and the mammalian KDEL receptor upon exit from the 15 degrees C compartment. Eur J Cell Biol *68*, 398-410.

Vollenweider, F., Kappeler, F., Itin, C., and Hauri, H.P. (1998). Mistargeting of the lectin ERGIC-53 to the endoplasmic reticulum of HeLa cells impairs the secretion of a lysosomal enzyme. J. Cell Biol *142*, 377-389.

Supplementary Data Legends

Movie 1: **Live imaging of GFP-ERGIC-53 (slow imaging).** HeLa cells expressing GFP-ERGIC-53 were treated with sodium butyrate overnight and imaged every 10 sec for 15 min. Several moving structures undergoing fusion, splitting, disappearance and re-emergence are seen. Movie is 50x accelerated relative to real time.

Movie 2: **Live imaging of GFP-ERGIC-53 (4D imaging).** Cells treated as in movie 1 were imaged in the xyz directions every 10 sec for 33 min. Several moving structures undergoing fusion, splitting, disappearance and re-emergence are seen. 50x accelerated.

Movie 3: **Live imaging of GFP-ERGIC-53 (fast imaging).** Cells treated as in movie 1 were imaged every 0.2 sec for 1 min. Several stationary and fast moving structures are seen. 100x accelerated.

Movie 4: **H89 blocks GFP-ERGIC-53 in the ER.** Cells were imaged during H89 block every 10 sec for 18 min. Note that the ERGIC structures in the periphery and in the Golgi area disappear simultaneously while fluorescence of the ER increases. 100x accelerated.

Movie 5: **Recovery from H89 block.** Cells were imaged during recovery from the H89 block every 10 sec for 26 min. Note that the ERGIC structures in the periphery and in the Golgi area emerge simultaneously while the fluorescence of the ER decreases. 100x accelerated.

Movie 6: **GFP-ERGIC-53 tubule formation during rewarming from 16°C.** Cells were imaged every 0.6 sec for 1 min 54 sec. Several elongated structures are seen to move randomly. 100x accelerated.

Movie 7: **Sorting of GFP-ERGIC-53 and ssDsRed in the ERGIC.** Cells were imaged during rewarming from a 16 ∀C block every 10 sec for 20 min. Several co-labeled structures are seen to segregate in the periphery. ER fluorescence of ssDsRed diminishes with time due to transport of ssDsRed to the Golgi. 50x accelerated.

Conclusions and perspectives

1. ERGIC: previous and up-dated view

Prior to the outcome of the work presented in this thesis, the ERGIC characteristics were continuously debated. Live imaging data describing the ERGIC as a collection of vesicular tubular clusters moving from the ER to the Golgi (Presley et al., 1997) (Scales et al., 1997), were difficult to reconcile with biochemical and immuno-electron microscopy results where no such movement has been observed (Klumperman et al., 1998). The findings of the present work in which the fate of the ERGIC was addressed in living cells shed light on this controversy. When vesicular tubular clusters were identified as the transport intermediates between the ER and the Golgi (Presley et al., 1997) (Scales et al., 1997), only the anterograde marker VSV-G-GFP was examined. In accord, data presented in this thesis show that the anterograde carriers, as labeled by the membrane-bound VSV-G-GFP and the luminal ssDsRed, are pleiomorphic tubular structures directed toward the Golgi. This cannot be interpreted as a maturing ERGIC (Lippincott-Schwartz et al., 2000) since VSV-G-GFP and ssDsRed are not ERGIC markers. Recycling of ERGIC-53, the bona fide marker of the ERGIC, was reported to bypass the Golgi and to be via tubules (Klumperman et al., 1998), the current data confirm such a recycling pathway (see results section).

Whether the ERGIC defines a true compartment or is constituted by a collection of tubulo-vesicular structures shuttling between the ER and the Golgi, provides a completely different view about trafficking in the early secretory pathway. If the ERGIC defines a stationary organelle, a function(s) has to be investigated. On the other hand, if the ERGIC clusters are just transport carriers, then it could be envisaged that this is the only role they have. Here, by video time-lapse imaging of GFP-ERGIC-53, a fluorescent version of ERGIC-53, the marker of the ERGIC, it was possible to show that this compartment is a true organelle for two major reasons. 1. ERGIC clusters are long-lived, thus could not be transport carriers for the fast anterograde and retrograde cargo trafficking between the ER and the Golgi. 2. Anterograde cargo is sorted from GFP-ERGIC-53 in ERGIC clusters, which are not consumed by the segregation event (see

results section). Such a stable ERGIC organelle is probably specific to higher eukaryotes, as no stationary intermediate compartment was described in *Saccharomyces cerevisae*. A stationary ERGIC organelle between the ER and the Golgi implicates central function(s) of this compartment in a trafficking intersection. One of these functions, as presented above, is the sorting of anterograde and retrograde cargo soon after they leave the ERES. The benefit of such an early sorting event is a more "economical" exit of anterograde cargo from the ER. For instance, recycling receptors like ERGIC-53 from the ERGIC rather than from the Golgi would save energy and time for the cell; the same receptor molecule could hence be re-used for several rounds of ER exit. The sorting function of the ERGIC could also be an initial backup system in the early secretory pathway. Indeed, the ER of higher eukaryotes is complex and might need a down-stream compartment where sorting of resident ER proteins from itinerant proteins could be completed. Another advantage for a cell to have a stationary intermediate compartment could be the regulation of the association of key components (such as SNAREs and tethering factors) with anterograde or retrograde transport carriers. Indeed, it is established that various but overlapping SNAREs localize to the different organelles of the early secretory pathway (Chen and Scheller, 2001) and that each pair of t- and v-SNAREs is engaged in distinct fusion events. These SNARE pairs could be gradually exchanged by transiting through an intermediate compartment rather than entirely replaced on the ER and on the Golgi membranes separately. Moreover, the sorting function of the ERGIC could determine the fate of a carrier that is exiting this organelle by localizing the correct v-SNARE, Rab and tethering factor that will allow targeting to the corresponding membrane. All these plausible functions and others should be investigated in more detail to fully characterize the stationary ERGIC compartment.

The models of stability and maturation in the early secretory pathway have been continuously debated. Since few years, data from many laboratories obtained by several techniques favored the maturation hypothesis (Aridor et al., 1995) (Rowe et al., 1996) (Mironov et al., 2003) (Bevis et al., 2002) (Puri and Linstedt, 2003). A number of these data were collected from experiments where all Golgi components were recycled back to the ER using conditions that either blocked ER exit and/or enhanced the retrograde pathway. The fact that the Golgi components could be completely relocalised to the ER,

lead to the assumption that the Golgi is a maturing compartment that needs the ER to reconstitute (Ward et al., 2001) (Puri and Linstedt, 2003) (Storrie et al., 1998). In this thesis, the notion of maturation is not the capacity of an organelle to reform from the ER or not. In fact, following the reconstruction of compartments, the components of which were totally recycled to the ER, does not reflect stability or maturation. Therefore, it is probably more appropriate to define maturation and stability as the means by which trafficking occurs between the ER and the Golgi. If transport is through stable compartments, the organelles should not be consumed by massive protein flows. Conversely, if traffic is a maturation process, there should be no stable intermediate stations during ER-to-Golgi or Golgi-to-ER transit. Besides, these traveling intermediate stations should be able to concomitantly move and sort material back to the previous station. Assessing both models in fixed cells is inappropriate as the difference resides in the dynamics of movement of the intermediate stations and not in their contents. In the present work, relocalizing GFP-ERGIC-53 from ERGIC clusters to the ER then following its exit was fundamental to show that the newly appearing GFP-ERGIC-53 stationary elements do not migrate to the Golgi, thus demonstrating their stability (see results section). My data do not entirely exclude the possibility of a maturation process, but they reject the idea that this would be the only means by which trafficking occurs. Indeed, I see that some of the fast moving GFP-ERGIC-53 structures that co-label with ssDsRed separate into retrograde and anterograde moving carriers, respectively; however these structures are a minority. It is hence likely that both trafficking mechanisms co-exist depending on the cell and cargo size and load.

2. ERGIC populations

Monitoring GFP-ERGIC-53 trafficking in living HeLa cells has revealed three types of moving populations: stationary spots, fast moving structures and transient tubules (see results section). The stationary spots are long-lived and undergo short-range movement. Fast moving structures are short-lived and, although they are elongated, they could be differentiated from tubules because these two populations have distinct speeds. Tubules are also rather short-lived. They are noticeably identifiable in a 15°C rewarming experiment. The amount of each GFP-ERGIC-53 population depends on different

conditions. At steady state, the majority of the population is represented by the stationary structures. Few fast moving entities (~ 20% of the total population) are observed, and virtually no tubules could be identified. In a 15°C rewarming experiment, 66% of the total population is moving. ~22% of the moving entities are tubules clearly emanating from stationary structures. To what do the different ERGIC populations correspond? What are the possible functions of the different ERGIC populations? What regulates the equilibrium between ERGIC populations? These questions and the possible approach (es) to address them will be discussed in the following paragraphs of this sub-section.

By light microscopy, ERGIC clusters are condensed in the Golgi area. This labeling does not correspond to a Golgi localization only, because immuno-electron microscopy data has revealed that ERGIC-53 positive clusters are concentrated close to the *cis*-Golgi (Klumperman et al., 1998). Following GFP-ERGIC-53 re-appearance from the ER in H89 washout experiments has revealed that the stationary clusters in the periphery of the cell and in the juxtanuclear region emerge simultaneously, suggesting that they are equivalent (see results section). To further explore this assumption, the same H89 recovery procedure could be done in dual time-lapse experiments with GFP-ERGIC-53 and various fluorescently labeled SNAREs and tethering factors that were previously mislocalized to the ER. If the recovery kinetics of SNAREs (such as Sec22, ykt6 and Gos 28) in the ERGIC peripheral clusters and in the Golgi area are similar, then these structures are identical. If in contrast the recovery time of SNAREs in the periphery of the cell is faster than in the Golgi area or *vice versa* than these ERGIC structures are not identical. In this case, further investigation by dual imaging GFP-ERGIC-53 and other fluorescently labeled proteins as tethering factors like p115 (Sapperstein et al., 1995) and/or regulatory factors like LMA1 (Elazar et al., 2003) could give more information about the characteristics of these clusters. The fast moving structures outline a very intriguing population. These entities behave indistinguishably at 37°C and in a 15°C rewarming experiment. They move along microtubule tracks and seem to cross several stationary structures during their transit and ultimately fuse with them. To examine whether the fast moving structures indeed fuse with the stationary spots, their dynamics could be monitored in presence of the fusion inhibitor N-ethylmaleimide (NEM). If these entities indeed fuse with the target stationary clusters,

then the addition of NEM should block the fusion events resulting in an increase of the number of the fast moving structures inside the cell. If on the other hand fast moving structures are only intersecting the stationary clusters fortuitously during their transit, then the addition of NEM should have no effect on the dynamics of the fast moving structures. As NEM is a general fusion inhibitor, more specific fusion steps could be impeded using antibodies against particular fusion proteins involved in transport between the ER and the Golgi. An example is the use of antibodies against NSF or the expression of NSF dominant interfering ATP-hydrolysis deficient mutants (Dalal et al., 2004).

The majority of the fast moving structures (~71%) are devoid of anterograde cargo in cells rewarmed from 15°C to 37°C. The few that are cargo positive (29%) give the impression to cross several stationary ERGIC structures during their movement. This and the findings described above suggested that the fast moving structures act as intra-ERGIC carriers (see results section). To further investigate this possibility, the dynamics of the fast moving structures could be studied under conditions where only intra-ERGIC transport is detectable. This could be produced by blocking anterograde and retrograde transport from the ERGIC. If the movement of these structures persists under these conditions, then it could be firmly concluded that the fast moving elements are intra-ERGIC carriers. The dynamics of the fast moving structures are similar at 37°C and at very early times (few seconds) after rewarming from 15°C (Ben Tekaya and Hauri, unpublished). If these dynamics are also similar under steady state conditions and in BFA and/or AlF_4^- treated cells, then it would validate the notion that fast moving structures are intra-ERGIC carriers. Preliminary data using a BFA-like effect in ldlF cells (Hobbie et al., 1994) incubated at 40°C for 15 h to inhibit COPI activity, show that the dynamics of fast moving structures are essentially unaffected (Ben Tekaya and Hauri, unpublished). One drawback of this procedure is that traffic between the ER and the ERGIC is still intact under some of these block conditions. Thus, it would still be possible that the fast moving structures are ERGIC to ER and/or ER to ERGIC transport carriers. This is unlikely because H89 block shows that fast moving structures disappear quickly after the addition of the drug while the recycling of GFP-ERGIC-53 to the ER proceeds; and the recovery from H89 treatment reveals that these structures appear only after almost full recovery of the stationary clusters and often seem to protrude from them. The

fact that the majority of GFP-ERGIC-53 fast moving structures are cargo negative could be explained in two mutually non exclusive ways: either these structures have already segregated ssDsRed, or they were never positive for anterograde cargo. In cells that were not incubated at 15°C, GFP-ERGIC-53 and ssDsRed fast moving structures hardly ever colocalize, even in the presence of high cargo concentrations. The very few entities that do colocalize behave as the ones seen in a 15°C rewarming experiment. Hence, the colocalization of GFP-ERGIC-53 and ssDsRed in the fast moving structures could be interpreted as a result of cargo concentration in the ERGIC during a 15°C block. This further supports the idea of fast moving structures being intra-ERGIC carriers. Probably, if more cargo is concentrated in the ERGIC, more fast moving structures will be positive. This could be investigated by two approaches: 1. Dual live imaging, during a 15°C rewarming experiment, of GFP-ERGIC-53 and fluorescently labeled VIP36 and/or KDEL receptor. The advantage of these two proteins is that they are concentrated in the ERGIC at 15°C and not partially in the ER as it is the case for ssDsRed; thus, the results could be directly compared to the ones obtained with ssDsRed. 2. Concentrating GFP-ERGIC-53 and ssDsRed in the ERGIC by BFA and/or AlF_4^- and dual live imaging of the fast moving co-labeled structures during the block and not during the recovery as done with the 15°C rewarming experiment.

Fast moving structures are very sensitive to H89 as they instantly disappear after the addition of this drug (Ben Tekaya and Hauri, unpublished). It could be interpreted that these structures are COPII-coated, and the moment the coat components are mislocalized to the cytosol in the presence of H89 (Lee and Linstedt, 2000) (Aridor and Balch, 2000), these structures disappear perhaps by fusing with the ER. This is unlikely though, for two reasons. First, if the fast moving structures were COPII-coated vehicles, we would expect to see them at initial ER exit steps and thus they would be the earliest structures emerging in a recovery from H89 experiment. But this is not the case. Second, COPII spots speed and half-life are completely dissimilar to the fast moving structures (Hammond and Glick, 2000) (Stephens et al., 2000). The other interpretation is that this high H89 sensitivity is caused by a specific kinase regulating the trafficking of the fast moving structures. As soon as this kinase is inhibited, the transport of the fast moving structures abruptly stops. If this is the case, the specific kinase would have a concomitant effect on ER exit and on intra-ERGIC transport. Interestingly, H89 blocks

intra-Golgi trafficking as well (Muniz et al., 1997), suggesting that this H89-sensitive kinase acts at later steps in the early secretory pathway. Recently, an H89-like effect was reported in cells expressing DGKι, a diacylglycerol kinase (Nagaya et al., 2001). Classical members of the DGK family phophorylate diacylglycerol to produce phosphatidic acid so that the action of protein kinase C, which requires diaclyglycerol for activation, is attenuated (Sakane and Kanoh, 1997). Phosphatidic acid generated by the action of phospholipase D has also been shown to regulate protein traffic from the Golgi complex. It was thus proposed that the effects of DGKι are exerted through its PH domain sequestrating the target lipid(s) involved in the control of ER-to-Golgi transport (Nagaya et al., 2001). It would be interesting to examine the effect of DGKι over-expression on the fast moving GFP-ERGIC-53 structures. It would be additionally very exciting to uncover its mode of function. When the GFP-ERGIC-53 stably expressing cells are treated with tunicamycin, sodium butyrate for 42 h, or high amounts of the transfection reagent FuGENE 6, ERGIC fast moving structures appear as elongated tubules comparable to the ones seen in a 15°C rewarming experiment (Ben Tekaya and Hauri, unpublished). Sodium butyrate induces gene expression by hyper-acetylating histones (Kruh, 1982). FuGENE 6 is a multi-component lipid-based transfection reagent. Low temperature and these compounds have seemingly nothing in common. But one could perceive that 15°C, long sodium butyrate incubation times and high amounts of FuGENE 6 result in elevated concentrations of GFP-ERGIC-53 in the ERGIC. This will lead to higher loads of proteins to be transported between ERGIC clusters; hence larger carriers are engaged to accomplish optimal and fast trafficking. Interestingly, in dual time-lapse imaging experiments, when a 15°C block is combined with high amounts of FuGENE 6, ssDsRed and GFP-ERGIC-53 colocalize in tubular structures during rewarming (Ben Tekaya and Hauri, unpublished). The advantage for a cell to have tubular fast moving structures rather than an increased number of fast moving structures is to minimize the energy consuming budding and fusion events. What mediates the transformation of small fast moving structures into tubular ones is completely undetermined. Morphologically this could be investigated using high resolution imaging microscopy such as correlative video laser scanning microscopy and video laser scanning tomography. One can imagine that lipid homeostasis is changed under high protein concentrations conditions (Morris and Homann, 2001), thus inducing

morphological transformations. The features of the lipids involved could be speculated from the tunicamycin effect, which is not due to a general alteration of the quality control machinery, since no tubules are observed with thapsigargin (Ben Tekaya and Hauri, unpublished). Tunicamycin is an antibiotic that interferes with the first step in the dolichol pathway of N-glycosylation by inhibiting the addition of an N-acetylglucosamine phosphate residue to dolichyl phosphate, resulting in a lack of functional lipid-linked oligosaccharide precursors (Schwarz, 1991) (Rine et al., 1983). The regulation of trafficking via lipids has already been reported. Indeed, it was shown that phospholipid metabolism is implicated in the control of membrane traffic particularly at the distal stage of the secretory pathway (Kahn and Gilman, 1986) (De Camilli et al., 1996) (Siddhanta and Shields, 1998) (Roth, 1999). Furthermore, the presence of phosphatidylinositol(3,4)P_2 in the membranes has been shown to be required for binding COPII coat protein complex (Yoshihisa et al., 1993). Also, association of an isoform of phosphatidylinositol-4-kinase with the ER was described (Wong et al., 1997). Thus, methods interfering with the dolichol biosynthesis would be a useful option to further investigate this issue.

3. Potential machineries controlling ERGIC populations

As described in the Introduction section, several machineries, such as coats, SNARES, motors, Rabs and tethering factors, control trafficking in the early secretory pathway. It is obvious that the components of these machineries are involved in regulating and probably distinguishing the various ERGIC populations, outlined in this thesis, from each others and from other transport carriers in the early secretory pathway. Nevertheless, to date it is not possible to clearly state how, when and where the several trafficking regulators act in the ERGIC and if some of them are specific to different ERGIC populations. It is hence of major interest to dissect the molecular mechanisms taking place in the ERGIC and thus precisely defining the function(s) of its various populations.

The elementary trafficking effectors that are most likely controlling ERGIC dynamics and the exchange of material with the ER and the Golgi are COPII and COPI coats. Dual time-lapse imaging of GFP-ERGIC-53 and for example a DsRed-tagged version of Sec13, a component of the COPII coat, and analysis of the segregation of

these two proteins during rewarming from 15°C will allow to assess the relationship between ERES and ERGIC clusters. It will clarify data from immunofluorescence experiments showing that ERGIC and ERES markers colocalize at 15°C while this colocalization is only partial at 37°C (Hammond and Glick, 2000) (Ben-Tekaya and Hauri unpublished data). Following the recruitment of fluorescent COPII component to ERES and the recovery of GFP-ERGIC-53 from the ER to ERGIC clusters would be very informative about the dynamics of ERES and ERGIC clusters. Such an experiment could be performed using dual live imaging of GFP-ERGIC-53 and DsRed-Sec13 under H89 washout conditions. The influence of COPI coats on ERGIC dynamics is not clear. ERGIC stationary structures stain positive for COPI by immunofluorescence (see results section), suggesting that it is functional on these membranes. Trafficking of the fast moving structures seems to be COPI-independent, as these entities persist in ldlF cells incubated at 39.5°C (Ben-Tekaya and Hauri unpublished data). At this temperature the κ subunit of the COPI complex is unstable, which impairs the proper function of COPI coats (Hobbie et al., 1994). It was already shown that the ERGIC tubules formed in a 15°C rewarming experiment do not contain COPI components (Klumperman et al., 1998), implying that this trafficking step is either COPI-independent or the association of COPI to tubules is too fast to be visible in fixed cells. To dissect the actual contribution of COPI coats in the regulation of ERGIC dynamics, dual time lapse imaging experiments of a COPI subunit and ERGIC-53 will be informative. Alternatively, the different populations of the ERGIC could be followed under conditions where COPI is inhibited (BFA, AlF_4^-, antibody microinjection).

It is proposed that COPII-coated ERES act as a reservoir of SNAREs and other machinery molecules (Mossessova et al., 2003) (Miller et al., 2003); so would ERGIC clusters probably do. To investigate these possibilities, and once the relationships between COPII and ERGIC and SNAREs and ERGIC populations are established (as described above and in the “ERGIC populations” sub-section), triple-labeling experiments of COPII, ERGIC and SNAREs with or without ER/ERGIC blocks will directly illustrate whether COPII structures indeed concentrate SNAREs, if this is also the case for some ERGIC populations, and how the SNARE composition of a vehicle will determine its targeting and probably the trafficking route it takes.

The first feature that differentiates the various ERGIC populations described in the present work is their speeds. Stationary structures move with speeds of 0.2 σm/sec; while fast moving structures have speeds of 1 to 7 σm/sec, and tubules move at 1 σm/sec. These significant differences are probably the result of the action of distinct motor proteins. So far, the precise motor proteins involved in each step of ER-to-Golgi and Golgi-to-ER trafficking are not firmly established (Allan et al., 2002). It is possible however, to scrutinize which one of the motor proteins, known to act in the ER-Golgi interface, is regulating each trafficking population of the ERGIC. Microinjecting antibodies to specific subunits of motor complexes or over-expressing the corresponding proteins (Presley et al., 1997) will reveal which one of them specifically directs the movement of particular GFP-ERGIC-53 populations. Alternatively, the dynamics of GFP-ERGIC-53 could be followed in semi-intact cells. Adding cytosol depleted in one or the other motor proteins will precisely reveal which ERGIC population the depleted motor acts on as movement of the affected population will be inhibited. Rescue of this movement by the addition of the depleted motor protein will confirm its specific effect. It would be very challenging to unravel the extensive list of motor proteins acting on ERGIC populations. For that, it could be envisaged to biochemically separate ERGIC populations using differential centrifugation and gradients, as was already described (Ying et al., 2000) (Breuza *et al.*, in preparation). The separation should be done in the presence of detergents such as TX-100 where both membrane and cytosolic fractions could be analyzed. If this procedure is successful, the composition of each ERGIC population will be resolved by mass-spectrometry. Once the putative motors identified, it will be possible to assign each one to precise trafficking steps/populations by the microinjection/over-expression and/or the semi-intact cells procedures described above. Obviously, such a biochemical procedure when effective would also unravel in details the differences and similarities between ERGIC populations based on their composition in coats, SNAREs, regulatory components, tethering factors, etc.

The COPI independence of the dynamics of fast moving structures (described in the “ERGIC populations” sub-section) implies the involvement of another type of machinery in regulating this trafficking step. The plausible regulators of this specific transport step are Rabs, as Rab-dependent COPI-independent Golgi-to-ER trafficking steps were already described (White et al., 1999). A candidate Rab to investigate fast

moving structures dynamics, is Rab1b (Goud and McCaffrey, 1991). Indeed, it was recently shown that this specific Rab remains associated with ERGIC membranes after COPI inhibition using BFA (Breuza *et al.*, in preparation). To ascertain this hypothesis, fast dual imaging experiments of Rab1b and GFP-ERGIC-53 will be advantageous. Expressing Rab1b mutants, or microinjecting Rab1b antibodies (Plutner et al., 1991) and analyzing ERGIC fast moving structures will also clarify this issue. To this end, the ldlF cells stably expressing GFP-ERGIC-53, where the fast moving structures persist at the non-permissive temperature although COPI coats are destabilized (Ben Tekaya and Hauri, unpublished), would be a good model system. The same rationale of antibody microinjection and dual live imaging could be used to examine the possible COPI-independence of ERGIC tubules movement. In this case, Golgi-to-ER Rabs such as Rab33b and Rab 6 (Valsdottir et al., 2001) (White et al., 1999) (Girod et al., 1999) should be considered.

Multiple Rab proteins on a single vehicle could interact with distinct effectors, leading to translocation and also to targeted vehicle delivery. In this case, a vehicle might be linked by Rab GTPases to a motor protein as well as to tethering factors. So far, nothing is known about how the action of Rab proteins is coupled to motors and how this controls trafficking in the early secretory pathway. By deciphering the precise motor proteins and Rabs acting on ERGIC populations and by resolving their mode of action (as described above), it would be possible to depict the simultaneous effect of this two machineries on the different ERGIC populations. Characterizing the dynamics of these machineries in conjunction with the ERGIC populations by using triple-time lapse imaging will be a major breakthrough in the field.

4. Future directions

The notion of seeing is believing has its limitations. For this reason, techniques that aim to improve the optical resolution in live specimens are continuously developed. Several powerful approaches, which are based on illumination through multiple objectives (Theta, 4Pi, I5M) or increased contrast by using structured illumination (Gustafsson, 1999) are starting to see the light. New devices like the scanning near-field optical microscopy, could be used in the future to overcome the resolution limitations of TIR-FM

and epi-fluorescence (de Lange et al., 2001). Another alternative is to combine fluorescence live imaging with electron microscopy. Some new techniques such as transmission video microscopy, correlative video electron microscopy and correlative video tomography are starting to be used.

One of the next objectives of cell biology is to quantify the flow of materials, information and energy through the molecular networks. To achieve this, both the dynamic and kinetic parameters of the single processes within the networks —such as the movement and translocation of proteins, the protein–protein interactions and the enzymatic reactions — must be determined in living cells. Monitoring chemical reactions using single-molecule analysis will also be an important future goal. Finally, combining single-molecule-visualization, single-molecule-manipulation and single-molecule-electrophysiology techniques will be important to allow the further understanding of the nanobiology of living cells.

5. References

Allan, V. J., Thompson, H. M., and McNiven, M. A. (2002). Motoring around the Golgi. Nat Cell Biol *4*, E236-242.

Aridor, M., and Balch, W. E. (2000). Kinase signaling initiates coat complex II (COPII) recruitment and export from the mammalian endoplasmic reticulum. J Biol Chem *275*, 35673-35676.

Aridor, M., Bannykh, S. I., Rowe, T., and Balch, W. E. (1995). Sequential coupling between COPII and COPI vesicle coats in endoplasmic reticulum to Golgi transport. J Cell Biol *131*, 875-893.

Bevis, B. J., Hammond, A. T., Reinke, C. A., and Glick, B. S. (2002). De novo formation of transitional ER sites and Golgi structures in Pichia pastoris. Nat Cell Biol *4*, 750-756.

Chen, Y. A., and Scheller, R. H. (2001). SNARE-mediated membrane fusion. Nat Rev Mol Cell Biol *2*, 98-106.

Dalal, S., Rosser, M. F., Cyr, D. M., and Hanson, P. I. (2004). Distinct roles for the AAA ATPases NSF and p97 in the secretory pathway. Mol Biol Cell *15*, 637-648.

De Camilli, P., Emr, S. D., McPherson, P. S., and Novick, P. (1996). Phosphoinositides as regulators in membrane traffic. Science *271*, 1533-1539.

de Lange, F., Cambi, A., Huijbens, R., de Bakker, B., Rensen, W., Garcia-Parajo, M., van Hulst, N., and Figdor, C. G. (2001). Cell biology beyond the diffraction limit: near-field scanning optical microscopy. J Cell Sci *114*, 4153-4160.

Elazar, Z., Scherz-Shouval, R., and Shorer, H. (2003). Involvement of LMA1 and GATE-16 family members in intracellular membrane dynamics. Biochim Biophys Acta *1641*, 145-156.

Girod, A., Storrie, B., Simpson, J. C., Johannes, L., Goud, B., Roberts, L. M., Lord, J. M., Nilsson, T., and Pepperkok, R. (1999). Evidence for a COP-I-independent transport route from the Golgi complex to the endoplasmic reticulum. Nat Cell Biol *1*, 423-430.

Goud, B., and McCaffrey, M. (1991). Small GTP-binding proteins and their role in transport. Curr Opin Cell Biol *3*, 626-633.

Gustafsson, M. G. (1999). Extended resolution fluorescence microscopy. Curr Opin Struct Biol *9*, 627-634.

Hammond, A. T., and Glick, B. S. (2000). Dynamics of transitional endoplasmic reticulum sites in vertebrate cells. Mol Biol Cell *11*, 3013-3030.

Hobbie, L., Fisher, A. S., Lee, S., Flint, A., and Krieger, M. (1994). Isolation of three classes of conditional lethal Chinese hamster ovary cell mutants with temperature-dependent defects in low density lipoprotein receptor stability and intracellular membrane transport. J Biol Chem *269*, 20958-20970.

Kahn, R. A., and Gilman, A. G. (1986). The protein cofactor necessary for ADP-ribosylation of Gs by cholera toxin is itself a GTP binding protein. J Biol Chem *261*, 7906-7911.

Klumperman, J., Schweizer, A., Clausen, H., Tang, B. L., Hong, W., Oorschot, V., and Hauri, H. P. (1998). The recycling pathway of protein ERGIC-53 and dynamics of the ER-Golgi intermediate compartment. J Cell Sci *111*, 3411-3425.

Kruh, J. (1982). Effects of sodium butyrate, a new pharmacological agent, on cells in culture. Mol Cell Biochem *42*, 65-82.

Lee, T. H., and Linstedt, A. D. (2000). Potential role for protein kinases in regulation of bidirectional endoplasmic reticulum-to-Golgi transport revealed by protein kinase inhibitor H89. Mol Biol Cell *11*, 2577-2590.

Lippincott-Schwartz, J., Roberts, T. H., and Hirschberg, K. (2000). Secretory protein trafficking and organelle dynamics in living cells. Annu Rev Cell Dev Biol *16*, 557-589.

Miller, E. A., Beilharz, T. H., Malkus, P. N., Lee, M. C., Hamamoto, S., Orci, L., and Schekman, R. (2003). Multiple cargo binding sites on the COPII subunit Sec24p ensure capture of diverse membrane proteins into transport vesicles. Cell *114*, 497-509.

Mironov, A. A., Mironov, A. A., Jr., Beznoussenko, G. V., Trucco, A., Lupetti, P., Smith, J. D., Geerts, W. J., Koster, A. J., Burger, K. N., Martone, M. E.*, et al.* (2003). ER-to-Golgi carriers arise through direct en bloc protrusion and multistage maturation of specialized ER exit domains. Dev Cell *5*, 583-594.

Morris, C. E., and Homann, U. (2001). Cell surface area regulation and membrane tension. J Membr Biol *179*, 79-102.

Mossessova, E., Bickford, L. C., and Goldberg, J. (2003). SNARE selectivity of the COPII coat. Cell *114*, 483-495.

Muniz, M., Martin, M. E., Hidalgo, J., and Velasco, A. (1997). Protein kinase A activity is required for the budding of constitutive transport vesicles from the trans-Golgi network. Proc Natl Acad Sci U S A *94*, 14461-14466.

Nagaya, H., Saito, Y., and Warashina, H. (2001). Simultaneous ipsilateral fractures of distal and proximal ends of the radius. J Orthop Sci *6*, 439-443.

Plutner, H., Cox, A. D., Pind, S., Khosravi-Far, R., Bourne, J. R., Schwaninger, R., Der, C. J., and Balch, W. E. (1991). Rab1b regulates vesicular transport between the endoplasmic reticulum and successive Golgi compartments. J Cell Biol *115*, 31-43.

Presley, J. F., Cole, N. B., Schroer, T. A., Hirschberg, K., Zaal, K. J., and Lippincott-Schwartz, J. (1997). ER-to-Golgi transport visualized in living cells. Nature *389*, 81-85.

Puri, S., and Linstedt, A. D. (2003). Capacity of the golgi apparatus for biogenesis from the endoplasmic reticulum. Mol Biol Cell *14*, 5011-5018.

Rine, J., Hansen, W., Hardeman, E., and Davis, R. W. (1983). Targeted selection of recombinant clones through gene dosage effects. Proc Natl Acad Sci U S A *80*, 6750-6754.

Roth, M. G. (1999). Lipid regulators of membrane traffic through the Golgi complex. Trends Cell Biol *9*, 174-179.

Rowe, T., Aridor, M., McCaffery, J. M., Plutner, H., Nuoffer, C., and Balch, W. E. (1996). COPII vesicles derived from mammalian endoplasmic reticulum microsomes recruit COPI. J Cell Biol *135*, 895-911.

Sakane, F., and Kanoh, H. (1997). Molecules in focus: diacylglycerol kinase. Int J Biochem Cell Biol *29*, 1139-1143.

Sapperstein, S. K., Walter, D. M., Grosvenor, A. R., Heuser, J. E., and Waters, M. G. (1995). p115 is a general vesicular transport factor related to the yeast endoplasmic reticulum to Golgi transport factor Uso1p. Proc Natl Acad Sci U S A *92*, 522-526.

Scales, S. J., Pepperkok, R., and Kreis, T. E. (1997). Visualization of ER-to-Golgi transport in living cells reveals a sequential mode of action for COPII and COPI. Cell *90*, 1137-1148.

Schwarz, R. T. (1991). Manipulation of the biosynthesis of protein-modifying glycoconjugates by the use of specific inhibitors. Behring Inst Mitt, 198-208.

Siddhanta, A., and Shields, D. (1998). Secretory vesicle budding from the trans-Golgi network is mediated by phosphatidic acid levels. J Biol Chem *273*, 17995-17998.

Stephens, D. J., Lin-Marq, N., Pagano, A., Pepperkok, R., and Paccaud, J. P. (2000). COPI-coated ER-to-Golgi transport complexes segregate from COPII in close proximity to ER exit sites. J Cell Sci *113*, 2177-2185.

Storrie, B., White, J., Rottger, S., Stelzer, E. H., Suganuma, T., and Nilsson, T. (1998). Recycling of golgi-resident glycosyltransferases through the ER reveals a novel pathway and provides an explanation for nocodazole-induced Golgi scattering. J Cell Biol *143*, 1505-1521.

Valsdottir, R., Hashimoto, H., Ashman, K., Koda, T., Storrie, B., and Nilsson, T. (2001). Identification of rabaptin-5, rabex-5, and GM130 as putative effectors of rab33b, a regulator of retrograde traffic between the Golgi apparatus and ER. FEBS Lett *508*, 201-209.

Ward, T. H., Polishchuk, R. S., Caplan, S., Hirschberg, K., and Lippincott-Schwartz, J. (2001). Maintenance of Golgi structure and function depends on the integrity of ER export. J Cell Biol *155*, 557-570.

White, J., Johannes, L., Mallard, F., Girod, A., Grill, S., Reinsch, S., Keller, P., Tzschaschel, B., Echard, A., Goud, B., and Stelzer, E. H. (1999). Rab6 coordinates a novel Golgi to ER retrograde transport pathway in live cells. J Cell Biol *147*, 743-760.

Wong, K., Meyers dd, R., and Cantley, L. C. (1997). Subcellular locations of phosphatidylinositol 4-kinase isoforms. J Biol Chem *272*, 13236-13241.

Ying, M., Flatmark, T., and Saraste, J. (2000). The p58-positive pre-golgi intermediates consist of distinct subpopulations of particles that show differential binding of COPI and COPII coats and contain vacuolar H(+)-ATPase. J Cell Sci *113 (Pt 20)*, 3623-3638.

Yoshihisa, T., Barlowe, C., and Schekman, R. (1993). Requirement for a GTPase-activating protein in vesicle budding from the endoplasmic reticulum. Science *259*, 1466-1468.